Nuclei in the Cosmos School
2025

STELLAR EVOLUTION

Alessandro Chieffi
INAF, Italy

NASA/Space Telescope Science Institute

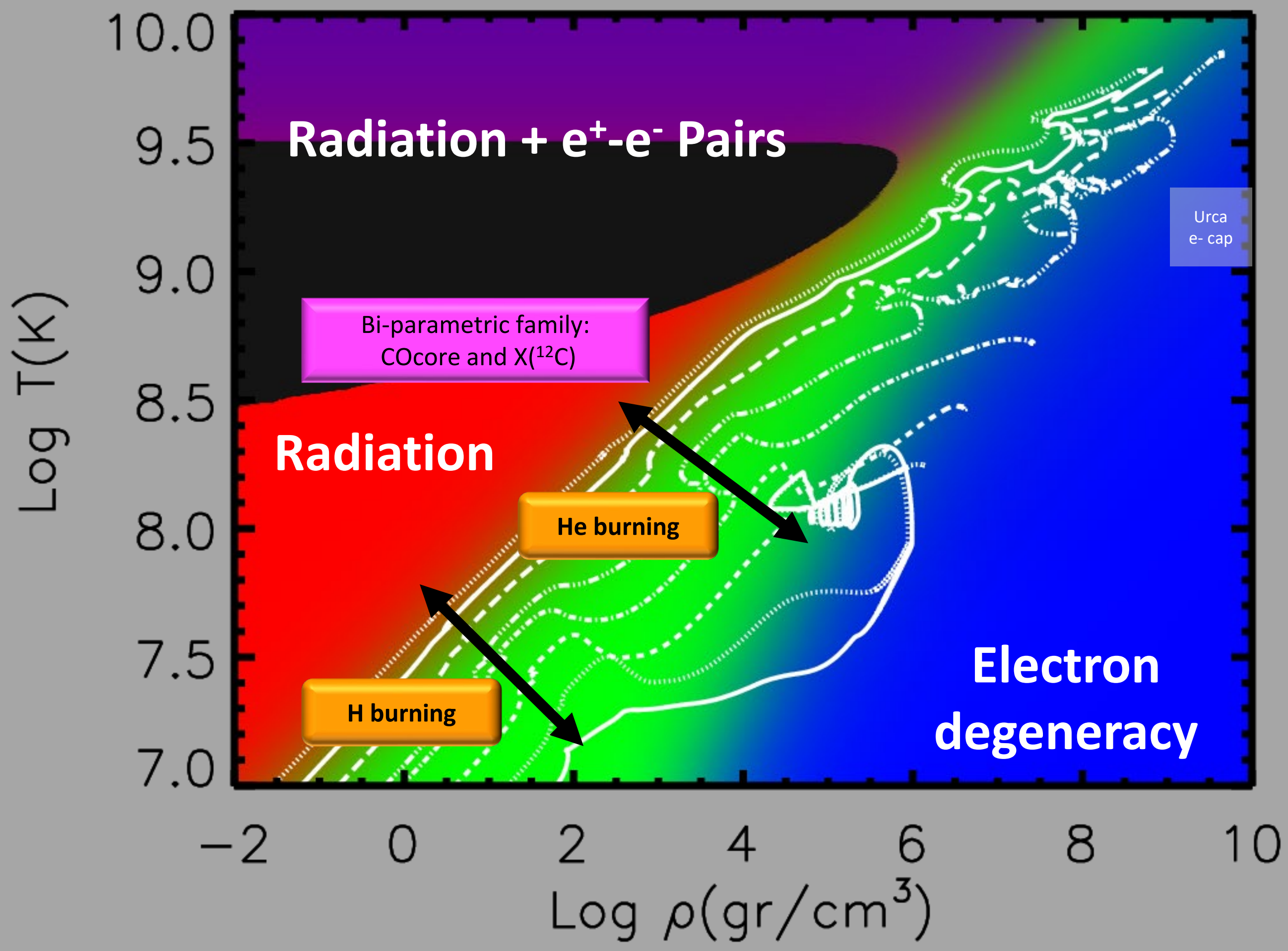

Radiation + e+-e- Pairs
Bi-parametric family:
COcore and X(12C)
Radiation
He burning
H burning
Urca
e- cap
Electron
degeneracy
Log T(K)
Log ρ(gr/cm3)
10.0
9.5
9.0
8.5
8.0
7.5
7.0
−2
0
2
4
6
8
10

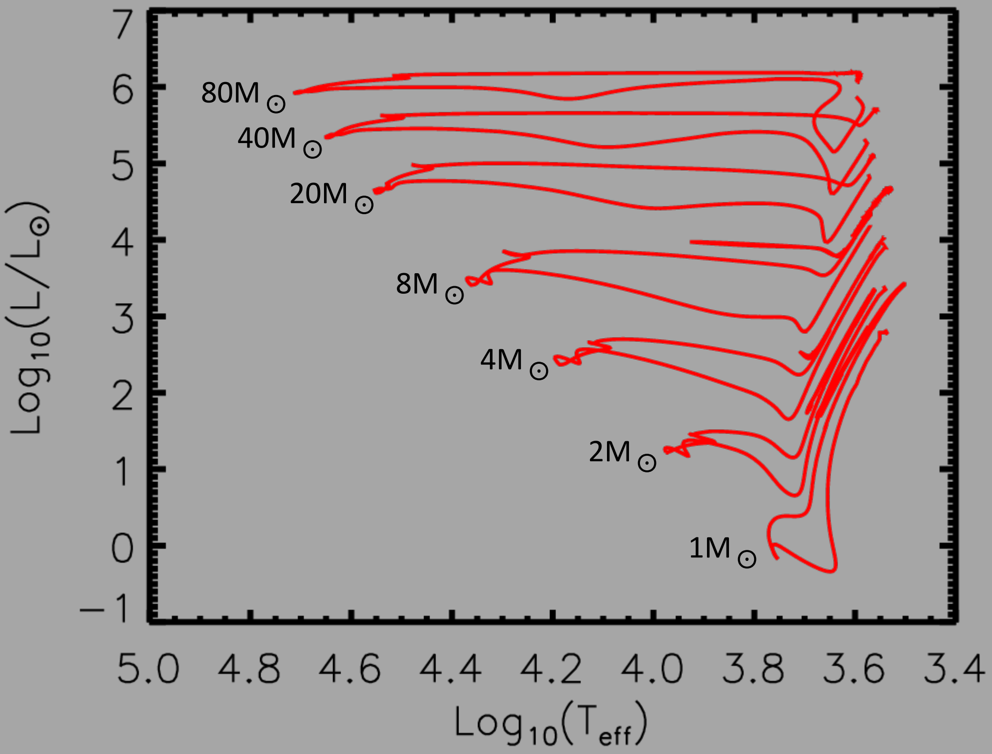
80M⊙
40M⊙
20M⊙
8M⊙
4M⊙
2M⊙
1M⊙
7
6
5
4
3
2
1
0
−1
5.0
4.8
4.6
4.4
4.2
4.0
3.8
3.6
3.4
Log10(L/L⊙)
Log10(Teff)

Shell He burning (the E-AGB)

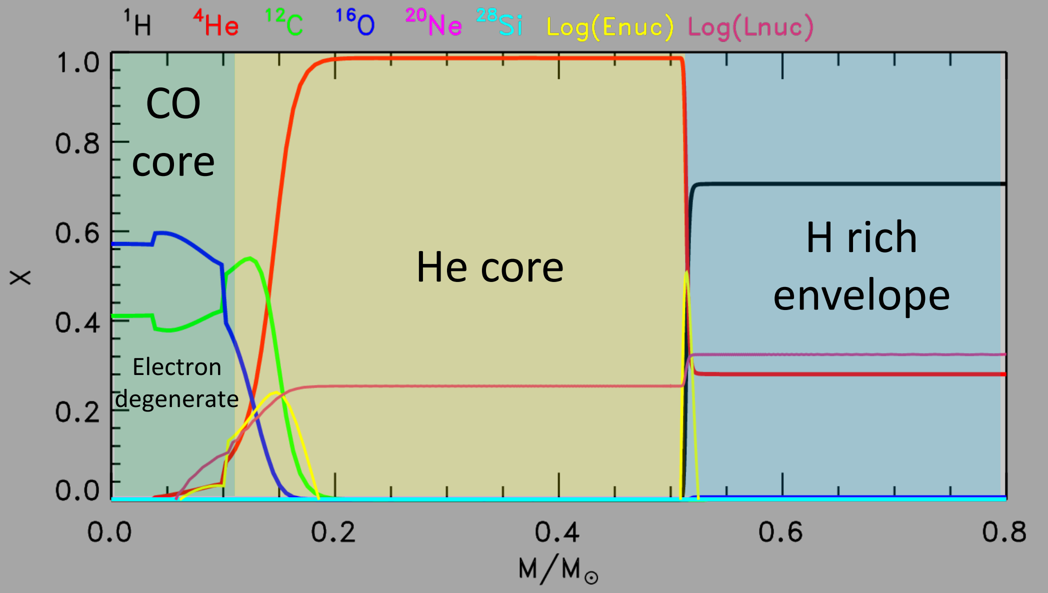

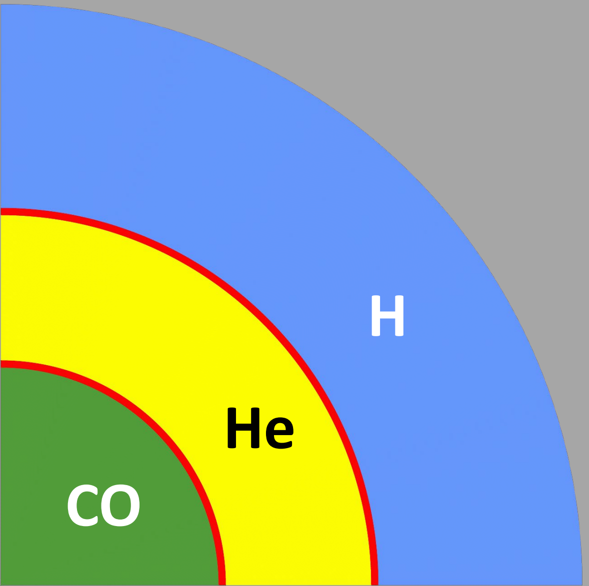

1) The efficiency of the He burning shell increases with the mass of the CO core because it is NOT self-regulated.
2) The growth of the CO core mass implies the increase of the temperature inside the core
3) The power of the He burning shell forces the H rich mantle to expand and cool down: the border of the convective envelope penetrates inward (in mass)

4) Neutrino energy losses push the maximum teperature far from the center
5) Mass Loss becomes stronger and stronger ($10^{-7} – 10^{-4}$ $M_\odot$/yr)

E-AGB lifetime ranges between 30 Myr (2 $M_\odot$) and 0.6 Myr (9 $M_\odot$)

Shell He burning (the E-AGB)

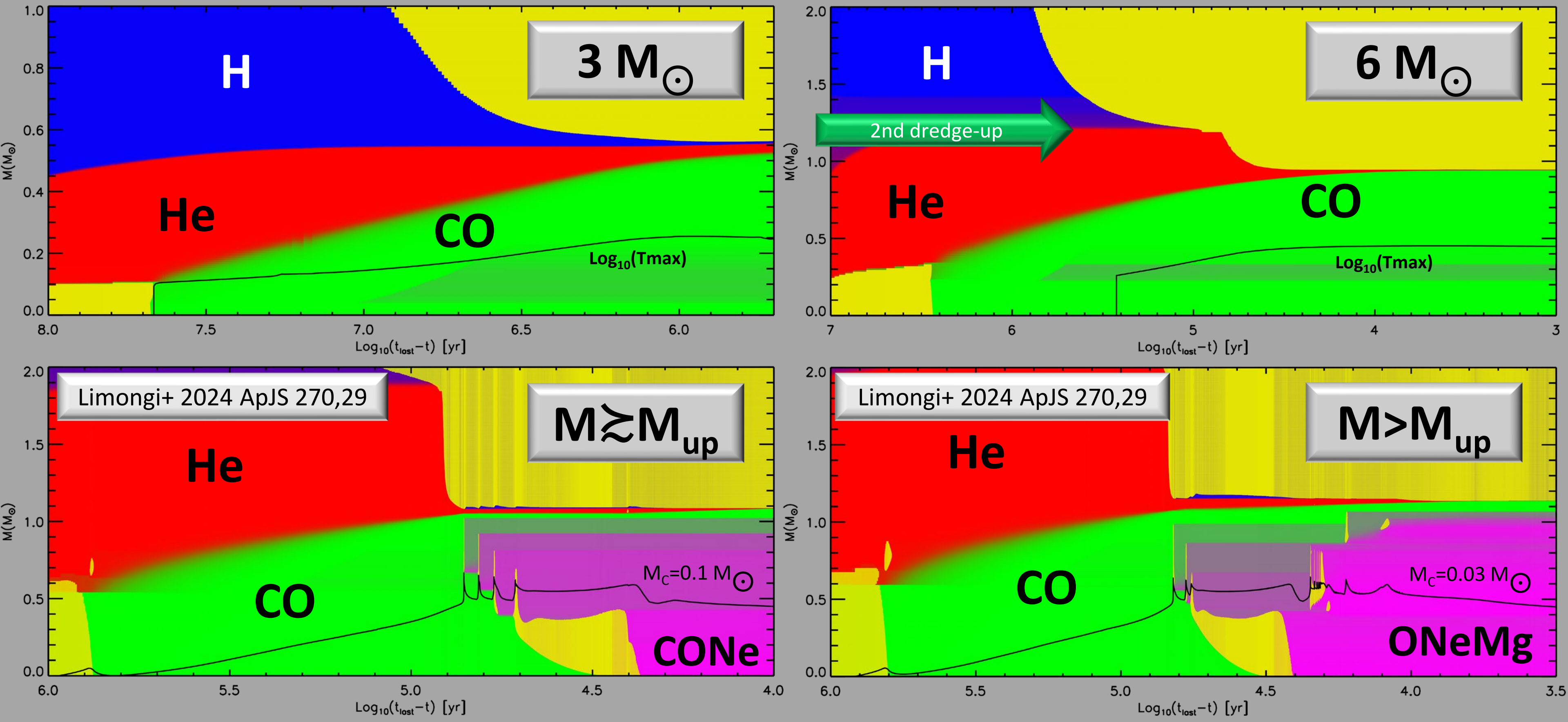

Shell He burning (the E-AGB)

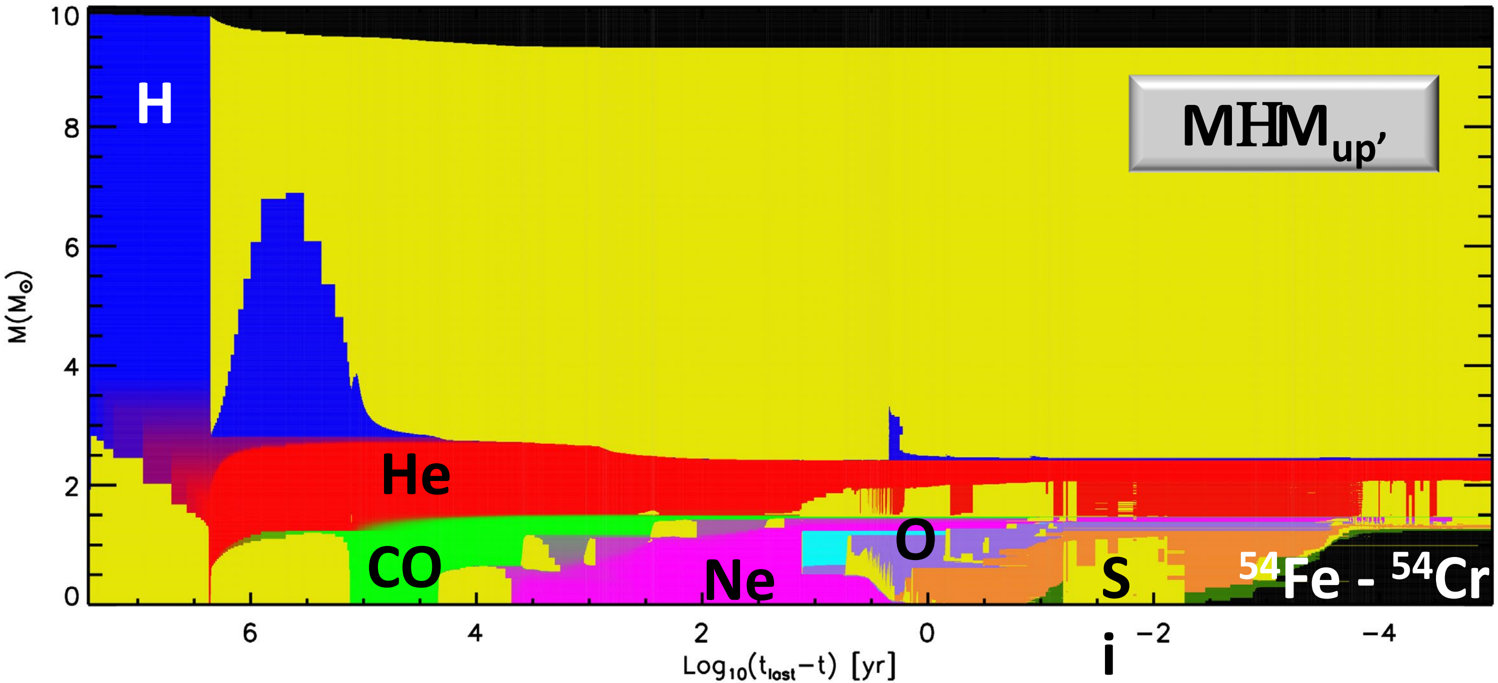

Limongi+ 2024 ApJS 270,29

Stars that ignite Ne in electron degenerate conditions lift the degeneracy and evolve as massive stars

Shell He burning (the E-AGB)

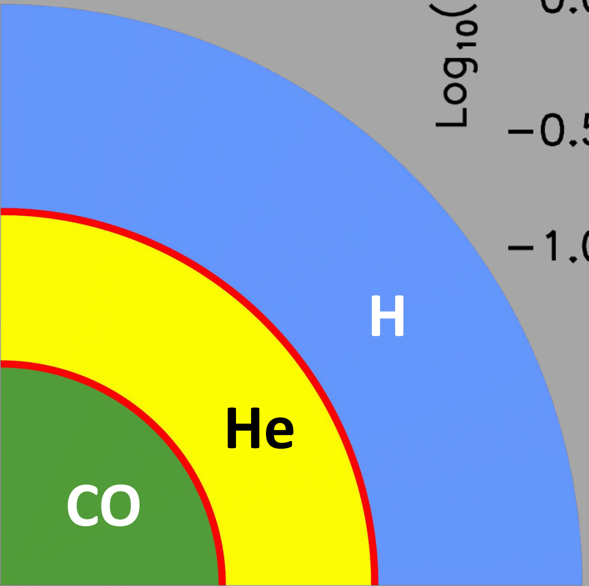

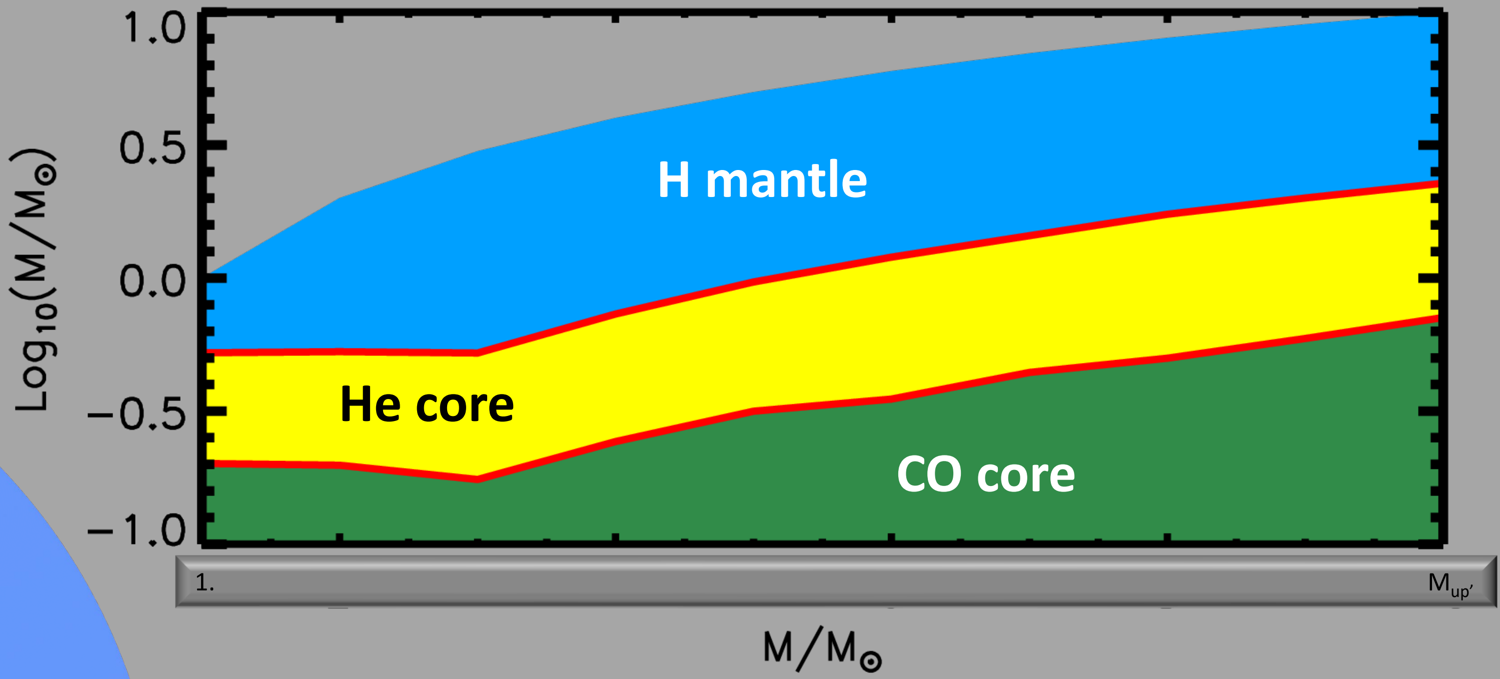

Shell He burning (the E-AGB)

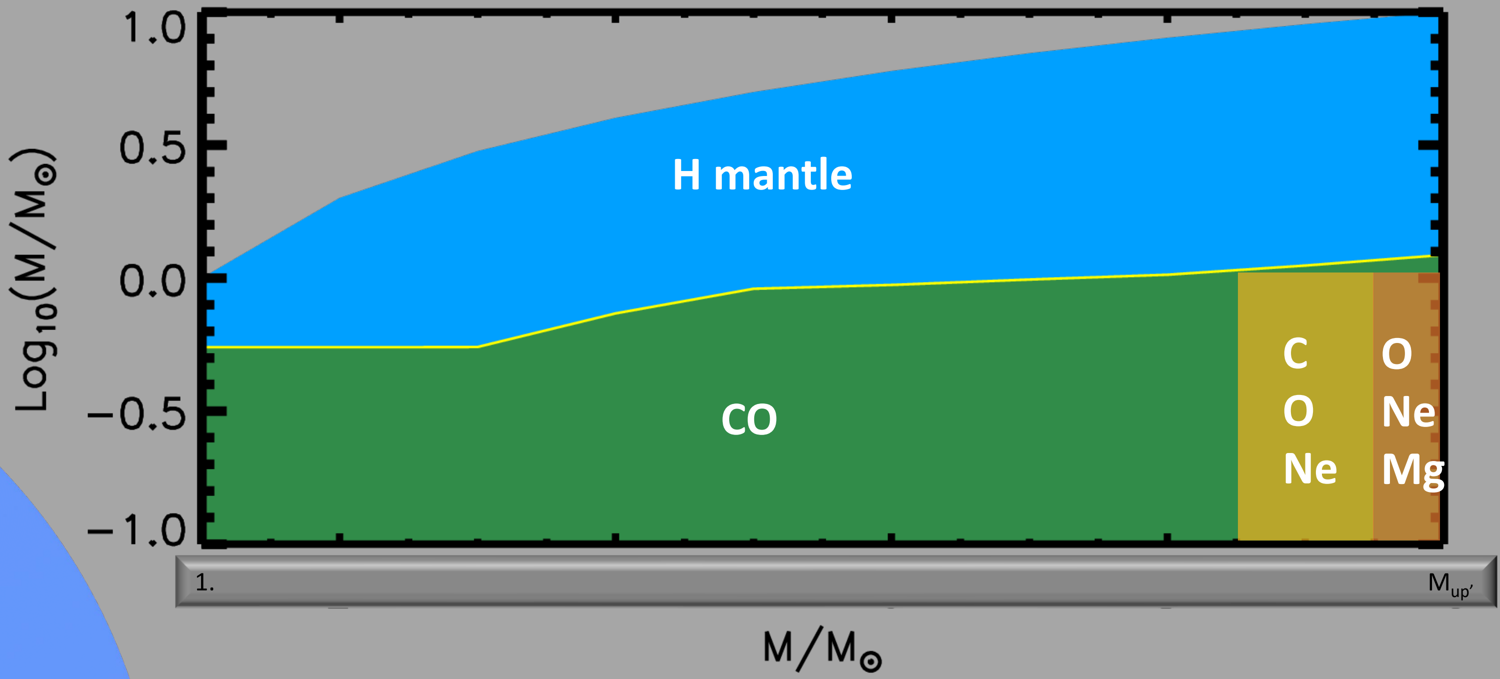

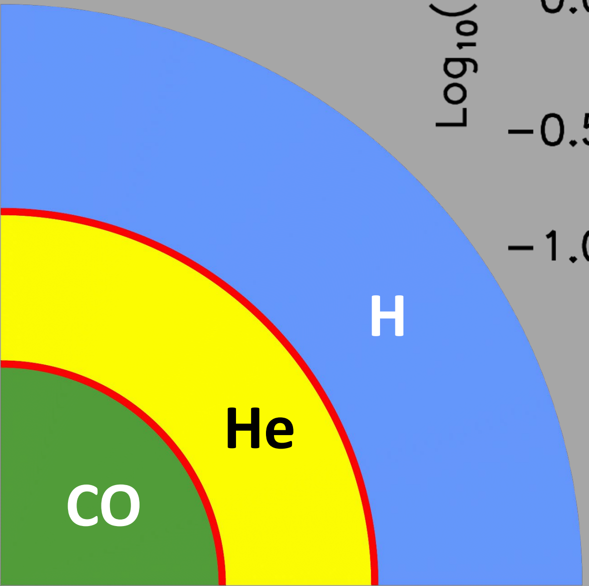

Scheme of a Thermal Pulse cycle

Q. Jl R. astr. Soc. (1970) 11, 12–22

Stellar Evolution in Globular Clusters

Martin Schwarzschild

(George Darwin Lecture delivered in Burlington House on 1969 October 10)

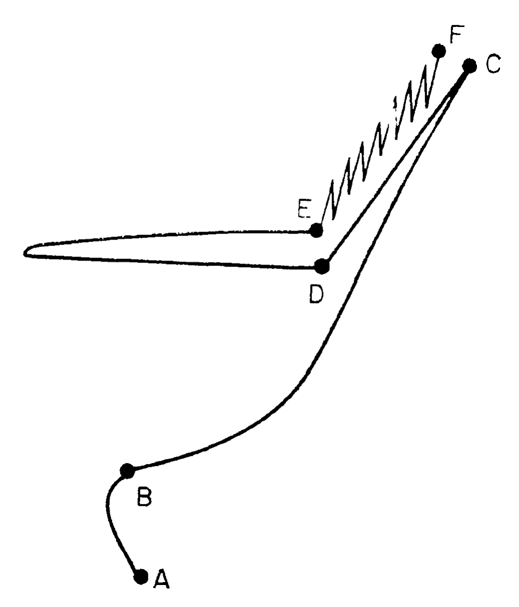

Finally, I come to my last major problem, namely the impasse in which we find ourselves in our attempt to follow the evolution of a globular-cluster star all the way through the second red-giant phase and beyond. Our present situation is simply that we are stuck just a little beyond point E in our figure. You may counter me with the question: What can be the problem; since clearly the numerical techniques are in hand to cover the second red-giant phase by computing through flash cycle after flash cycle in detail, why don't you compute if you cannot think? The answer to this question can be derived with a short bit of arithmetic. If we estimate the second red-giant phase to last for, say, several times 10^7 years, and if we accept that a typical flash cycle takes several times 10^5 years, then one has to conclude that a star may undergo of the order of 100 flash cycles to get through its second red-giant phase. Next, one has to compute several hundred fairly complex models if one wants to follow through one flash cycle with reasonable reliability. Finally, I think we all agree that the whole computation should be done for several stars to cover the relevant ranges in mass and composition. Thus the whole computing job we are contemplating turns out to be of such a magnitude that, in spite of the speed and capacity of modern computers, I know of no institution which could and would assign the necessary computer time to such an undertaking. No, I feel we are once again forced to try to think.

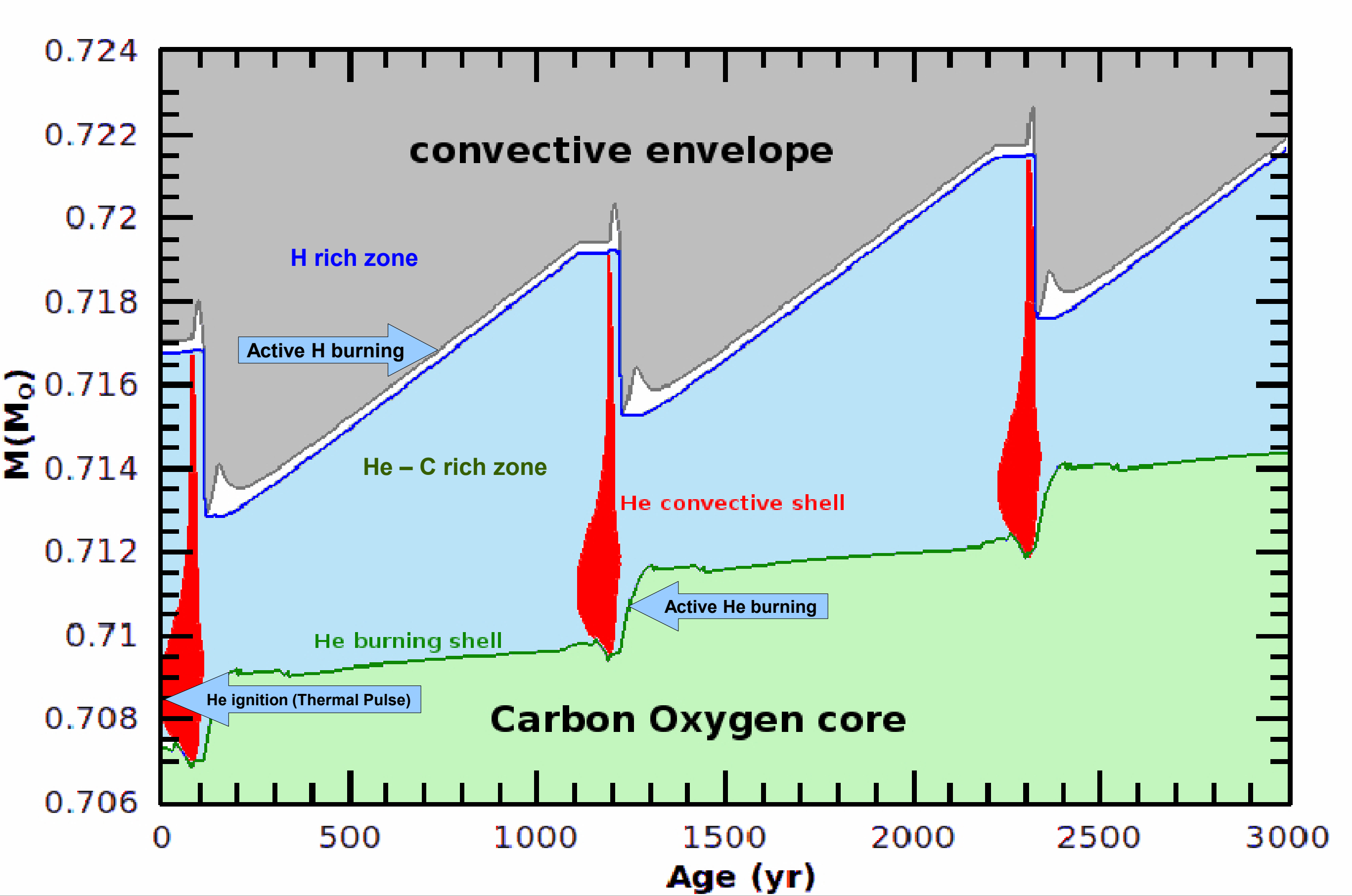

Lugaro&Chieffi, Astronomy with radioactivities, 2010, Chapter III

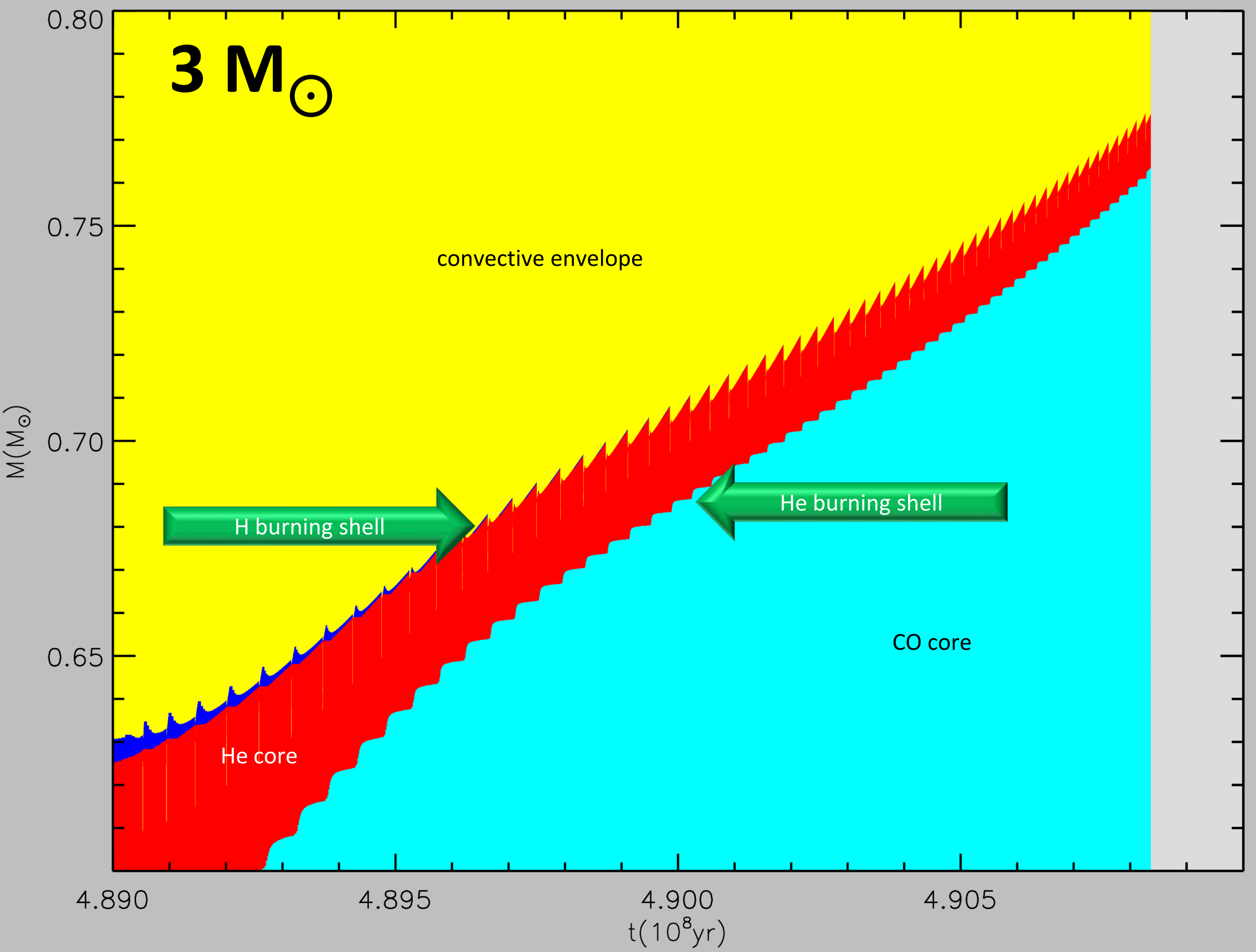

3 M⊙
convective envelope
H burning shell
He burning shell
He core
CO core
0.80
0.75
0.70
0.65
M(M⊙)
4.890
4.895
4.900
4.905
t(10^8 yr)

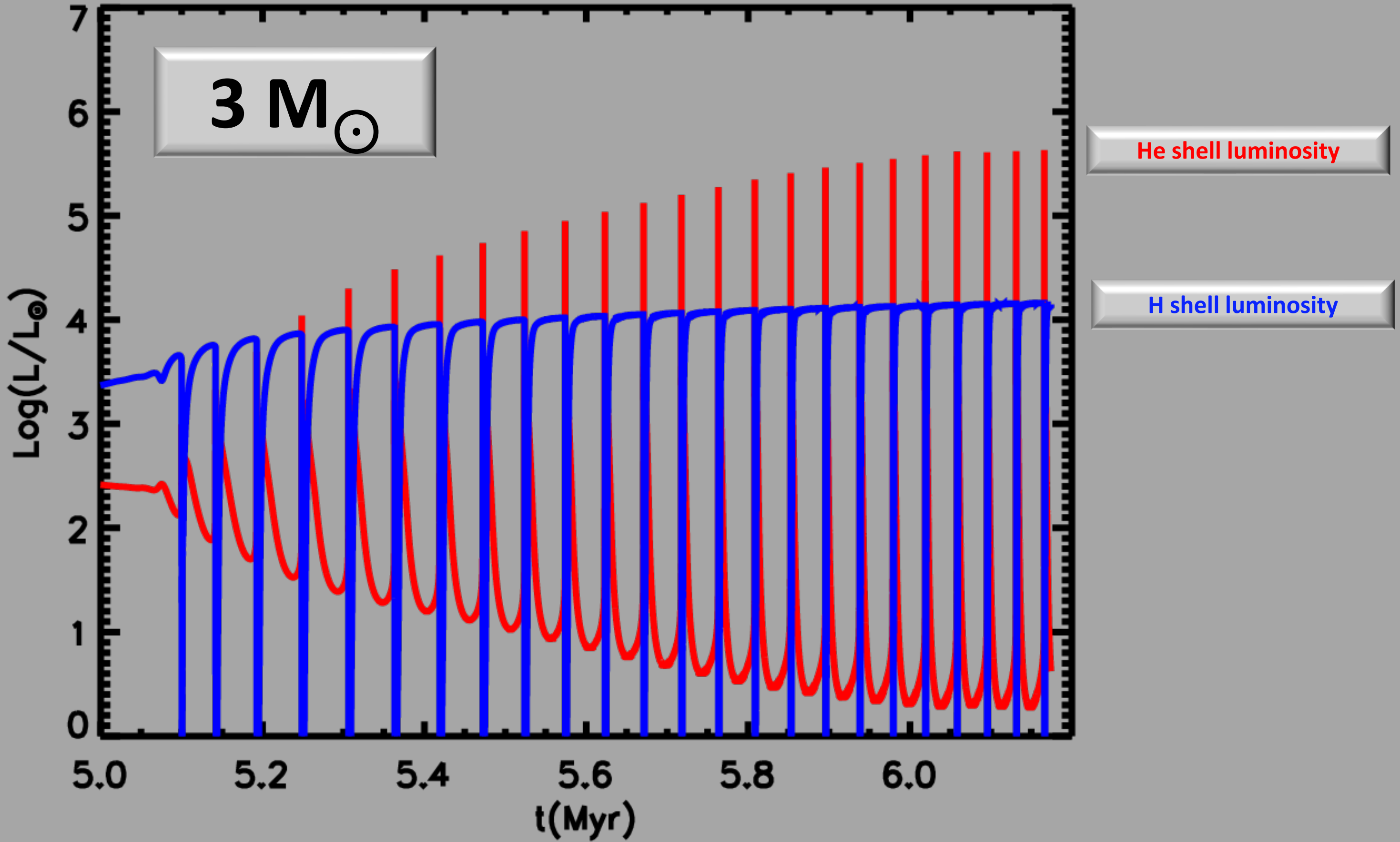

3 $M_\odot$
He shell luminosity
H shell luminosity
Log(L/L$_\odot$)
t(Myr)
0
1
2
3
4
5
6
7
5.0
5.2
5.4
5.6
5.8
6.0

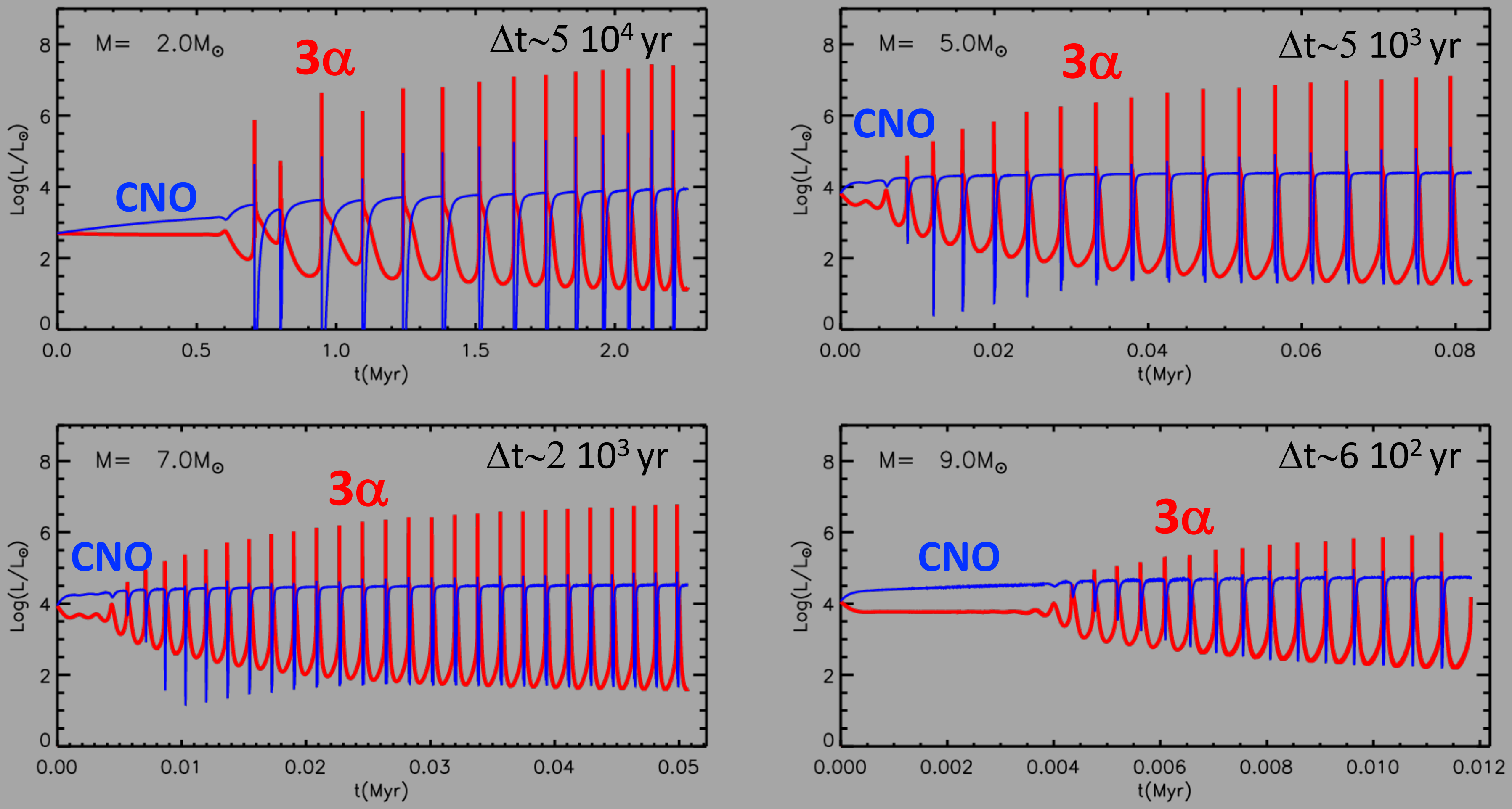

M= 2.0M⊙
Δt~5 10⁴ yr
3α
CNO
Log(L/L⊙)
t(Myr)
M= 5.0M⊙
Δt~5 10³ yr
3α
CNO
Log(L/L⊙)
t(Myr)
M= 7.0M⊙
Δt~2 10³ yr
3α
CNO
Log(L/L⊙)
t(Myr)
M= 9.0M⊙
Δt~6 10² yr
3α
CNO
Log(L/L⊙)
t(Myr)

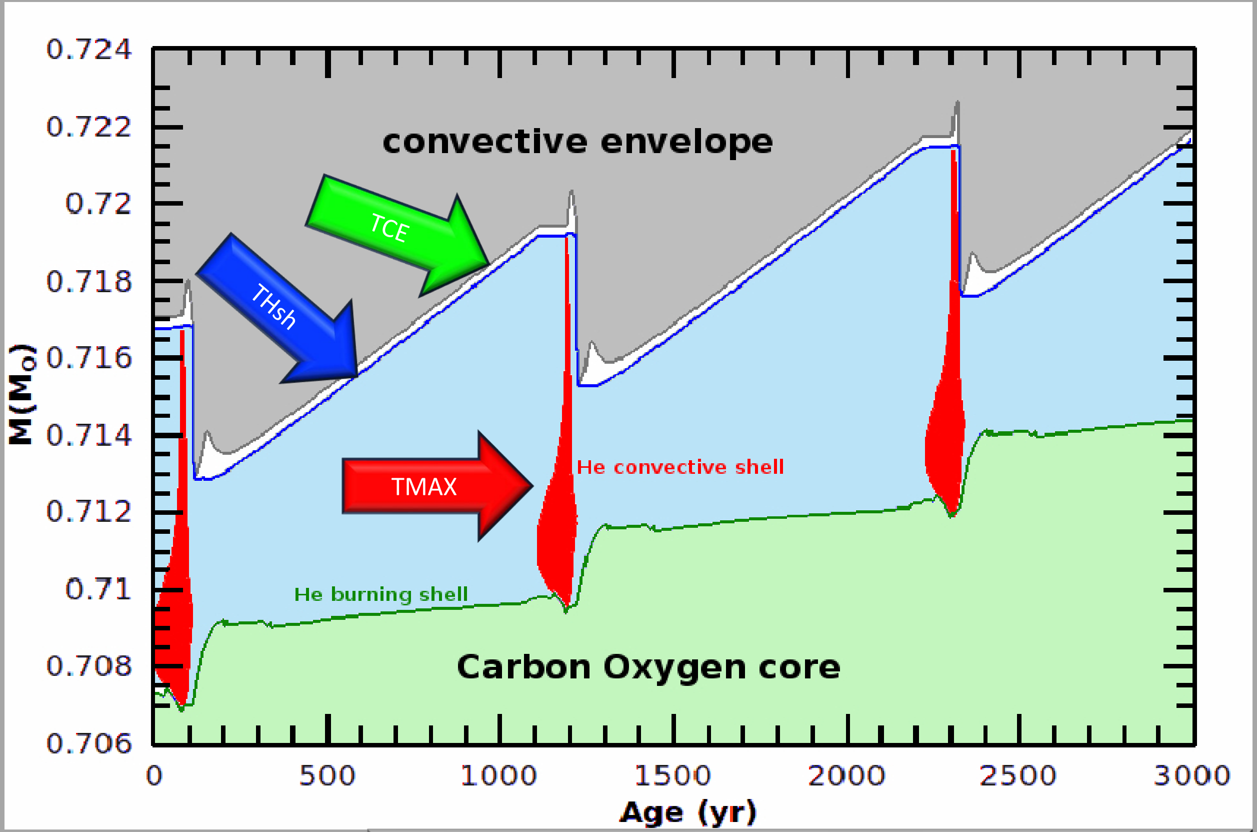

Lugaro&Chieffi, Astronomy with radioactivities, 2010, Chapter III

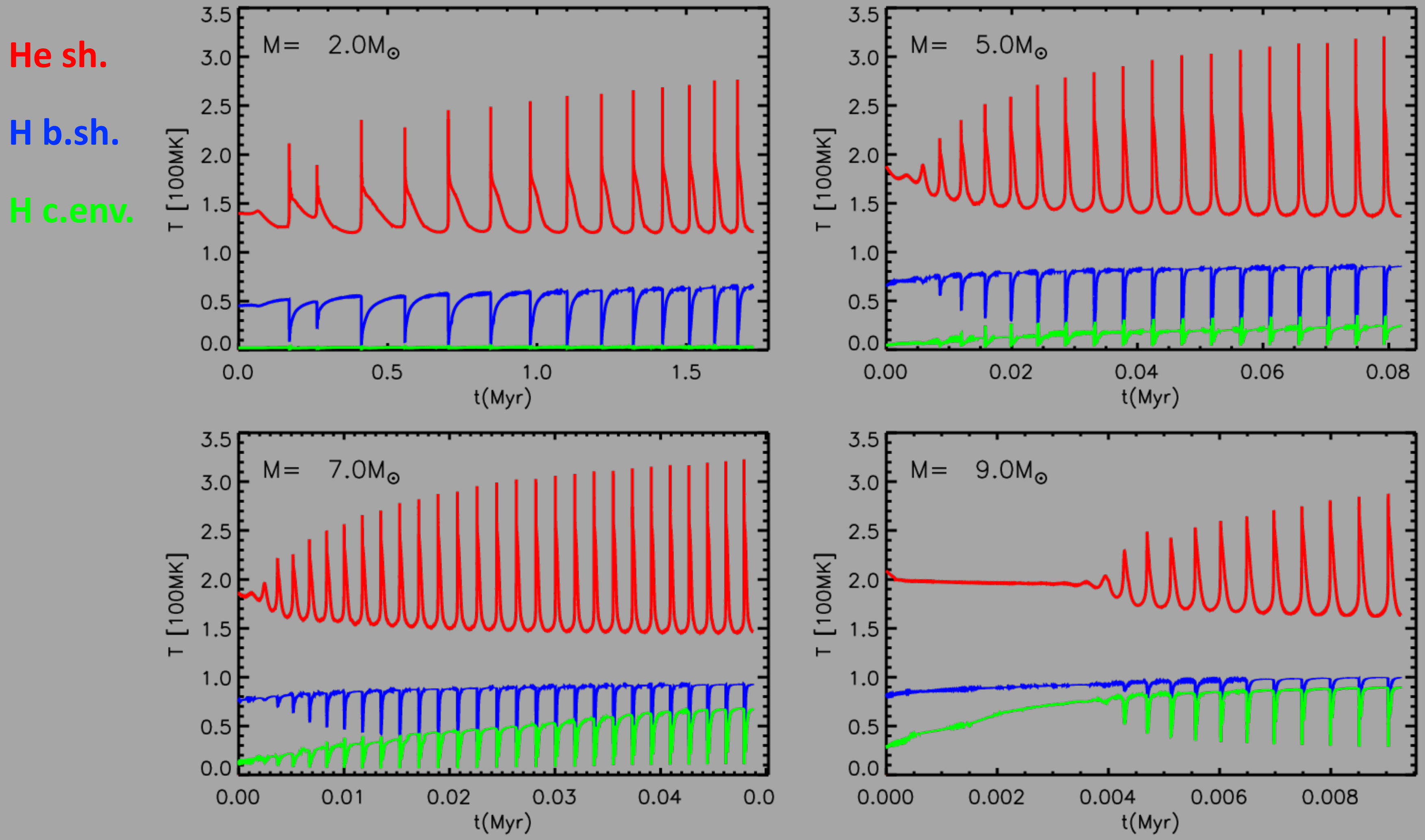

He sh.
H b.sh.
H c.env.
M= 2.0M$_\odot$
M= 5.0M$_\odot$
M= 7.0M$_\odot$
M= 9.0M$_\odot$
T [100MK]
t(Myr)

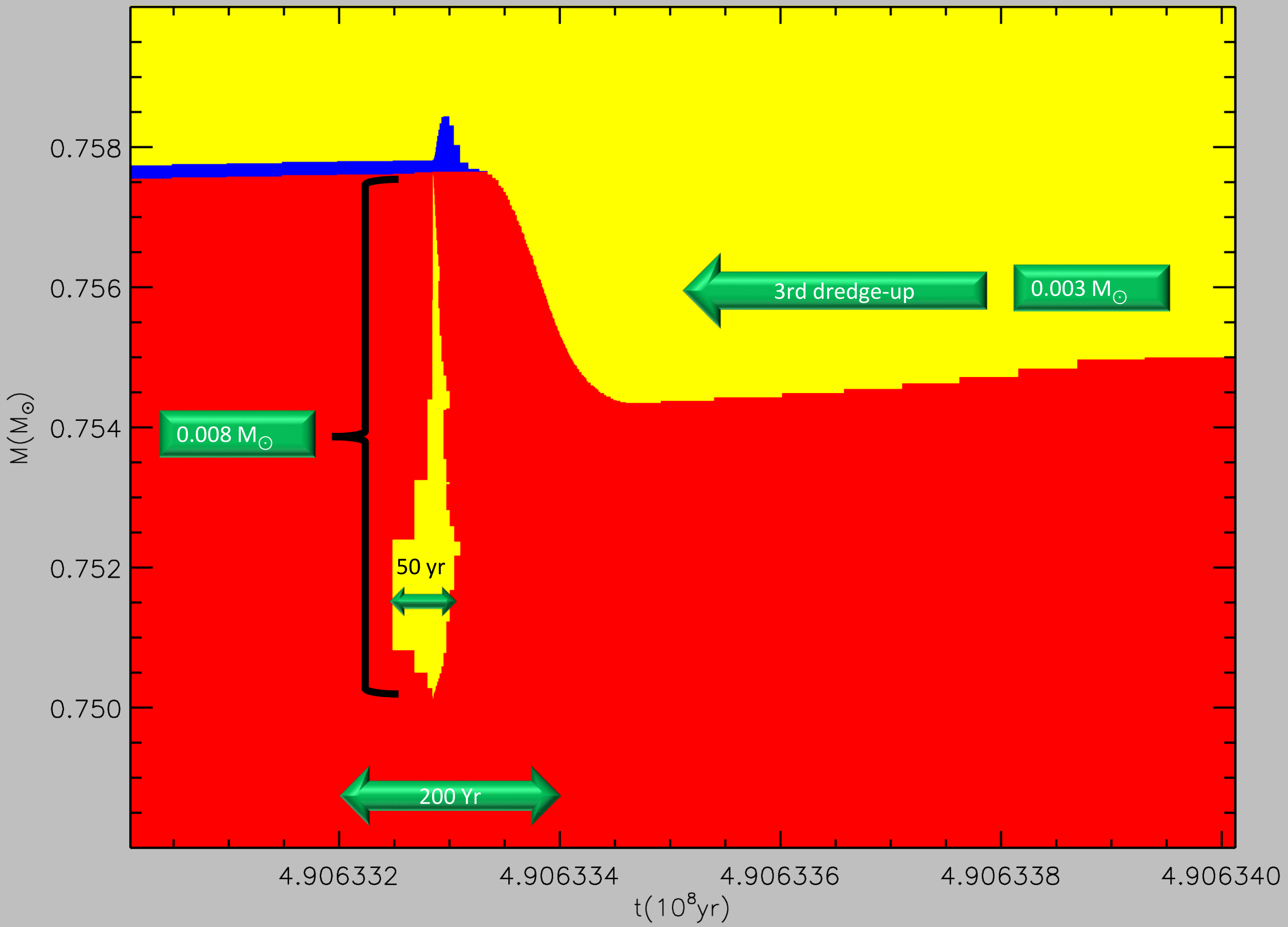
0.758
0.756
0.754
0.752
0.750
M(M⊙)
4.906332
4.906334
4.906336
4.906338
4.906340
t(10^8yr)
3rd dredge-up
0.003 M⊙
0.008 M⊙
50 yr
200 Yr

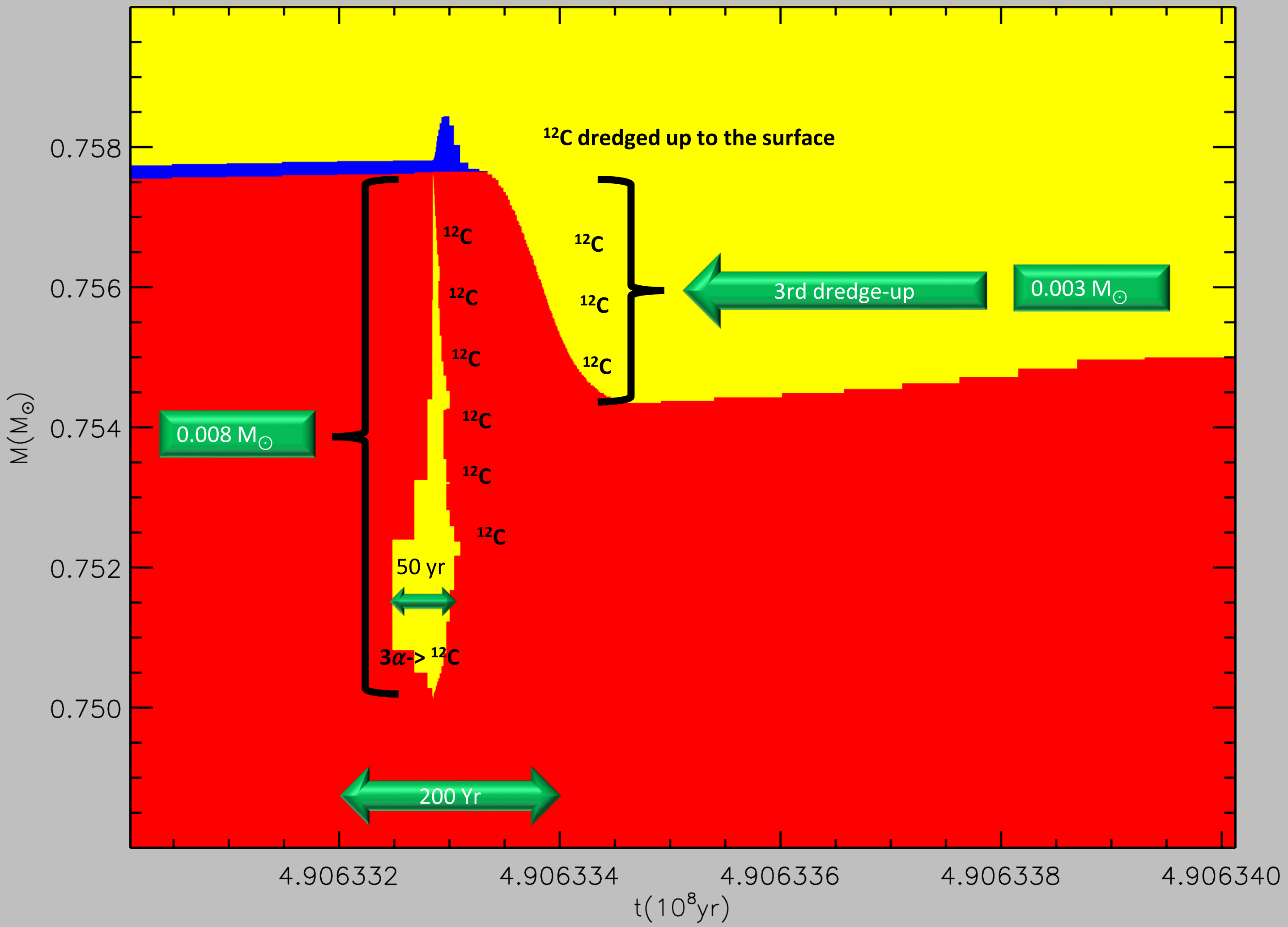

0.758
0.756
0.754
0.752
0.750
M(M⊙)
4.906332
4.906334
4.906336
4.906338
4.906340
t(10⁸yr)
¹²C dredged up to the surface
¹²C
3rd dredge-up
0.003 M⊙
0.008 M⊙
50 yr
3α-> ¹²C
200 Yr

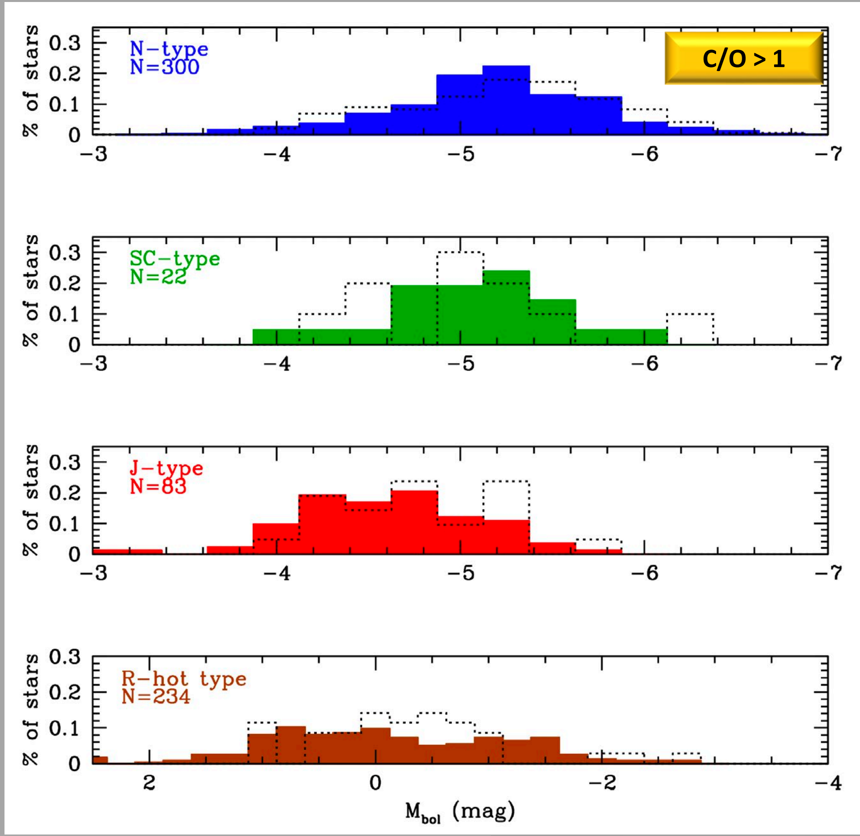

Abia+ 2022, AA 664,45

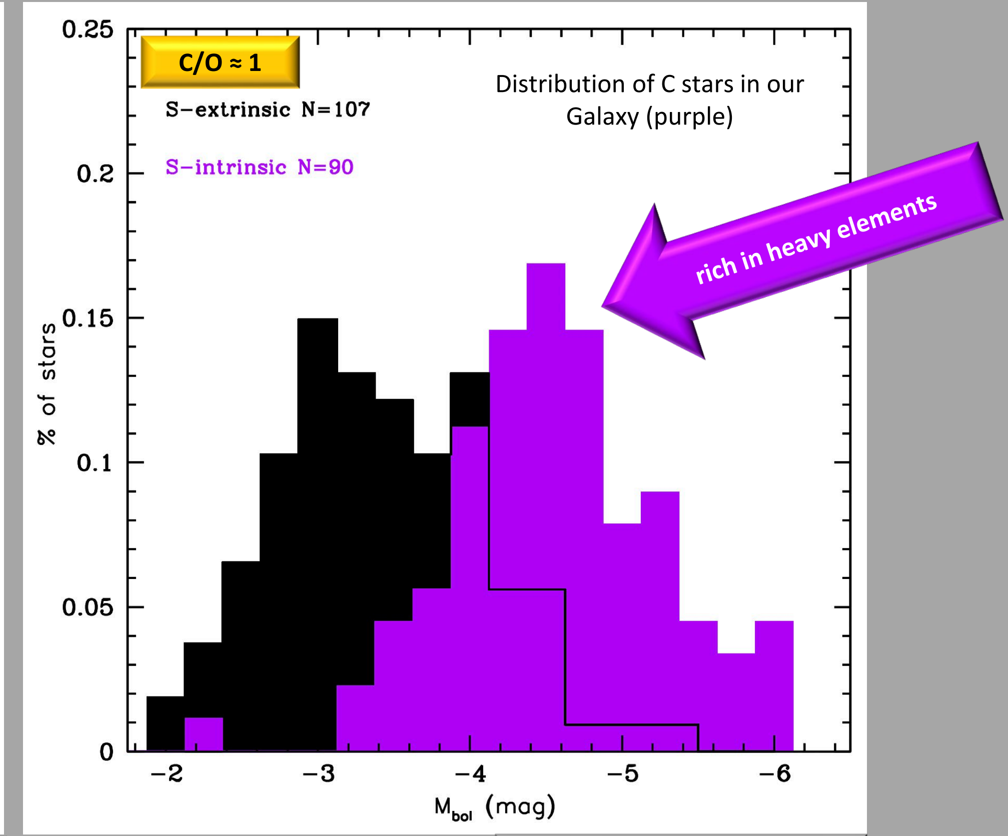

Abia+ 2022, AA 664,45

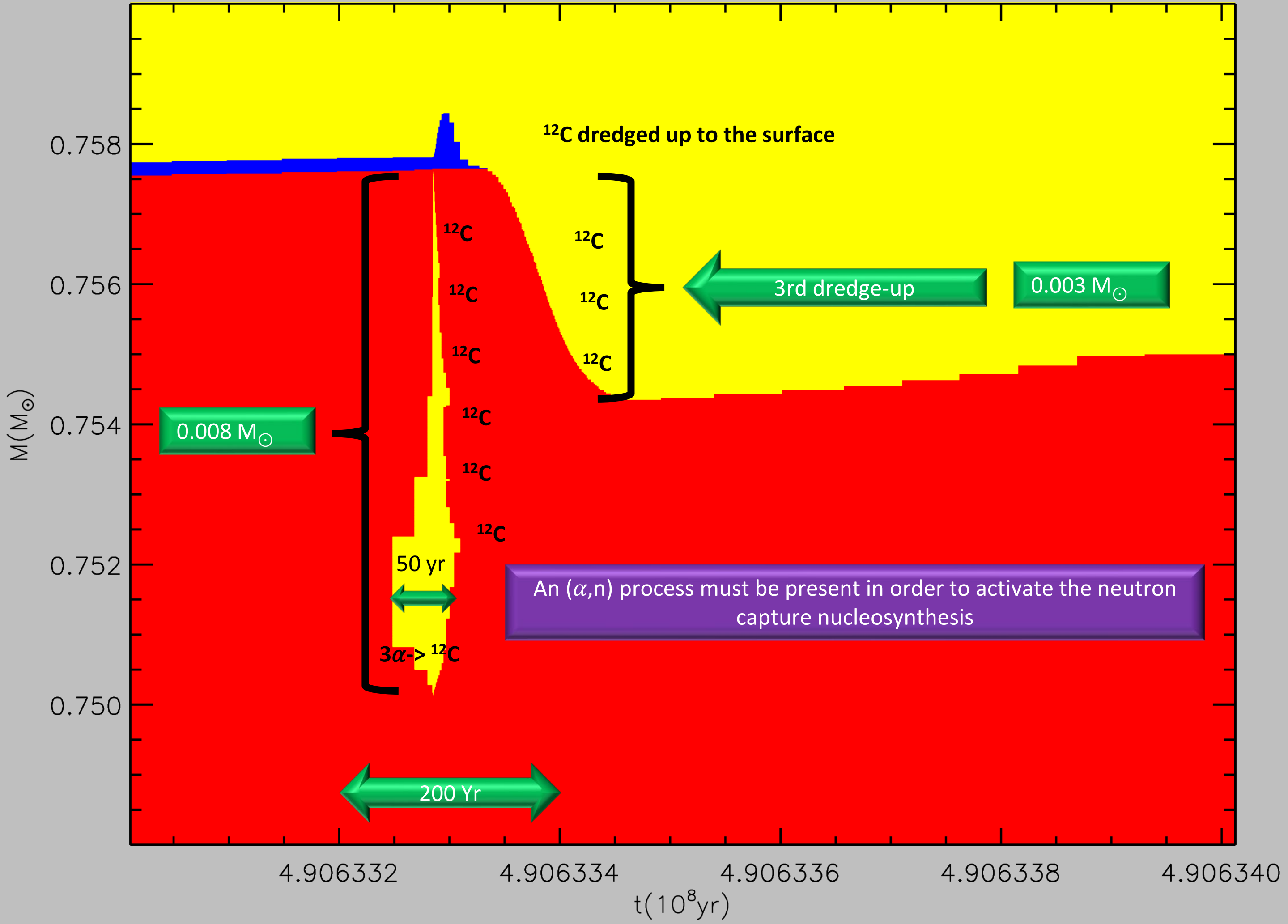

0.758
0.756
0.754
0.752
0.750
M(M☉)
4.906332
4.906334
4.906336
4.906338
4.906340
t(10^8yr)
12C dredged up to the surface
12C
3rd dredge-up
0.003 M☉
0.008 M☉
50 yr
3α-> 12C
An (α,n) process must be present in order to activate the neutron capture nucleosynthesis
200 Yr

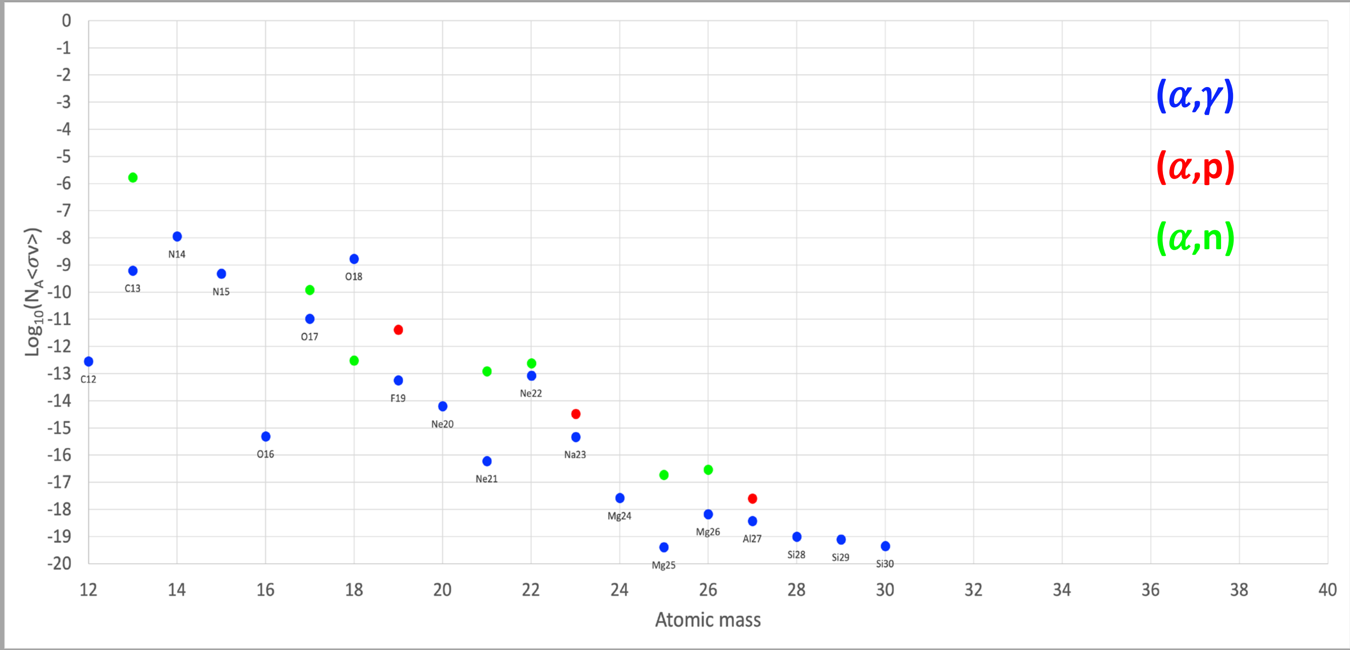

Log10(NA<σv>)
Atomic mass
(α,γ)
(α,p)
(α,n)
C12
C13
N14
N15
O16
O17
O18
F19
Ne20
Ne21
Ne22
Na23
Mg24
Mg25
Mg26
Al27
Si28
Si29
Si30

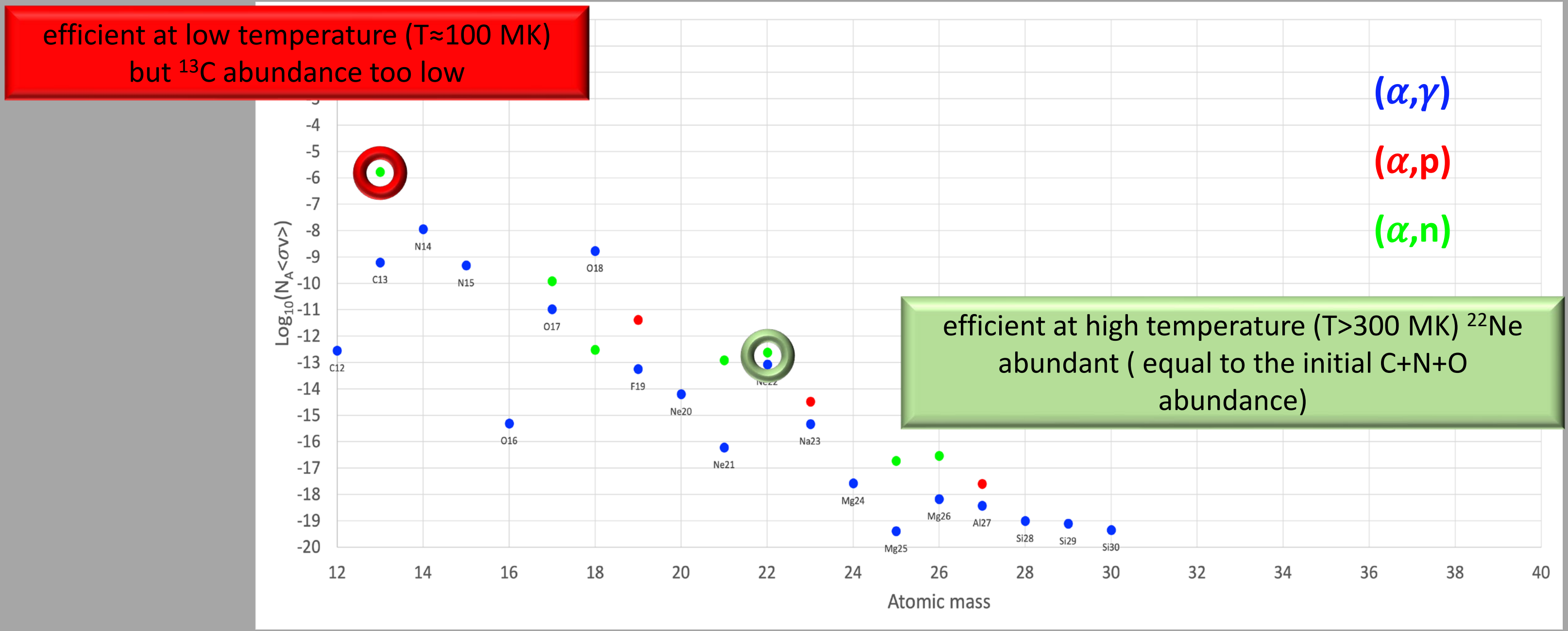

efficient at low temperature (T≈100 MK) but ¹³C abundance too low
efficient at high temperature (T>300 MK) ²²Ne abundant (equal to the initial C+N+O abundance)
(α,γ)
(α,p)
(α,n)
Log10(NA<σv>)
Atomic mass
C12
C13
N14
N15
O16
O17
O18
F19
Ne20
Ne21
Na23
Mg24
Mg25
Mg26
Al27
Si28
Si29
Si30

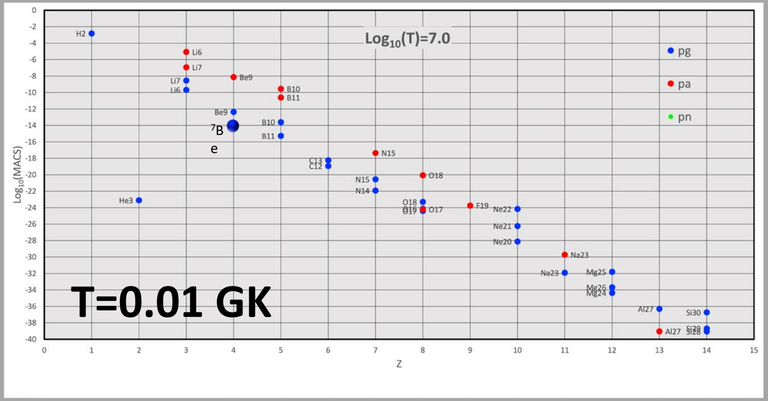

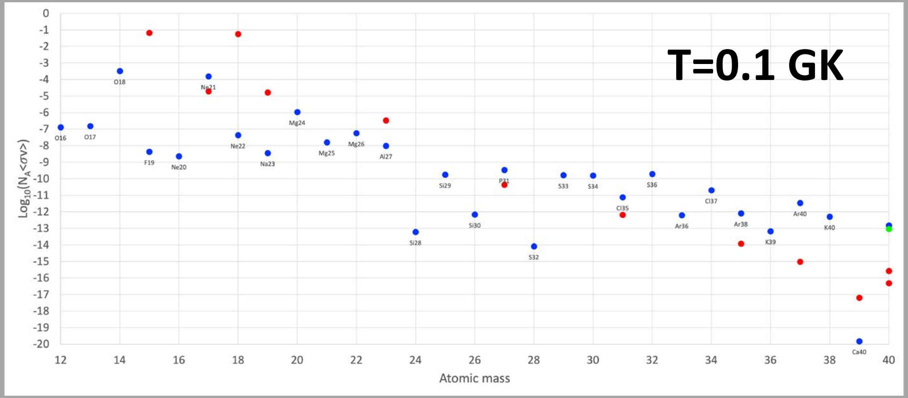

(p,γ)

(p,α)

(p,n)

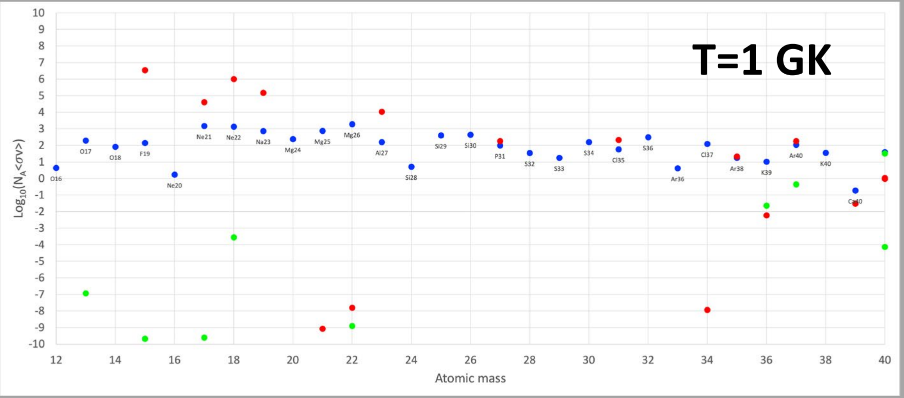

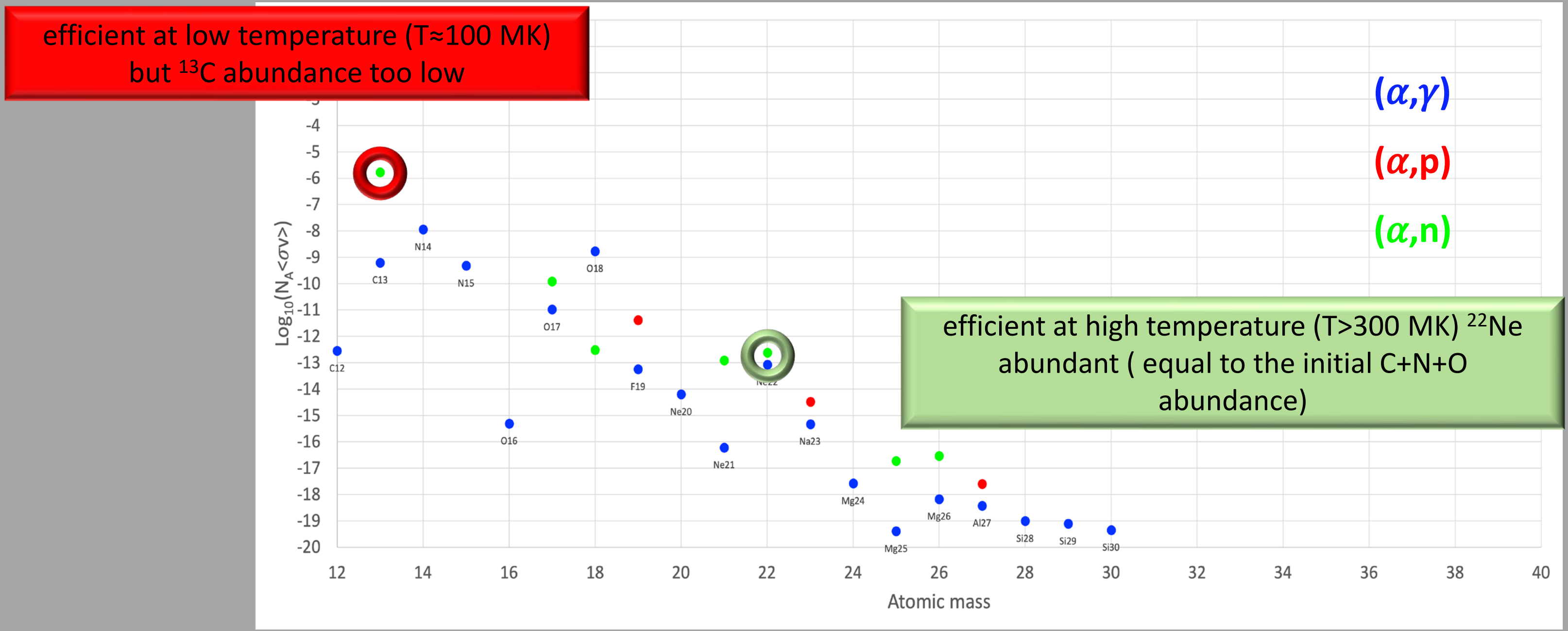

efficient at low temperature (T≈100 MK) but 13C abundance too low
(α,γ)
(α,p)
(α,n)
efficient at high temperature (T>300 MK) 22Ne abundant (equal to the initial C+N+O abundance)
C12
C13
N14
N15
O16
O17
O18
F19
Ne20
Ne21
Ne22
Na23
Mg24
Mg25
Mg26
Al27
Si28
Si29
Si30
Log10(NA<σv>)
Atomic mass
-4
-5
-6
-7
-8
-9
-10
-11
-12
-13
-14
-15
-16
-17
-18
-19
-20
12
14
16
18
20
22
24
26
28
30
32
34
36
38
40

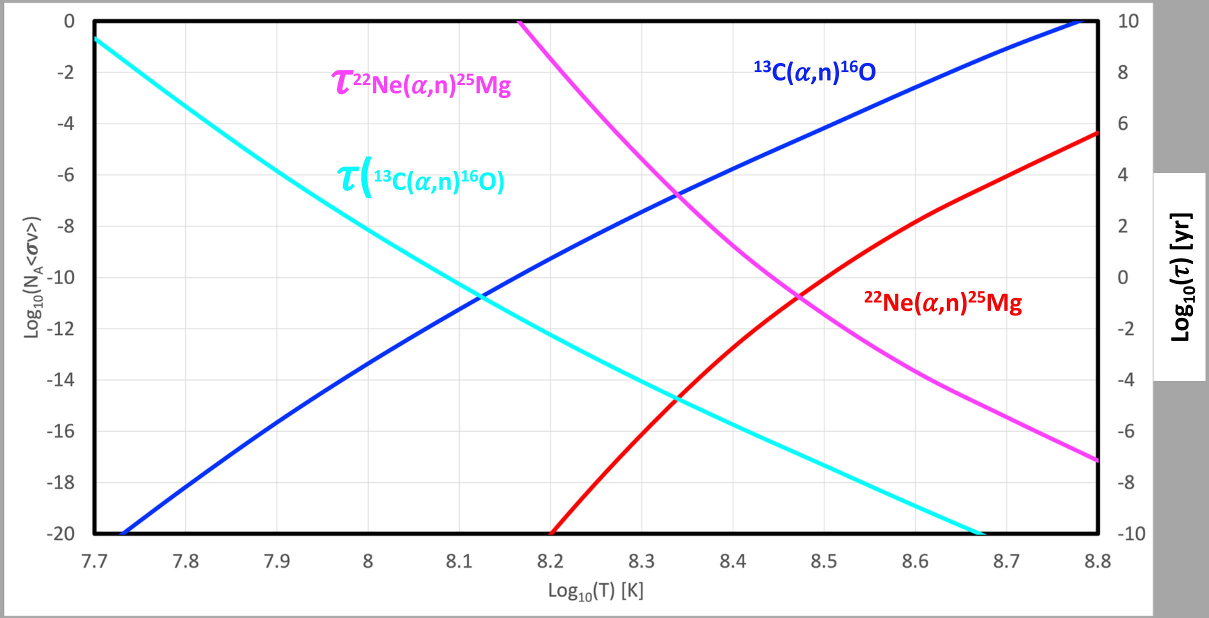

τ 22Ne(α,n)25Mg
13C(α,n)16O
τ(13C(α,n)16O)
22Ne(α,n)25Mg
Log10(NA<σv>)
Log10(τ) [yr]
Log10(T) [K]
0
-2
-4
-6
-8
-10
-12
-14
-16
-18
-20
10
8
6
4
2
0
-2
-4
-6
-8
-10
7.7
7.8
7.9
8
8.1
8.2
8.3
8.4
8.5
8.6
8.7
8.8

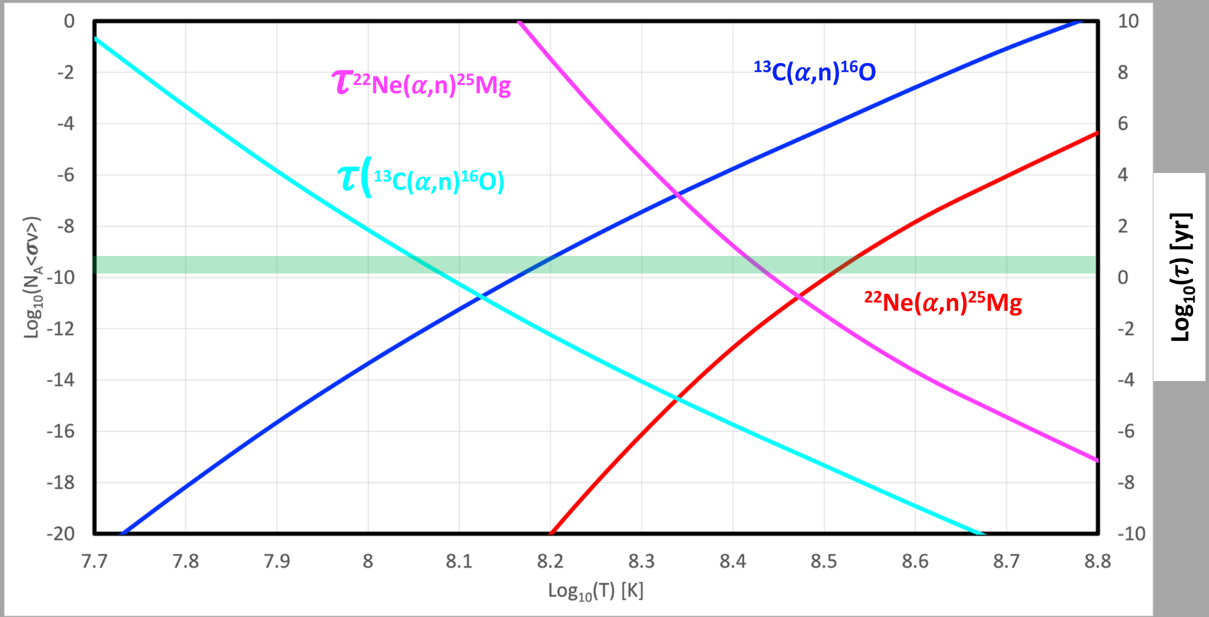

τ ^{22}Ne(α,n)^{25}Mg
^{13}C(α,n)^{16}O
τ(^{13}C(α,n)^{16}O)
^{22}Ne(α,n)^{25}Mg
Log$_{10}$(N$_A$<σv>)
Log$_{10}$(τ) [yr]
Log$_{10}$(T) [K]
0
-2
-4
-6
-8
-10
-12
-14
-16
-18
-20
10
8
6
4
2
0
-2
-4
-6
-8
-10
7.7
7.8
7.9
8
8.1
8.2
8.3
8.4
8.5
8.6
8.7
8.8

^{22}Ne is very abundant because it is the outcome of the initial CNO -> ^{14}N -> ^{22}Ne

$^{22}Ne(\alpha,n)^{25}Mg$ T > 300 MK $M>5M_\odot$

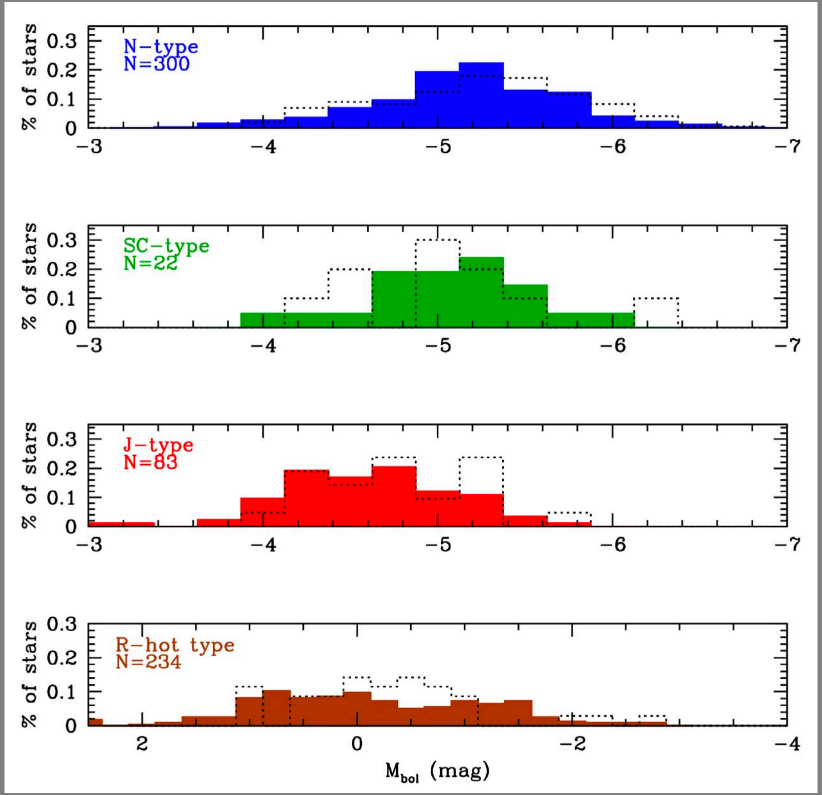

Abia+ 2022, AA 664,45

^{22}Ne is very abundant because it is the outcome of the initial CNO -> ^{14}N -> ^{22}Ne

$^{22}Ne(\alpha,n)^{25}Mg$ T > 300 MK M>5M$_\odot$

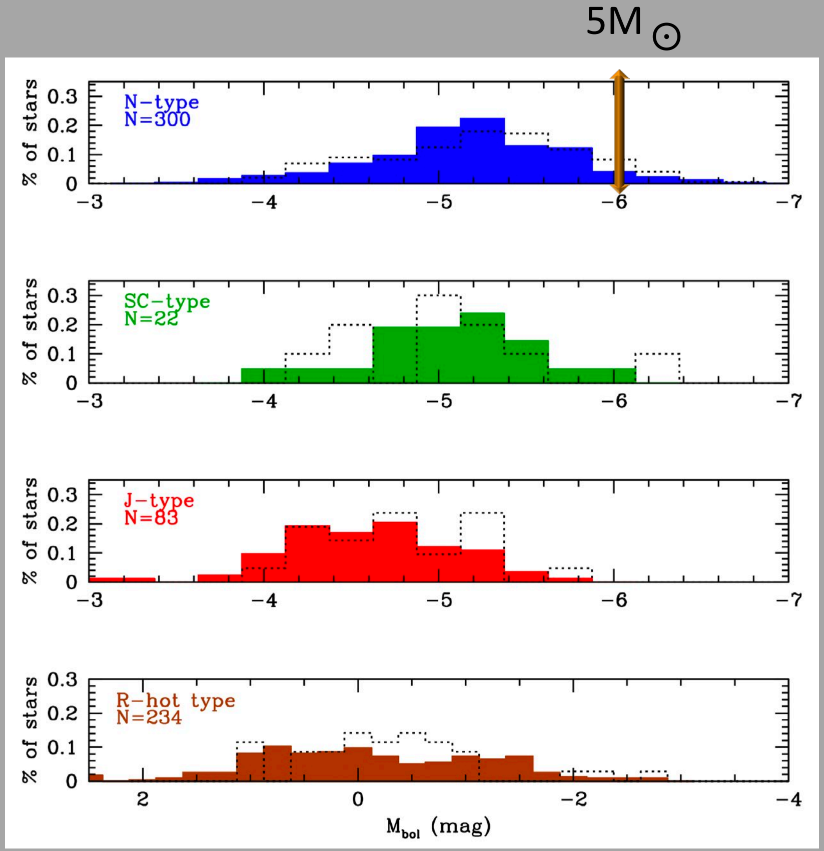

Abia+ 2022, AA 664,45

^{22}Ne is very abundant because it is the outcome of the initial CNO -> ^{14}N -> ^{22}Ne

$^{22}Ne(\alpha,n)^{25}Mg$ T > 300 MK M>5M$_{\odot}$

5M$_{\odot}$

Neutron density = 10^{10} [#/cm^3]

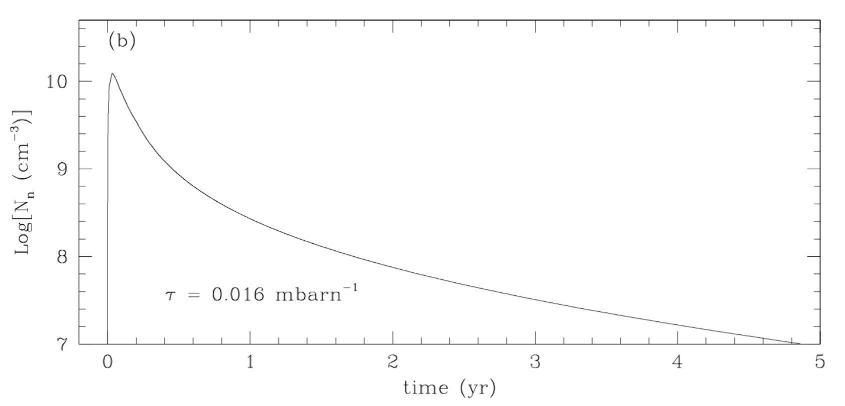

Lugaro&Chieffi, Astronomy with radioactivities, 2010, Chapter III

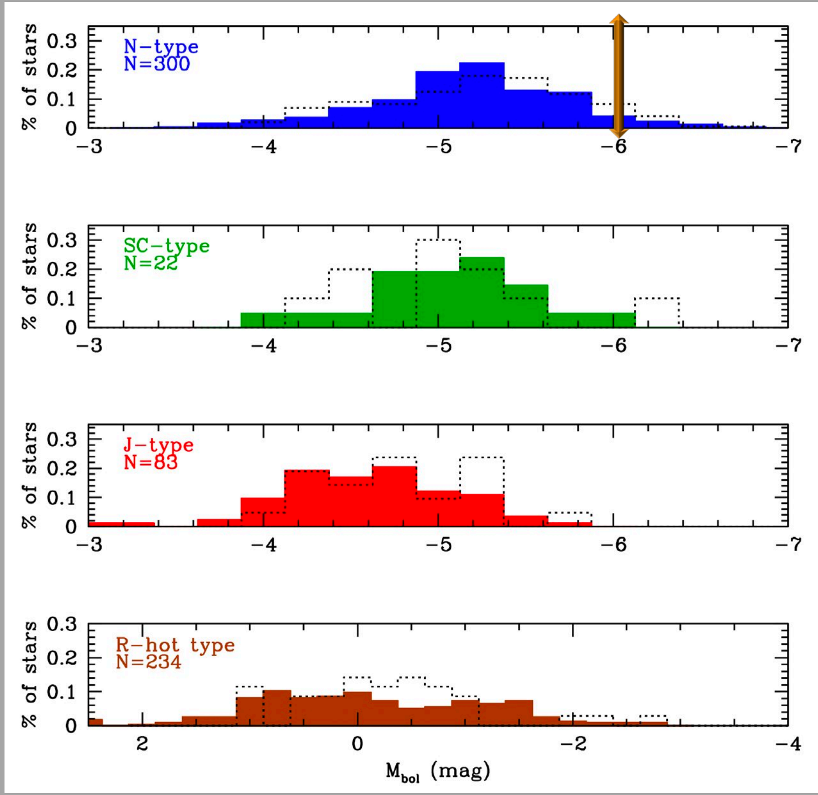

Abia+ 2022, AA 664,45

protons

83Nb 4.1 S ε: 100.00%	84Nb 9.5 S ε: 100.00% εp	85Nb 20.9 S ε: 100.00%	86Nb 56 S ε	87Nb 3.75 M ε: 100.00%	88Nb 14.55 M ε: 100.00%	89Nb 2.03 H ε: 100.00%	90Nb 14.60 H ε: 100.00%	91Nb 6.8E+2 Y ε: 100.00%	92Nb 3.47E+7 Y ε: 100.00% β- < 0.05%	93Nb STABLE 100%
82Zr 32 S ε: 100.00%	83Zr 41.6 S ε: 100.00% εp	84Zr 25.9 M ε: 100.00%	85Zr 7.86 M ε: 100.00%	86Zr 16.5 H ε: 100.00%	87Zr 1.68 H ε: 100.00%	88Zr 83.4 D ε: 100.00%	89Zr 78.41 H ε: 100.00%	90Zr STABLE 51.45%	91Zr STABLE 11.22%	92Zr STABLE 17.15%
81Y 70.4 S ε: 100.00%	82Y 8.30 S ε: 100.00%	83Y 7.08 M ε: 100.00%	84Y 4.6 S ε: 100.00%	85Y 2.68 H ε: 100.00%	86Y 14.74 H ε: 100.00%	87Y 79.8 H ε: 100.00%	88Y 106.626 D ε: 100.00%	89Y STABLE 100%	90Y 64.053 H β-: 100.00%	91Y 58.51 D β-: 100.00%
80Sr 106.3 M ε: 100.00%	81Sr 22.3 M ε: 100.00%	82Sr 25.55 D ε: 100.00%	83Sr 32.41 H ε: 100.00%	84Sr STABLE 0.56%	85Sr 64.84 D ε: 100.00%	86Sr STABLE 9.86%	87Sr STABLE 7.00%	88Sr STABLE 82.58%	89Sr 50.57 D β-: 100.00%	90Sr 28.90 Y β-: 100.00%
79Rb 22.9 M ε: 100.00%	80Rb 33.4 S ε: 100.00%	81Rb 4.570 H ε: 100.00%	82Rb 1.273 M ε: 100.00%	83Rb 86.2 D ε: 100.00%	84Rb 33.1 D ε: 96.20% β-: 3.80%	85Rb STABLE 72.17%	86Rb 18.642 D β-: 99.99% ε: 5.2E-3%	87Rb 4.81E+10 Y 27.83% β-: 100.00%	88Rb 17.773 M β-: 100.00%	89Rb 15.15 M β-: 100.00%
78Kr ≥2.3E+20 Y 0.35% 2ε	79Kr 35.04 H ε: 100.00%	80Kr STABLE 2.28%	81Kr 2.29E+5 Y ε: 100.00%	82Kr STABLE 11.58%	83Kr STABLE 11.49%	84Kr STABLE 57.00%	85Kr 3916.8 D β-: 100.00%	86Kr STABLE 17.30%	87Kr 76.3 M β-: 100.00%	88Kr 2.84 H β-: 100.00%
77Br 57.036 H ε: 100.00%	78Br 6.46 M ε ≥ 99.99% β- ≤ 0.01%	79Br STABLE 50.69%	80Br 17.68 M β-: 91.70% ε: 8.30%	81Br STABLE 49.31%	82Br 35.282 H β-: 100.00%	83Br 2.40 H β-: 100.00%	84Br 31.80 M β-: 100.00%	85Br 2.90 M β-: 100.00%	86Br 55.1 S β-: 100.00%	87Br 55.65 S β-: 100.00% β-n: 2.60%
76Se STABLE 9.37%	77Se STABLE 7.63%	78Se STABLE 23.77%	79Se 2.95E+5 Y β-: 100.00%	80Se STABLE 49.61% 2β-	81Se 18.45 M β-: 100.00%	82Se STABLE 8.73%	83Se 22.3 M β-: 100.00%	84Se 3.10 M β-: 100.00%	85Se 31.7 S β-: 100.00%	86Se 15.3 S β-: 100.00%
75As STABLE 100%	76As 1.0942 D β-: 100.00%	77As 38.83 H β-: 100.00%	78As 90.7 M β-: 100.00%	β-: 100.00%	β-: 100.00%	β- 00.00%	82As 19.1 S β-: 100.00%	N=50 β-: 100.00%	84As 3.24 S β-: 100.00% β-n: 0.28%	85As 2.021 S β-: 100.00% β-n: 59.40%

neutrons

83Nb 4.1 S ε: 100.00%	84Nb 9.5 S ε: 100.00% εp	85Nb 20.9 S ε: 100.00%	86Nb 56 S ε	87Nb 3.75 M ε: 100.00%	88Nb 14.55 M ε: 100.00%	89Nb 2.03 H ε: 100.00%	90Nb 14.60 H ε: 100.00%	91Nb 6.8E+2 Y ε: 100.00%	92Nb 3.47E+7 Y ε: 100.00% β- < 0.05%	93Nb STABLE 100%
82Zr 32 S ε: 100.00%	83Zr 41.6 S	84Zr 25.9 M	85Zr 7.86 M	86Zr 16.5 H ε: 100.00%	87Zr 1.68 H ε: 100.00%	88Zr 83.4 D ε: 100.00%	89Zr 78.41 H ε: 100.00%	90Zr STABLE 51.45%	91Zr STABLE 11.22%	92Zr STABLE 17.15%
[illegible]	[illegible]	[illegible]	[illegible]	[illegible]	86Y 14.74 H ε: 100.00%	87Y 79.8 H ε: 100.00%	88Y 106.626 D ε: 100.00%	89Y STABLE 100%	90Y 64.053 H β-: 100.00%	91Y 58.51 D β-: 100.00%
80Sr 106.3 M ε: 100.00%	81Sr 22.3 M ε: 100.00%	82Sr 25.55 D ε: 100.00%	83Sr 32.41 H ε: 100.00%	84Sr STABLE 0.56%	85Sr 64.84 D ε: 100.00%	86Sr STABLE 9.86%	87Sr STABLE 7.00%	88Sr STABLE 82.58%	89Sr 50.57 D β-: 100.00%	90Sr 28.90 Y β-: 100.00%
79Rb 22.9 M ε: 100.00%	80Rb 33.4 S ε: 100.00%	81Rb 4.570 H ε: 100.00%	82Rb 1.273 M ε: 100.00%	83Rb 86.2 D ε: 100.00%	84Rb 33.1 D ε: 96.20% β-: 3.80%	85Rb STABLE 72.17%	86Rb 18.642 D ε: 5.2E-3%	87Rb 4.81E+10 Y 27.83% β-: 100.00%	88Rb 17.773 M β-: 100.00%	89Rb 15.15 M β-: 100.00%
78Kr ≥2.3E+20 Y 0.35% 2ε	79Kr 35.04 H ε: 100.00%	80Kr STABLE 2.28%	81Kr 2.29E+5 Y ε: 100.00%	82Kr STABLE 11.58%	83Kr STABLE 11.49%	84Kr STABLE 57.00%	85Kr 3916.8 D	86Kr STABLE 17.30%	87Kr 76.3 M β-: 100.00%	88Kr 2.84 H β-: 100.00%
77Br 57.036 H ε: 100.00%	78Br 6.46 M ε ≥ 99.99% β- ≤ 0.01%	79Br STABLE 50.69%	80Br 17.68 M β-: 91.70% ε: 8.30%	81Br STABLE 49.31%	82Br 35.282 H β-: 100.00%	83Br	84Br	85Br	86Br 55.1 S β-: 100.00%	87Br 55.65 S β-: 100.00% β-n: 2.60%
76Se STABLE 9.37%	77Se STABLE 7.63%	78Se STABLE 23.77%	79Se 2.95E+5 Y β-: 100.00%	80Se STABLE 49.61% 2β-	81Se 18.45 M β-: 100.00%	82Se STABLE 8.73%	83Se 22.3 M β-: 100.00%	84Se 3.10 M β-: 100.00%	85Se 31.7 S β-: 100.00%	86Se 15.3 S β-: 100.00%
75As STABLE 100%	76As 1.0942 D β-: 100.00%	77As 38.83 H β-: 100.00%	78As 90.7 M β-: 100.00%	β-: 100.00%	β-: 100.00%	[illegible]	82As 19.1 S β-: 100.00%	β-: 100.00%	84As 3.24 S β-: 100.00% β-n: 0.28%	85As 2.021 S β-: 100.00% β-n: 59.40%

$$N_n \cdot < N_A \sigma v >_{in} = \frac{N_A}{\tau_i}$$

$$N_n = \frac{N_A}{< N_A \sigma v >_{in} \cdot \tau_i} \quad [\# \ cm^{-3}]$$

$N_n = 10^{10}$

$N_n = 2.2 \ 10^{8}$

Branching point

N=50

protons

neutrons


300 MK
$N_n \cdot \langle N_A \sigma v \rangle_{in} = \frac{N_A}{\tau_i}$
$N_n = \frac{N_A}{\langle N_A \sigma v \rangle_{in} \cdot \tau_i}$ [# cm^{-3}]
protons
neutrons
Branching point
N=50
Rb / Y
83Nb 4.1 S ε: 100.00%
84Nb 9.5 S ε: 100.00% εp
85Nb 20.9 S ε: 100.00%
86Nb 56 S ε
87Nb 3.75 M ε: 100.00%
88Nb
89Nb
90Nb 14.60 H ε: 100.00%
91Nb 6.8E+2 Y ε: 100.00%
92Nb 3.47E+7 Y ε: 100.00% β- < 0.05%
93Nb STABLE 100% 7.7
82Zr 32 S ε: 100.00%
86Zr 16.5 H ε: 100.00%
87Zr 1.68 H ε: 100.00%
88Zr 83.4 D ε: 100.00%
89Zr 78.41 H ε: 100.00%
90Zr STABLE 51.45% 6.4
91Zr STABLE 11.22% 7.1
92Zr STABLE 17.15% 6.8
86Y 14.74 H ε: 100.00%
87Y 79.8 H ε: 100.00%
88Y 106.626 D ε: 100.00%
89Y STABLE 100% 6.6
90Y 64.053 H β-: 100.00%
91Y 58.51 D β-: 100.00%
80Sr 106.3 M ε: 100.00%
81Sr 22.3 M ε: 100.00%
82Sr 25.55 D ε: 100.00%
83Sr 32.41 H ε: 100.00%
84Sr STABLE 0.56%
85Sr 64.84 D ε: 100.00%
86Sr STABLE 9.86% 7.1
87Sr STABLE 7.00% 7.3
88Sr STABLE 82.58% 5.9
89Sr 50.57 D β-: 100.00%
90Sr 28.90 Y β-: 100.00%
79Rb 22.9 M ε: 100.00%
80Rb 33.4 S ε: 100.00%
81Rb 4.570 H ε: 100.00%
82Rb 1.273 M ε: 100.00%
83Rb 86.2 D ε: 100.00%
84Rb 33.1 D ε: 96.20% β-: 3.80%
85Rb STABLE 72.17% 7.6
86Rb 18.642 D 7.5
87Rb 27.83% 6.3
88Rb 17.773 M β-: 100.00%
89Rb 15.15 M β-: 100.00%
78Kr ≥2.3E+20 Y 0.35% 2ε
79Kr 35.04 H ε: 100.00%
80Kr STABLE 2.28%
81Kr 2.29E+5 Y ε: 100.00%
82Kr STABLE 11.58% 7.0
83Kr STABLE 11.49% 7.7
84Kr STABLE 57.00% 6.8
85Kr 3916.8 D 6.9
86Kr STABLE 17.30% 5.3
87Kr 76.3 M β-: 100.00%
88Kr 2.84 H β-: 100.00%
77Br 57.036 H ε: 100.00%
78Br 6.46 M ε ≥ 99.99% β- ≤ 0.01%
79Br STABLE 50.69%
80Br 17.68 M β-: 91.70% ε: 8.30%
81Br STABLE 49.31% 7.6
82Br 35.282 H β-: 100.00%
83Br
84Br
85Br
86Br 55.1 S β-: 100.00%
87Br 55.65 S β-: 100.00% β-n: 2.60%
76Se STABLE 9.37%
77Se STABLE 7.63%
78Se STABLE 23.77%
79Se 2.95E+5 Y β-: 100.00%
80Se STABLE 49.61% 2β-
81Se 18.45 M β-: 100.00%
82Se STABLE 8.73%
83Se 22.3 M β-: 100.00%
84Se 3.10 M β-: 100.00%
85Se 31.7 S β-: 100.00%
86Se 15.3 S β-: 100.00%
75As STABLE 100%
76As 1.0942 D β-: 100.00%
77As 38.83 H β-: 100.00%
82As 19.1 S β-: 100.00%
84As 3.24 S β-: 100.00% β-n: 0.28%
85As 2.021 S β-: 100.00% β-n: 59.40%

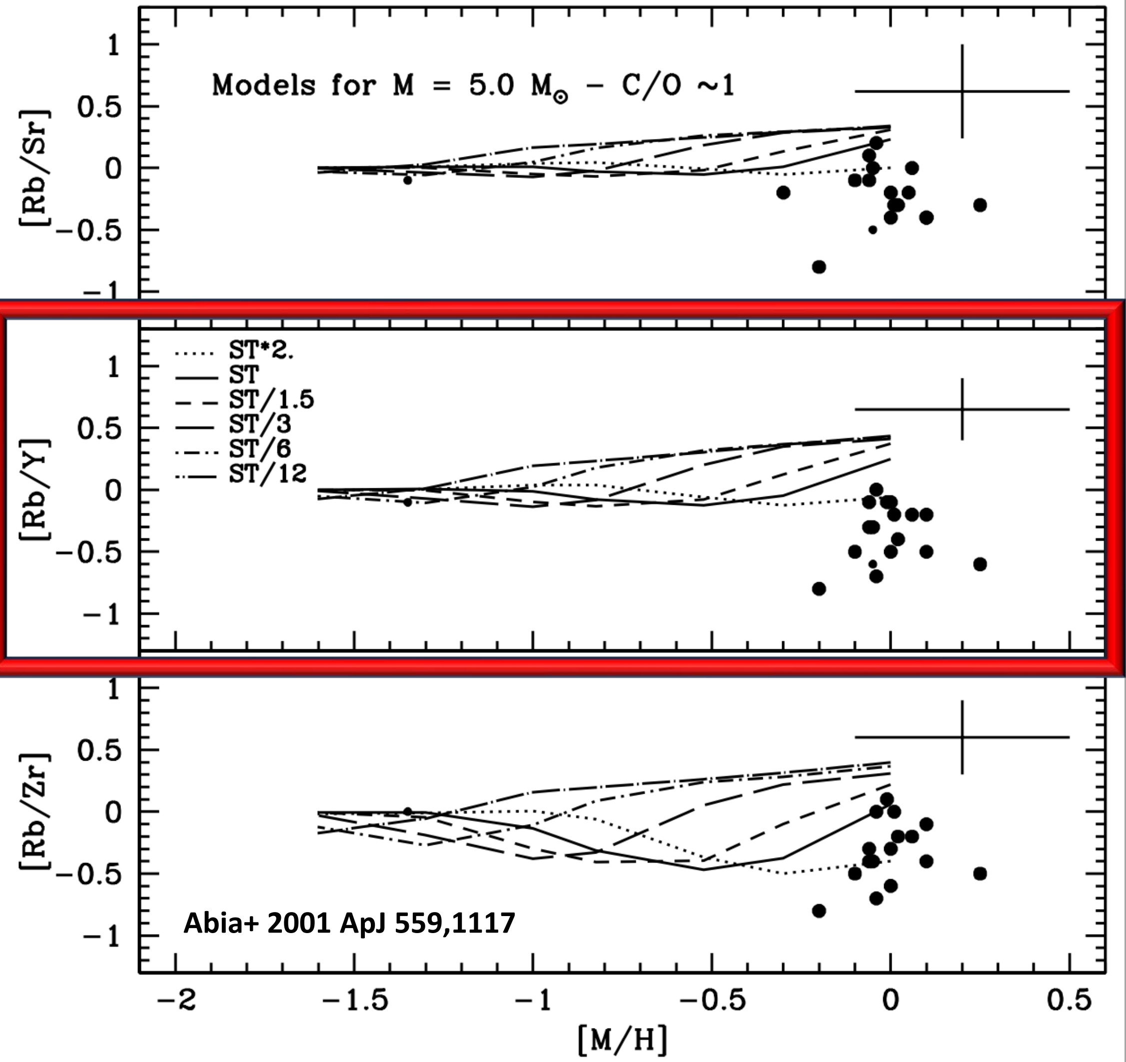
Models for M = 5.0 M☉ – C/O ~1
[Rb/Sr]
[Rb/Y]
[Rb/Zr]
[M/H]
ST*2.
ST
ST/1.5
ST/3
ST/6
ST/12
Abia+ 2001 ApJ 559,1117
1
0.5
0
−0.5
−1
−2
−1.5
−1
−0.5
0
0.5

^{22}Ne is very abundant because it is the outcome of the initial CNO -> ^{14}N -> ^{22}Ne

$^{22}Ne(\alpha,n)^{25}Mg$ T > 300 MK M>5M$_\odot$

Neutron density = 10^{10} [#/cm^3]

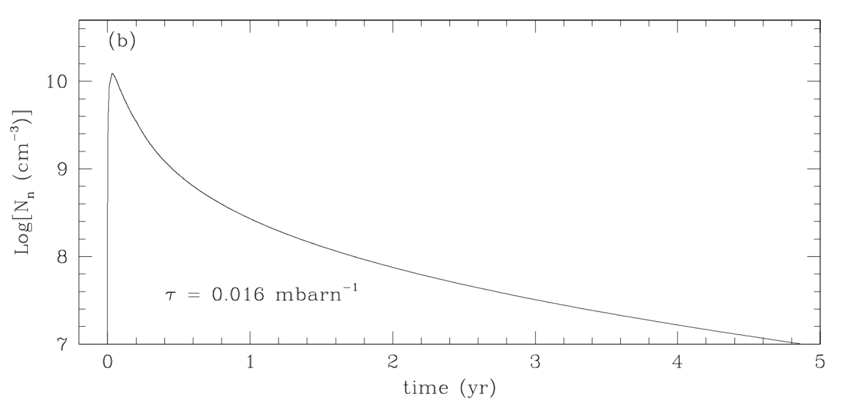

Lugaro&Chieffi, Astronomy with radioactivities, 2010, Chapter III

5M$_\odot$

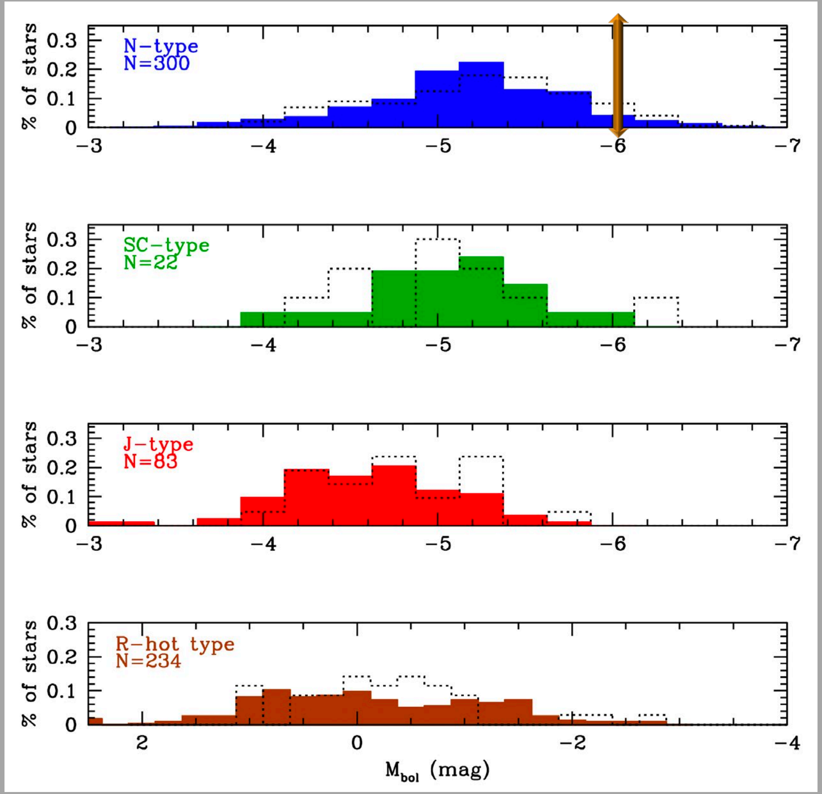

Abia+ 2022, AA 664,45

^{13}C NOT abundant because it is just the equilibrium value of the CNO cycle

$^{13}C(\alpha,n)^{16}O$ T > 90 MK $1.5<M/M_{\odot}<4$

Neutron density = 10^7 [#/cm^3]

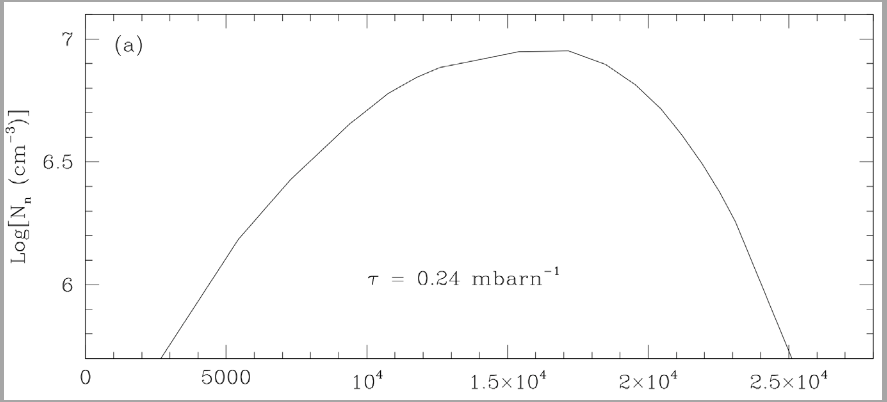

Lugaro&Chieffi, Astronomy with radioactivities, 2010, Chapter III

2M☉ 3M☉ 4M☉

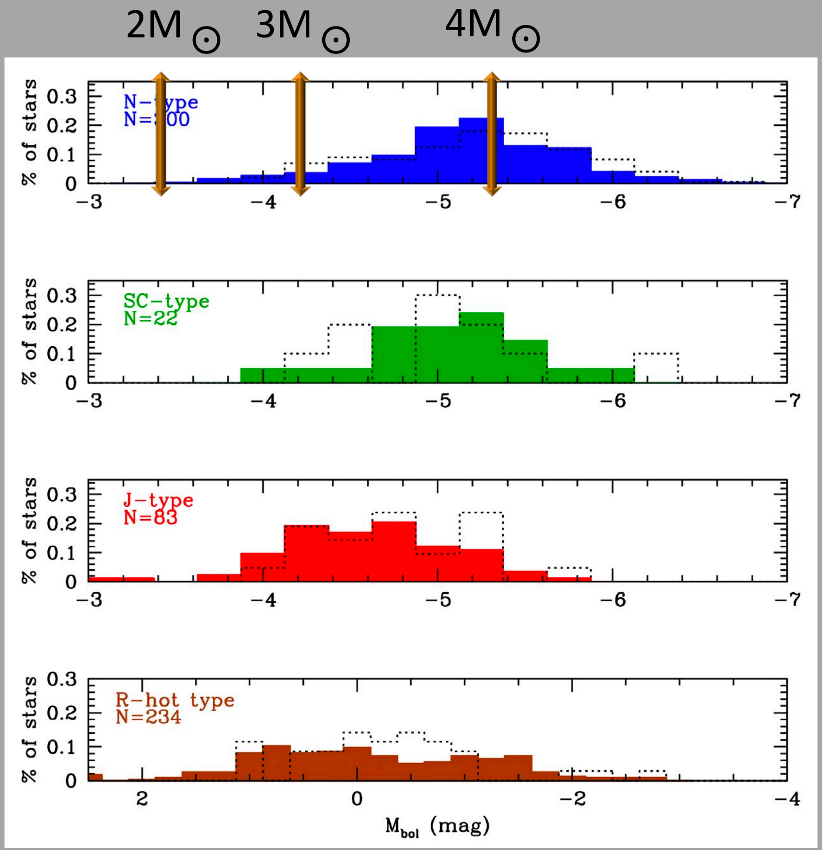

Abia+ 2022, AA 664,45

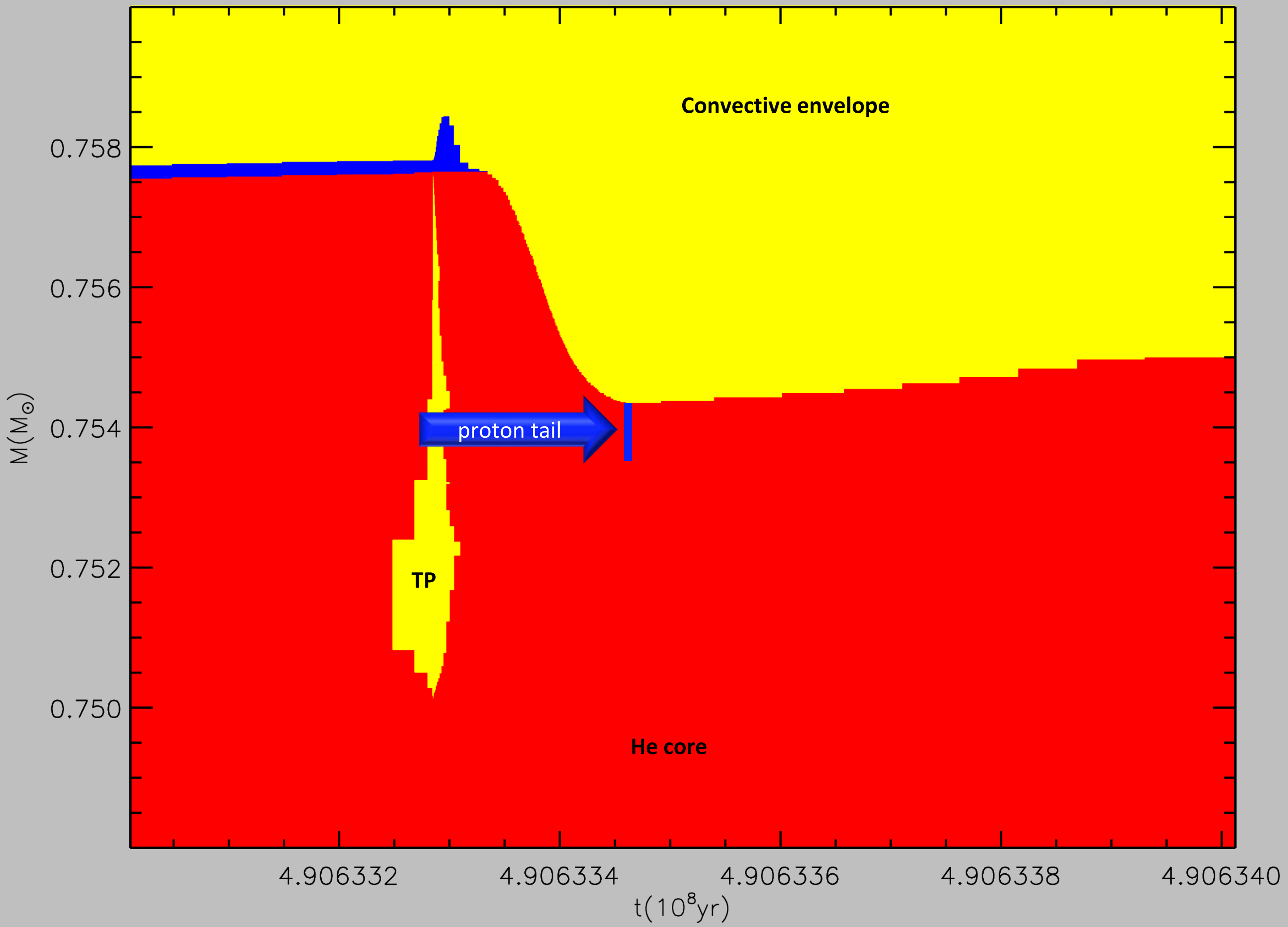

Convective envelope
proton tail
TP
He core
0.758
0.756
0.754
0.752
0.750
M(M⊙)
4.906332
4.906334
4.906336
4.906338
4.906340
t(10^8yr)

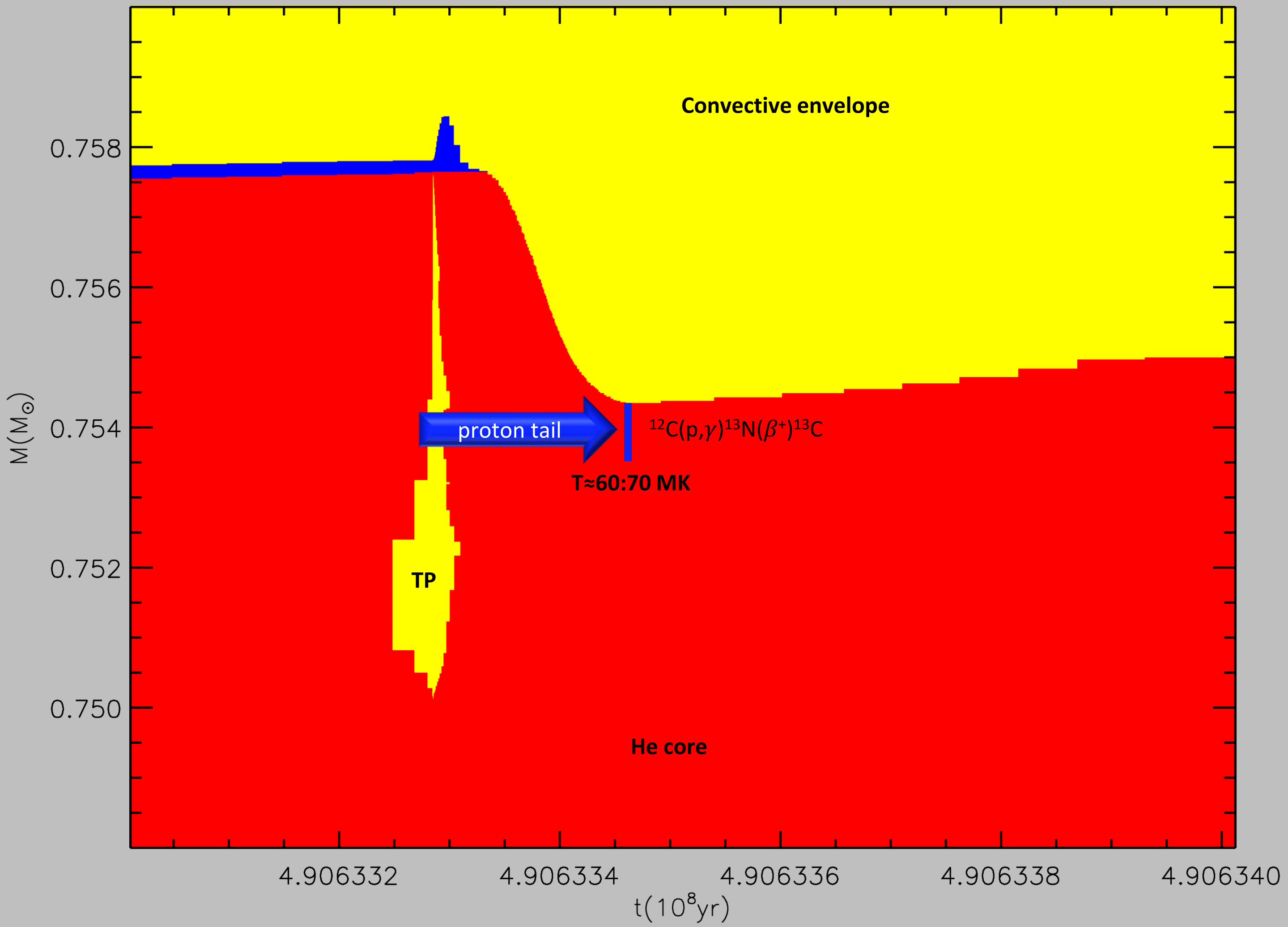

Convective envelope
proton tail
$^{12}C(p,\gamma)^{13}N(\beta^+)^{13}C$
T≈60:70 MK
TP
He core
0.758
0.756
0.754
0.752
0.750
M(M⊙)
4.906332
4.906334
4.906336
4.906338
4.906340
t(10^8yr)

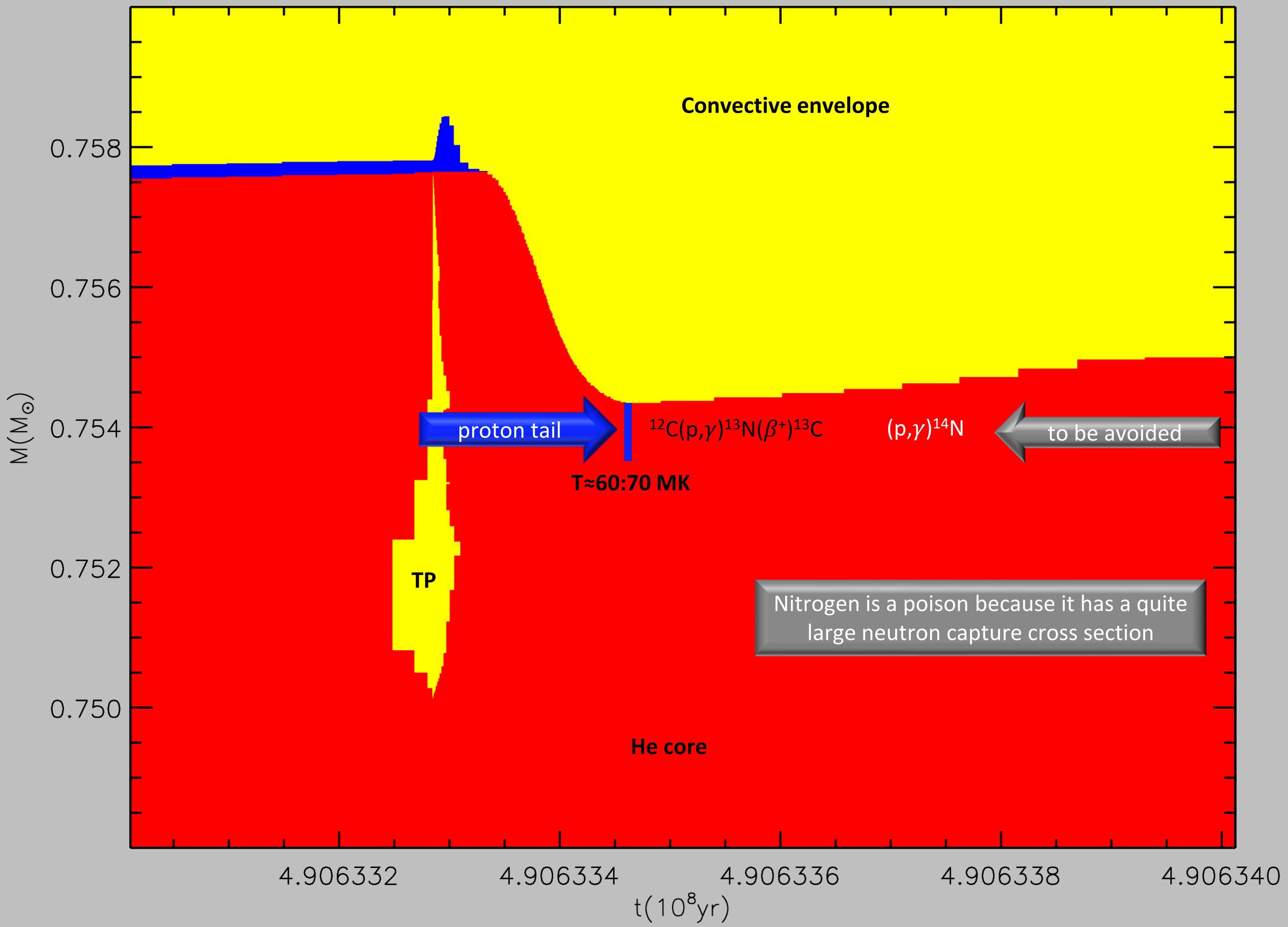

Convective envelope
proton tail
$^{12}C(p,\gamma)^{13}N(\beta^+)^{13}C$
$(p,\gamma)^{14}N$
to be avoided
T≈60:70 MK
TP
Nitrogen is a poison because it has a quite large neutron capture cross section
He core
0.758
0.756
0.754
0.752
0.750
$M(M_\odot)$
4.906332
4.906334
4.906336
4.906338
4.906340
$t(10^8 yr)$

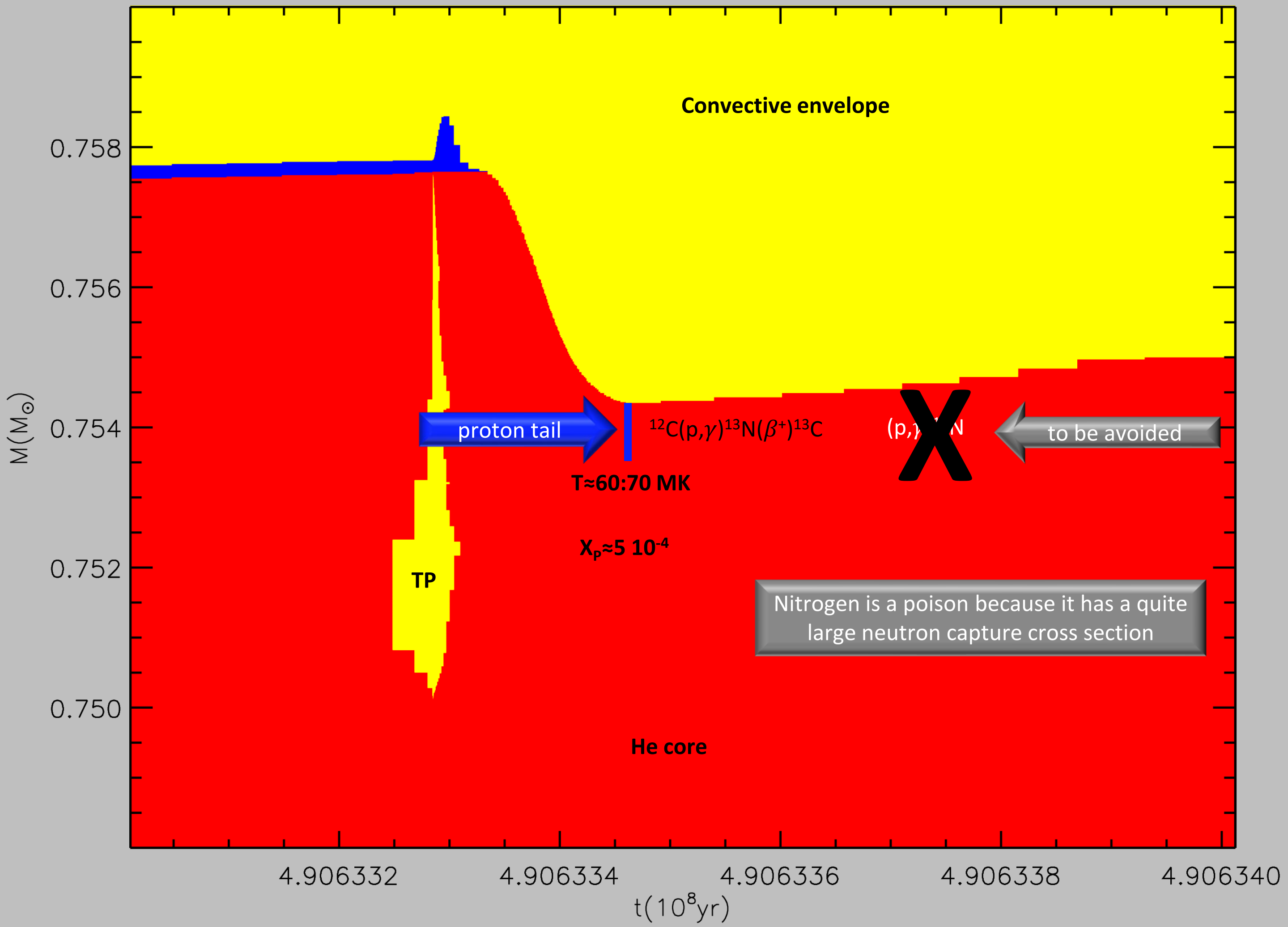
Convective envelope
proton tail
$^{12}C(p,\gamma)^{13}N(\beta^+)^{13}C$
(p,γ N
to be avoided
T≈60:70 MK
X_p≈5 10^{-4}
TP
Nitrogen is a poison because it has a quite large neutron capture cross section
He core
0.758
0.756
0.754
0.752
0.750
$M(M_\odot)$
4.906332
4.906334
4.906336
4.906338
4.906340
$t(10^8 yr)$

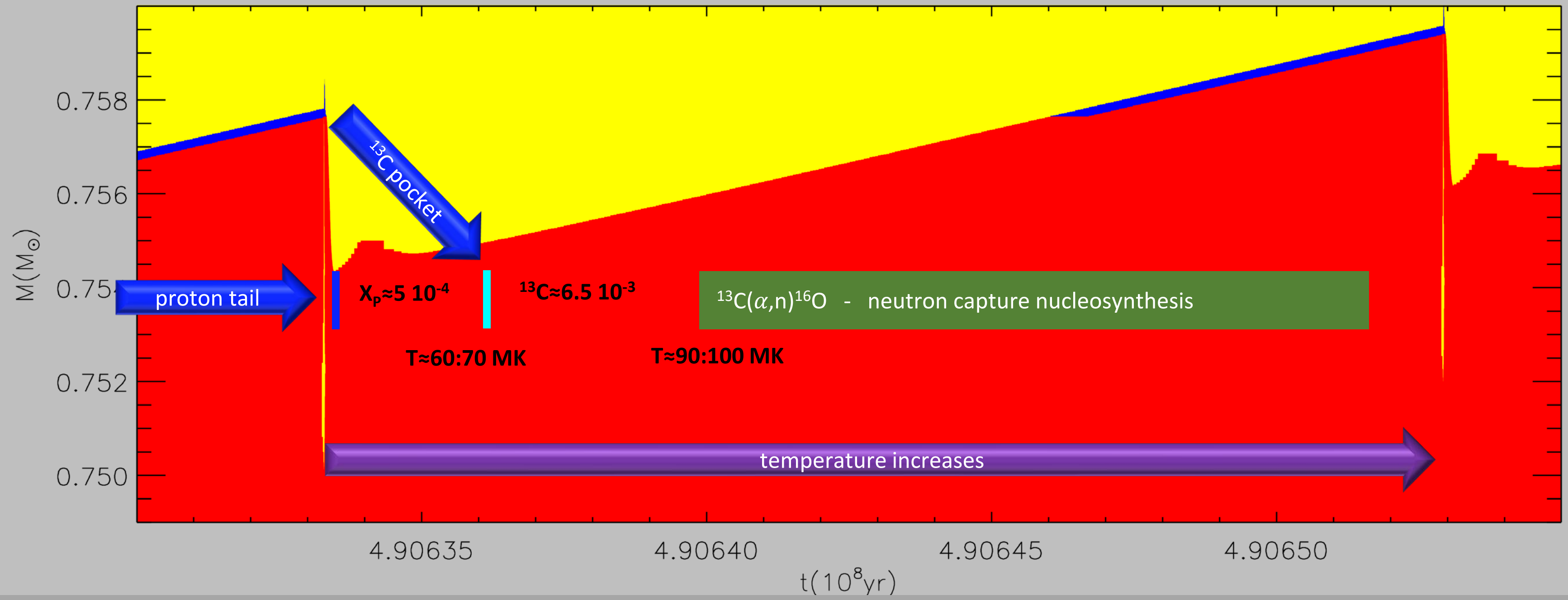

0.758
0.756
0.754
0.752
0.750
M(M⊙)
4.90635
4.90640
4.90645
4.90650
t(10^8yr)
13C pocket
proton tail
Xp≈5 10^-4
13C≈6.5 10^-3
13C(α,n)16O - neutron capture nucleosynthesis
T≈60:70 MK
T≈90:100 MK
temperature increases

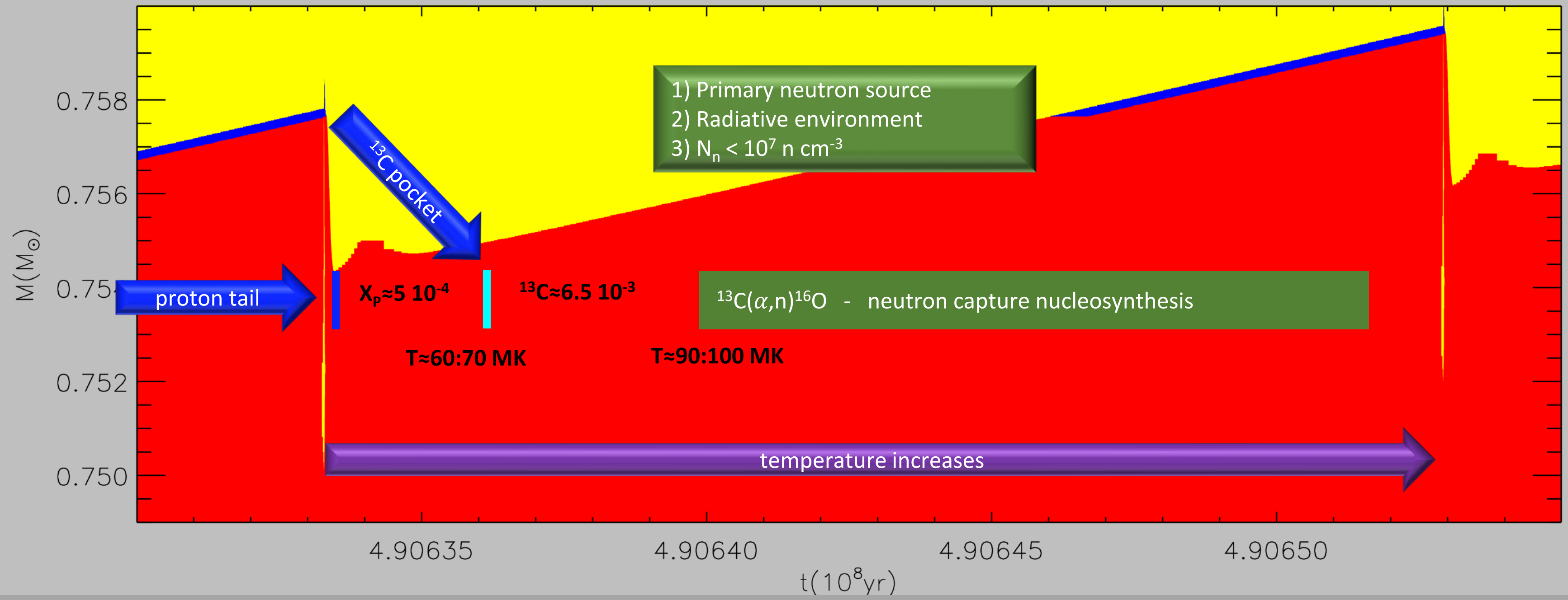
1) Primary neutron source
2) Radiative environment
3) $N_n < 10^7$ n cm^{-3}
^{13}C pocket
proton tail
$X_P \approx 5\ 10^{-4}$
$^{13}C \approx 6.5\ 10^{-3}$
$^{13}C(\alpha,n)^{16}O$ - neutron capture nucleosynthesis
T≈60:70 MK
T≈90:100 MK
temperature increases
0.758
0.756
0.754
0.752
0.750
$M(M_\odot)$
4.90635
4.90640
4.90645
4.90650
$t(10^8 yr)$

^{13}C NOT abundant because it is just the equilibrium value of the CNO cycle

$^{13}C(\alpha,n)^{16}O$ T > 90 MK $1.5<M/M_{\odot}<4$

Neutron density = 10^7 [#/cm^3]

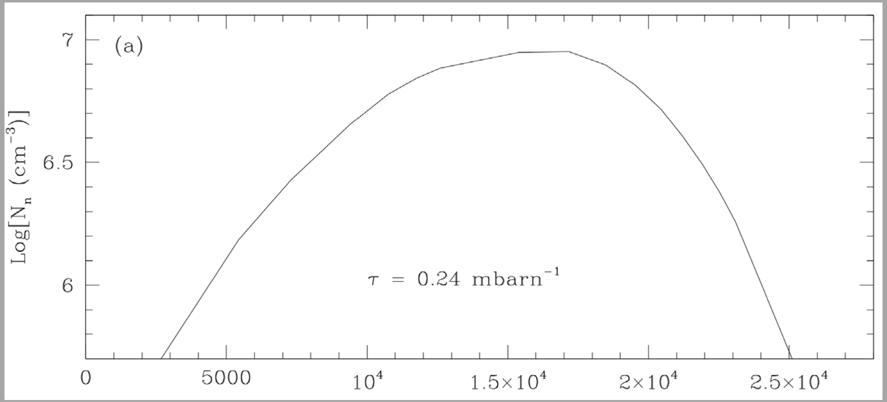

Lugaro&Chieffi, Astronomy with radioactivities, 2010, Chapter III

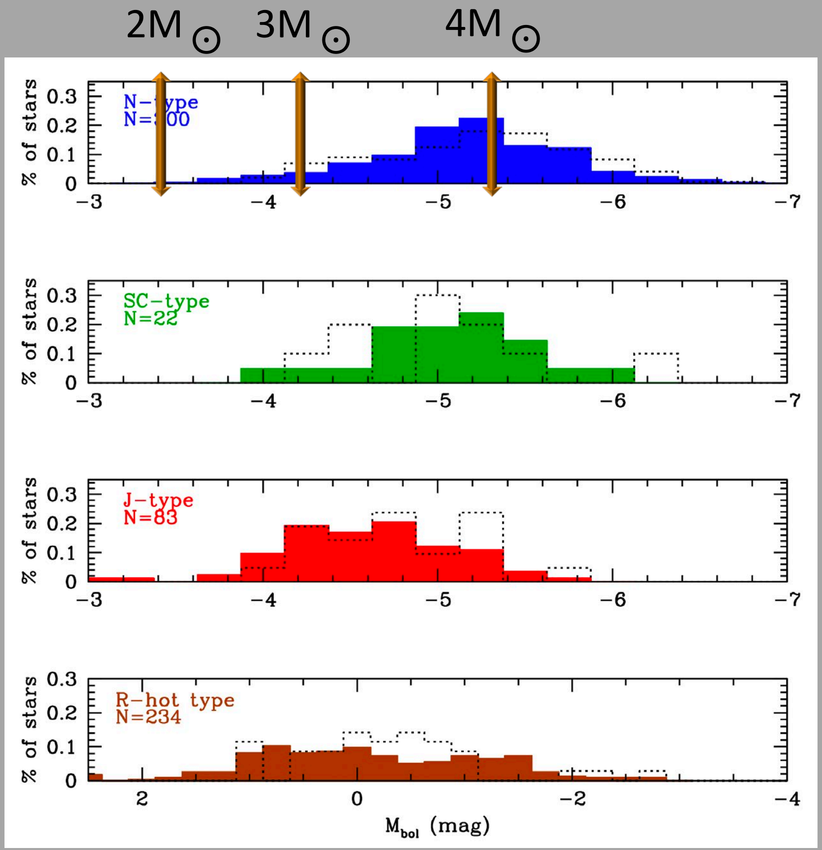

Abia+ 2022, AA 664,45

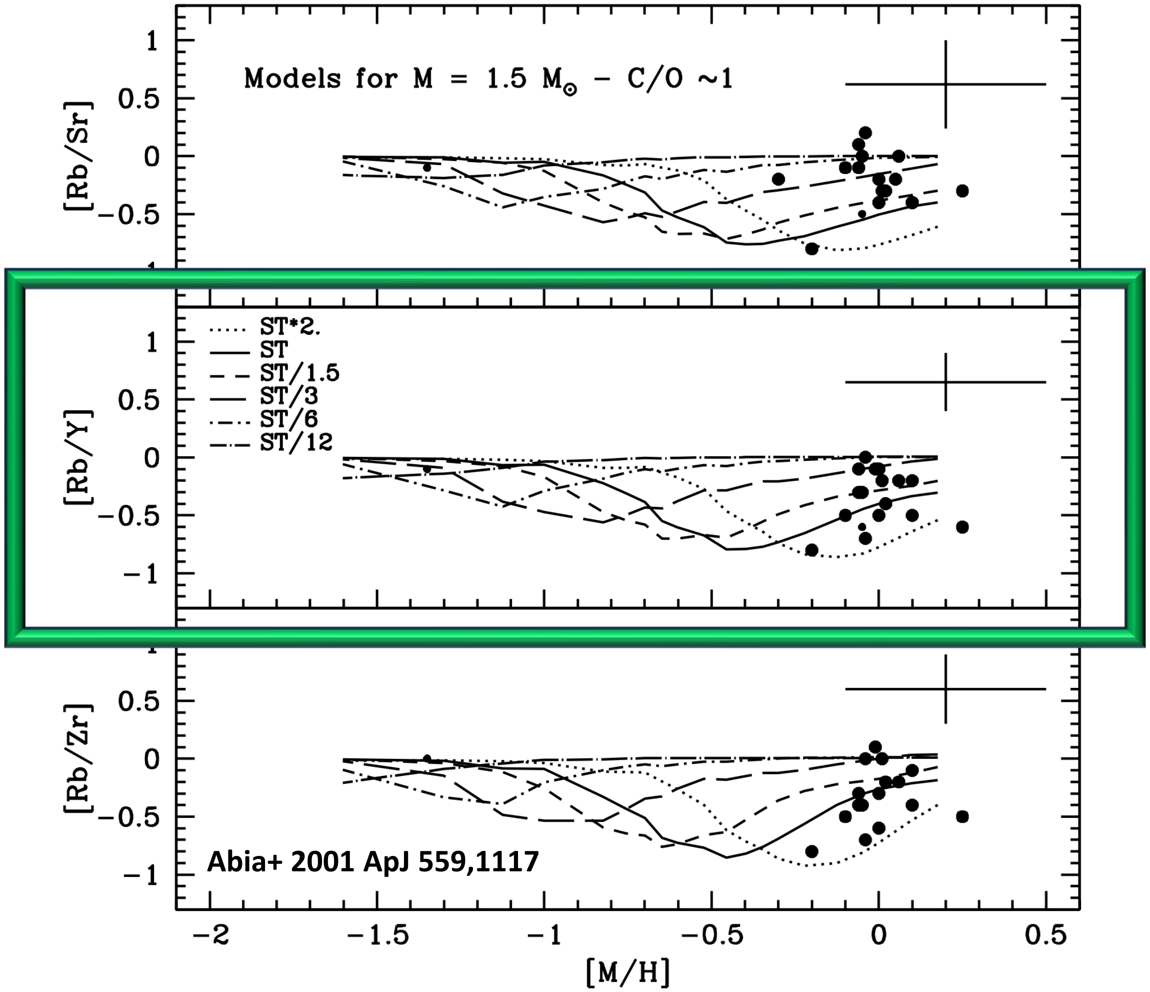

FIG. 3.—Comparison of the observed [Rb/Sr, Y, Zr] ratios vs. [M/H] with different theoretical predictions for a 1.5 $M_\odot$ TP-AGB star when the envelope reaches C/O $\gtrsim$ 1. Note that again the data points for IY Hya, VX Gem, and V CrB are plotted with smaller symbols.

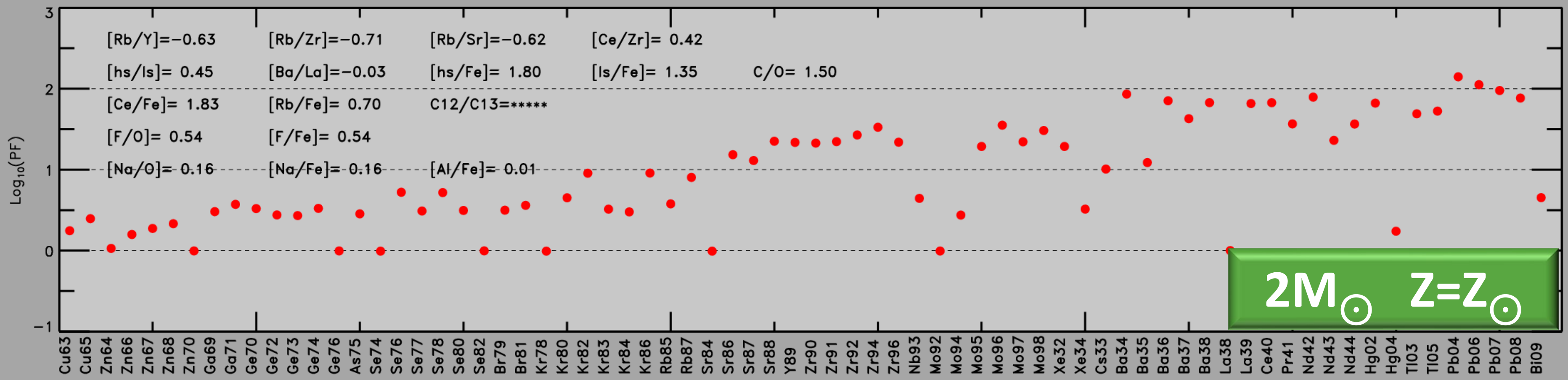

[Rb/Y]=−0.63
[Rb/Zr]=−0.71
[Rb/Sr]=−0.62
[Ce/Zr]= 0.42
[hs/ls]= 0.45
[Ba/La]=−0.03
[hs/Fe]= 1.80
[ls/Fe]= 1.35
C/O= 1.50
[Ce/Fe]= 1.83
[Rb/Fe]= 0.70
C12/C13=*****
[F/O]= 0.54
[F/Fe]= 0.54
[Na/O]= 0.16
[Na/Fe]= 0.16
[Al/Fe]= 0.01
Log10(PF)
3
2
1
0
−1
Cu63 Cu65 Zn64 Zn66 Zn67 Zn68 Zn70 Ga69 Ga71 Ge70 Ge72 Ge73 Ge74 Ge76 As75 Se74 Se76 Se77 Se78 Se80 Se82 Br79 Br81 Kr78 Kr80 Kr82 Kr83 Kr84 Kr86 Rb85 Rb87 Sr84 Sr86 Sr87 Sr88 Y89 Zr90 Zr91 Zr92 Zr94 Zr96 Nb93 Mo92 Mo94 Mo95 Mo96 Mo97 Mo98 Xe32 Xe34 Cs33 Ba34 Ba35 Ba36 Ba37 Ba38 La38 La39 Ce40 Pr41 Nd42 Nd43 Nd44 Hg02 Hg04 Tl03 Tl05 Pb04 Pb06 Pb07 Pb08 Bi09
2M⊙ Z=Z⊙

^{13}C pocket as simulated by Cristallo et al. ApJ 696, 797 (2009), ApJ 833, 181 (2016)

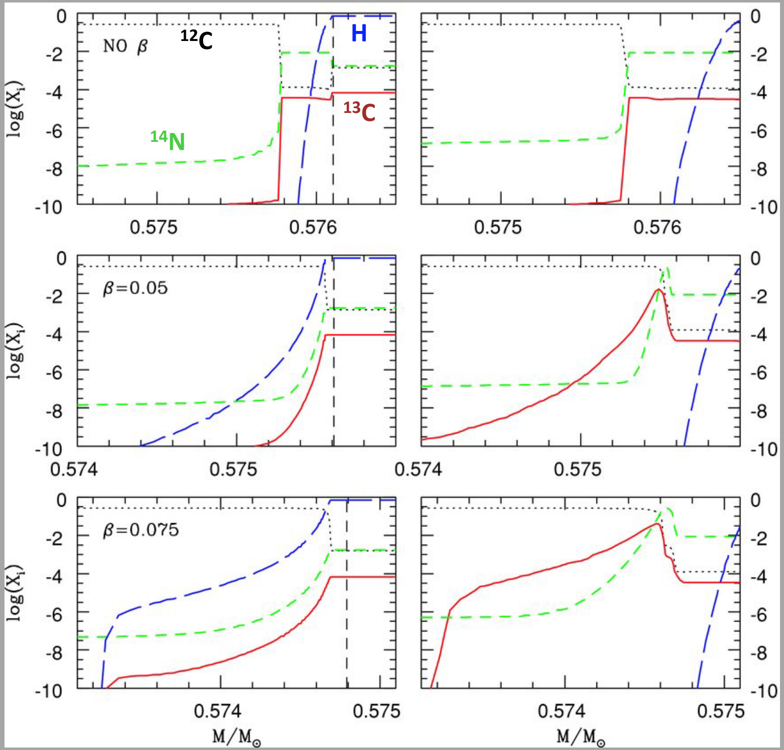

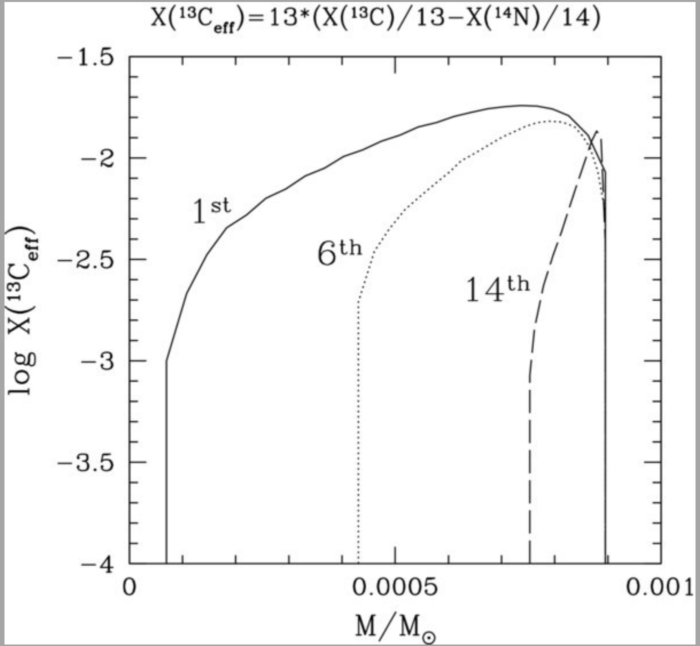

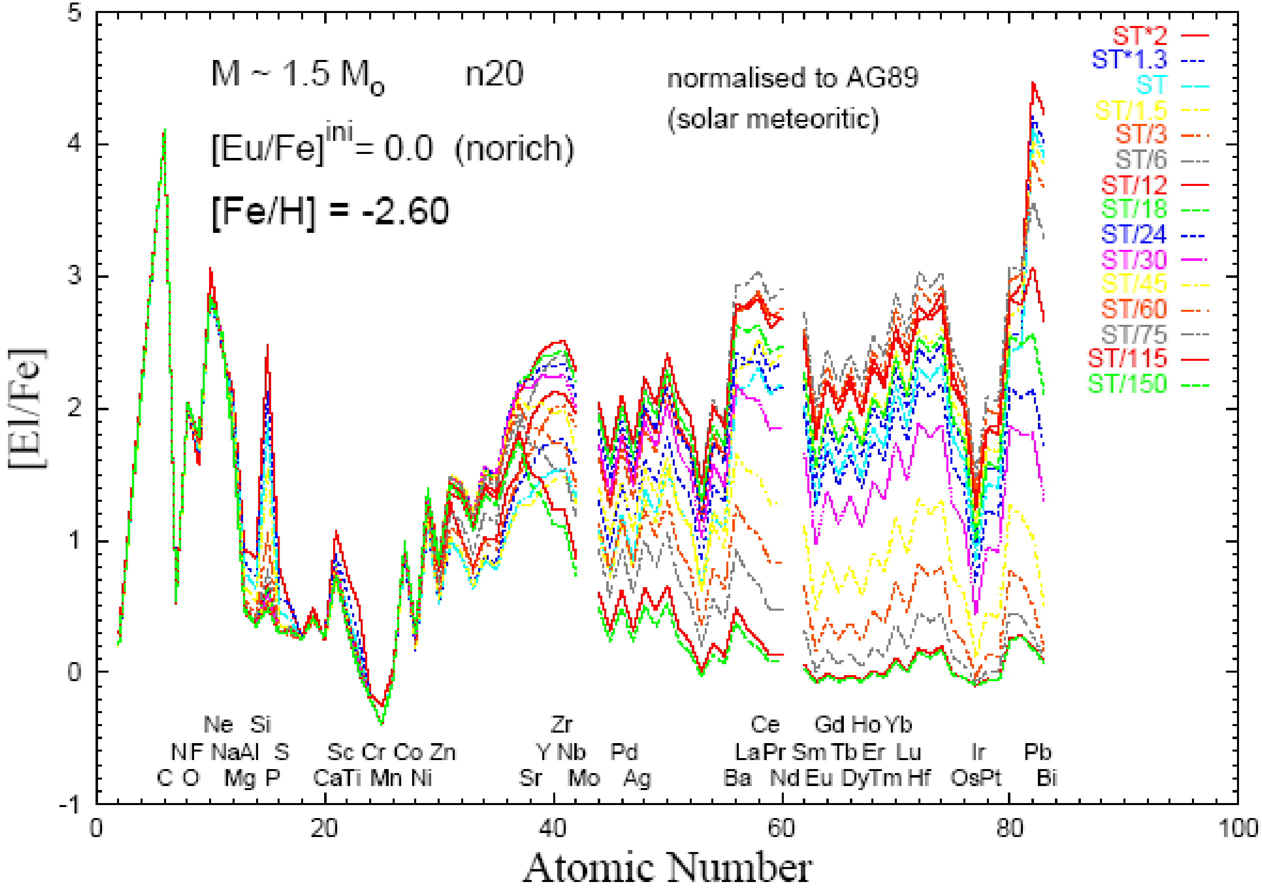
M ~ 1.5 M$_o$
n20
[Eu/Fe]^{ini}= 0.0 (norich)
[Fe/H] = -2.60
normalised to AG89
(solar meteoritic)
ST*2
ST*1.3
ST
ST/1.5
ST/3
ST/6
ST/12
ST/18
ST/24
ST/30
ST/45
ST/60
ST/75
ST/115
ST/150
[El/Fe]
Atomic Number
C O N F Ne Na Mg Al Si P S
Ca Sc Ti Cr Mn Co Ni Zn
Sr Y Zr Nb Mo Pd Ag
Ba La Ce Pr Nd Sm Eu Gd Tb Dy Ho Er Tm Yb Lu Hf
Os Ir Pt Pb Bi

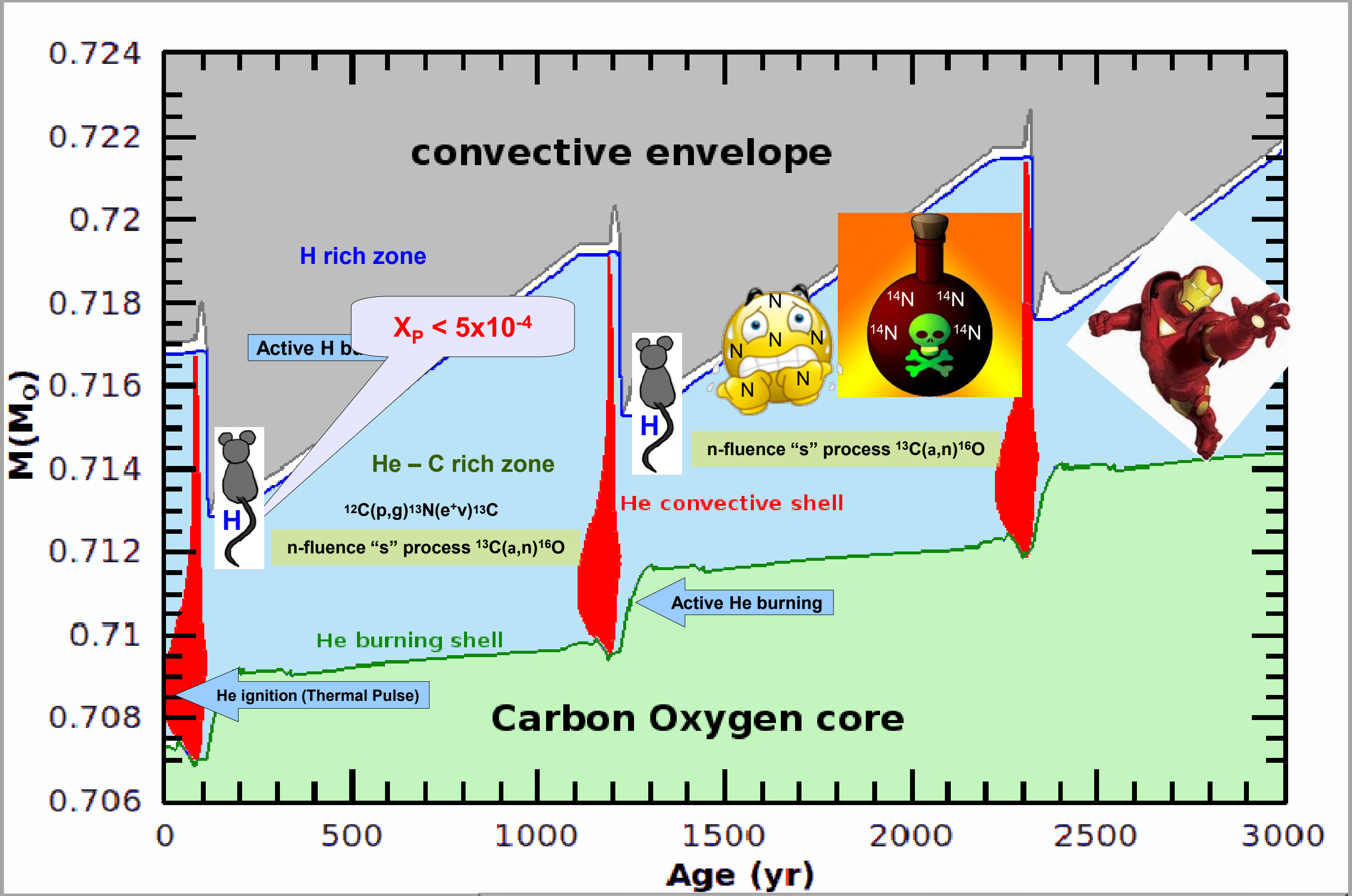

Lugaro&Chieffi, Astronomy with radioactivities, 2010, Chapter III

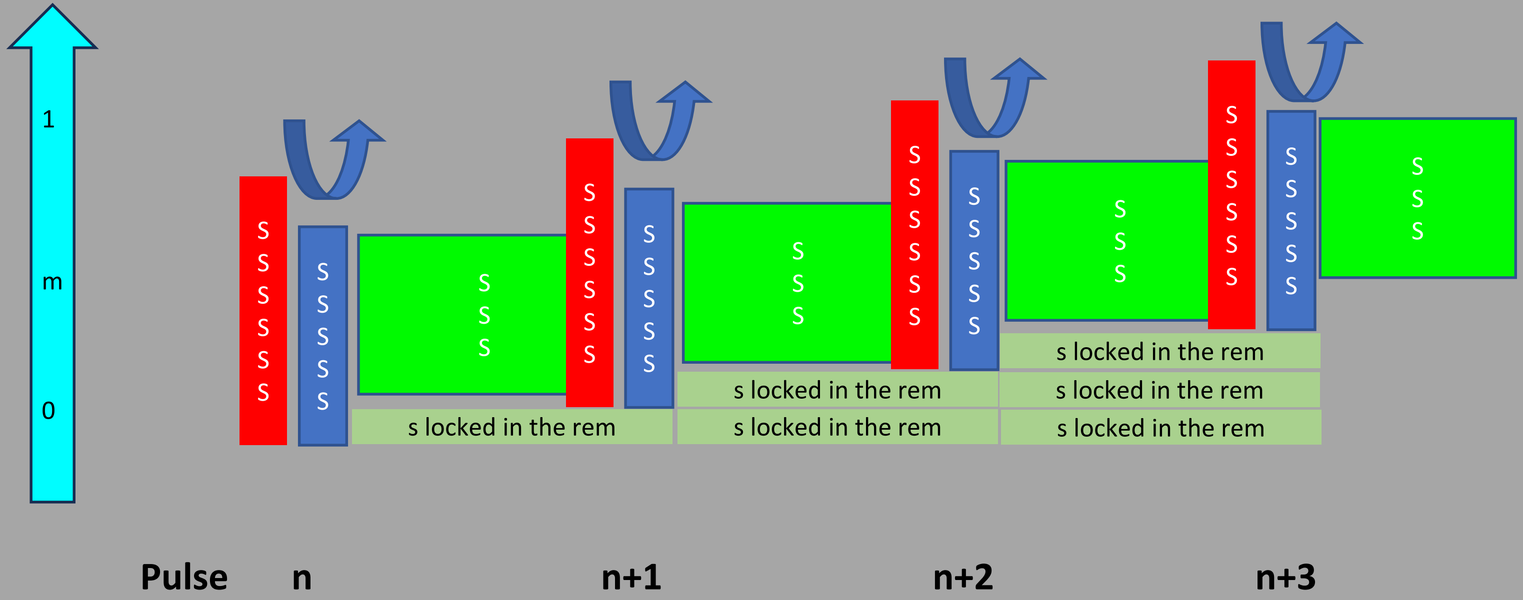
1
m
0
S S S S S S
S S S S S
S S S
s locked in the rem
S S S S S S
S S S S S
S S S
s locked in the rem
s locked in the rem
S S S S S S
S S S S S
S S S
s locked in the rem
s locked in the rem
s locked in the rem
S S S S S S
S S S S S
S S S
Pulse
n
n+1
n+2
n+3

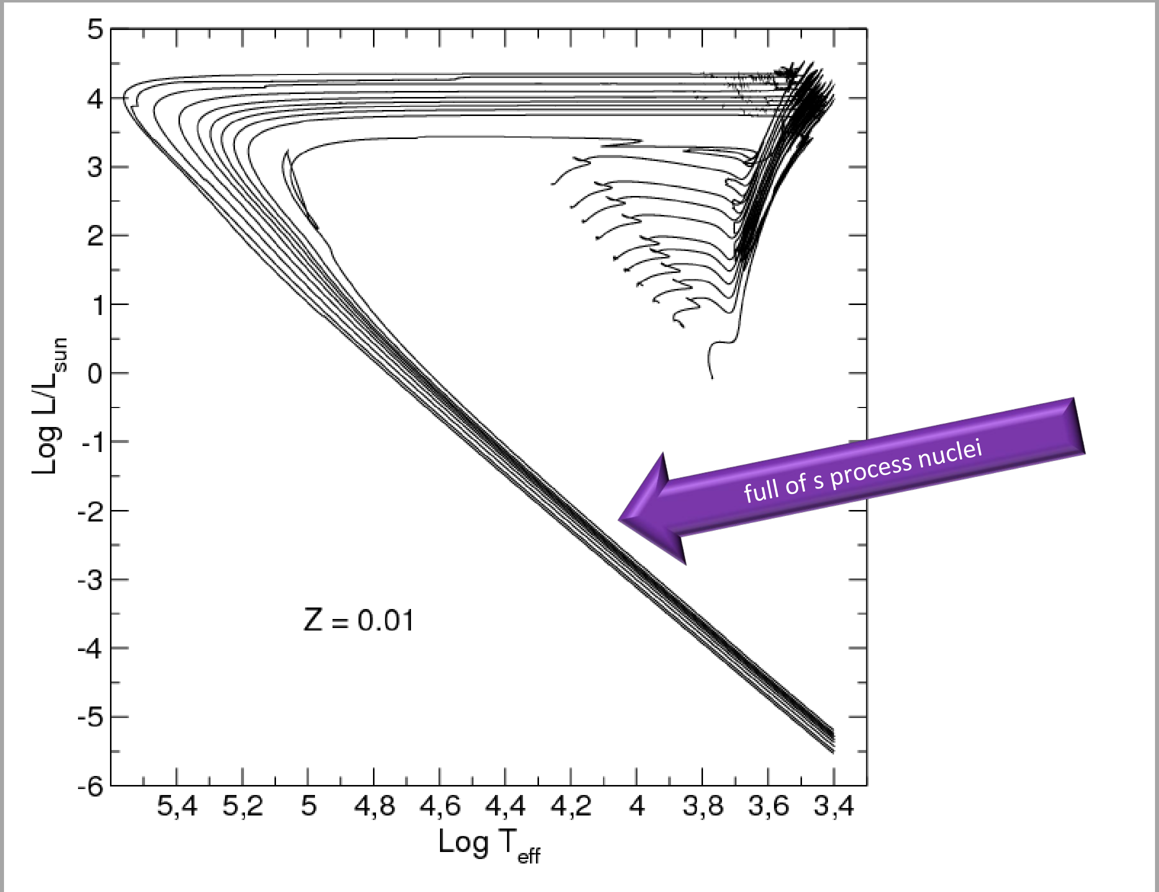

5
4
3
2
1
0
-1
-2
-3
-4
-5
-6
Log L/L$_{sun}$
5,4
5,2
5
4,8
4,6
4,4
4,2
4
3,8
3,6
3,4
Log T$_{eff}$
Z = 0.01
full of s process nuclei

Shell He burning (the E-AGB)

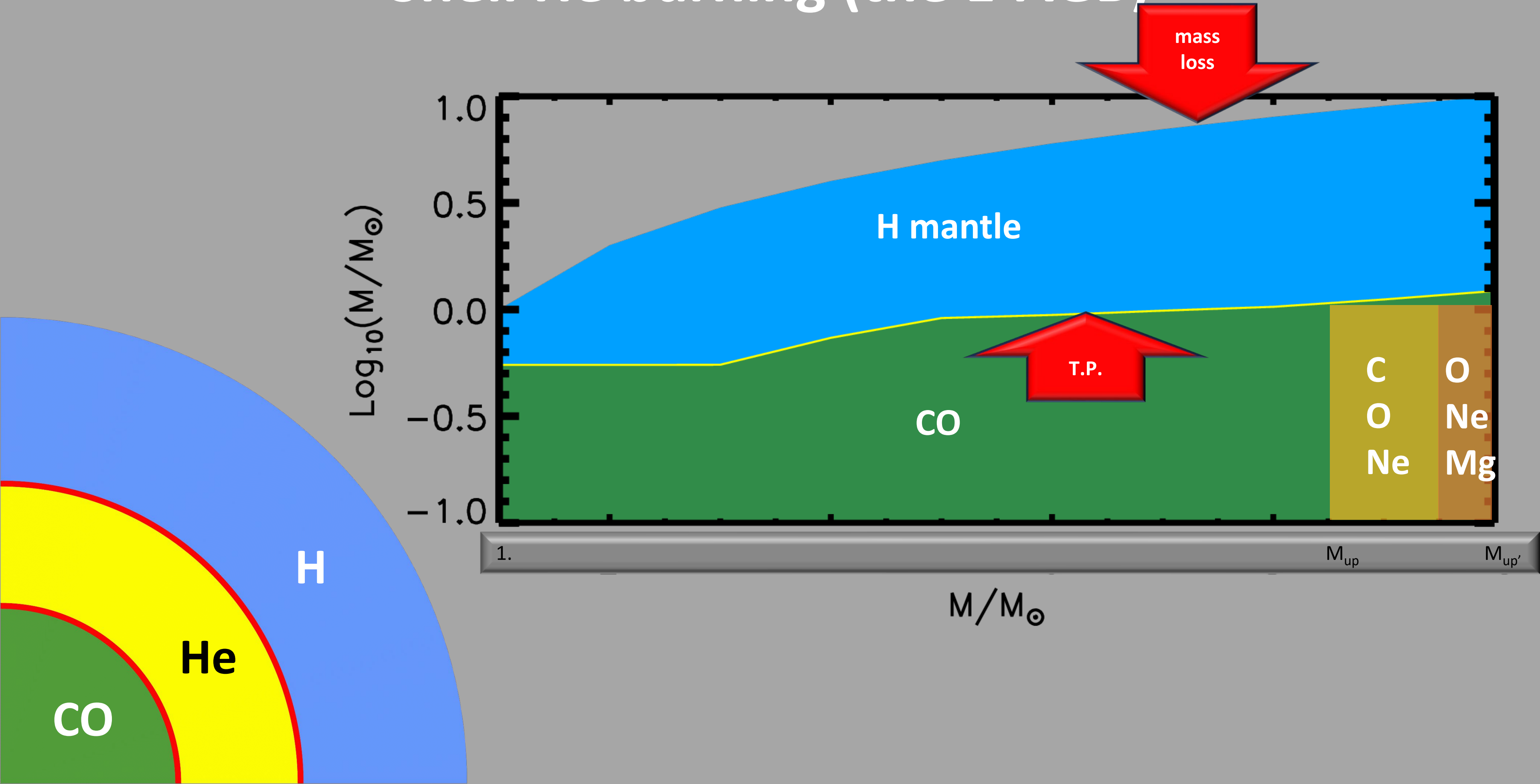

The evolution of the stars in the Thermally Pulsing phase is controlled by the competition between the growth of the electron degenerate core and the erosion of the mantle due to the mass loss

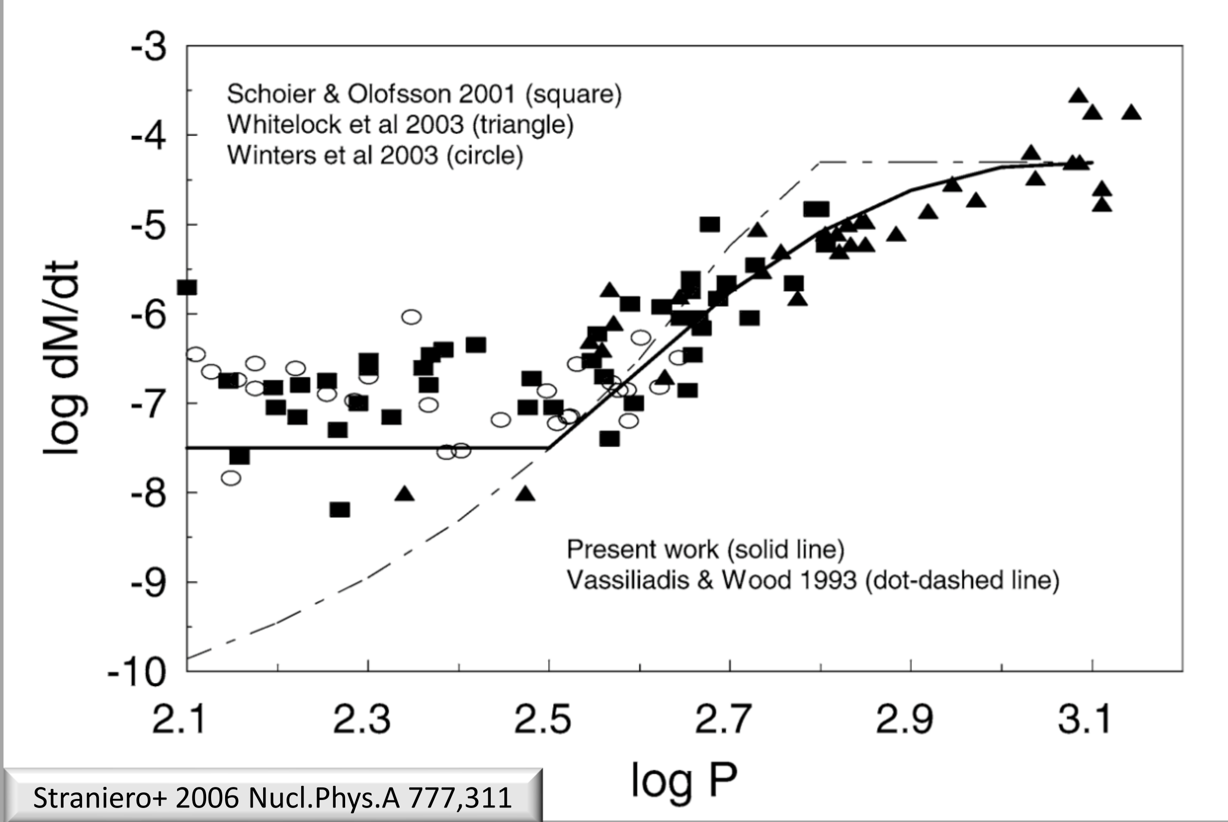

Straniero+ 2006 Nucl.Phys.A 777,311

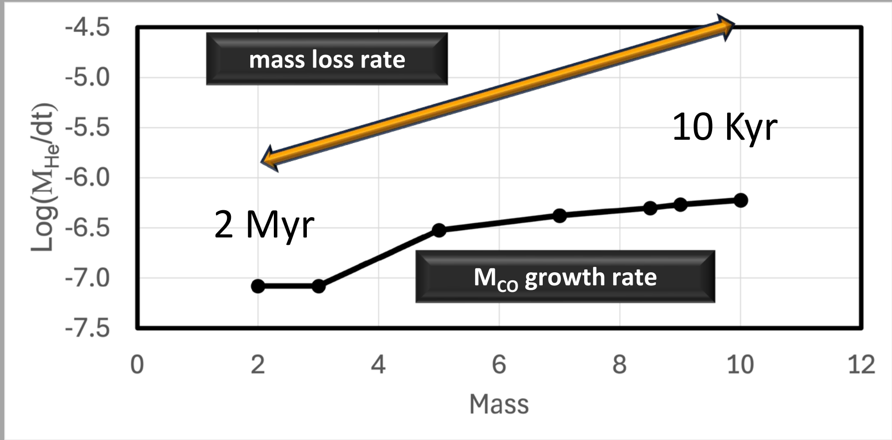
mass loss rate
10 Kyr
2 Myr
M_{CO} growth rate
Log(M_{He}/dt)
-4.5
-5.0
-5.5
-6.0
-6.5
-7.0
-7.5
0
2
4
6
8
10
12
Mass

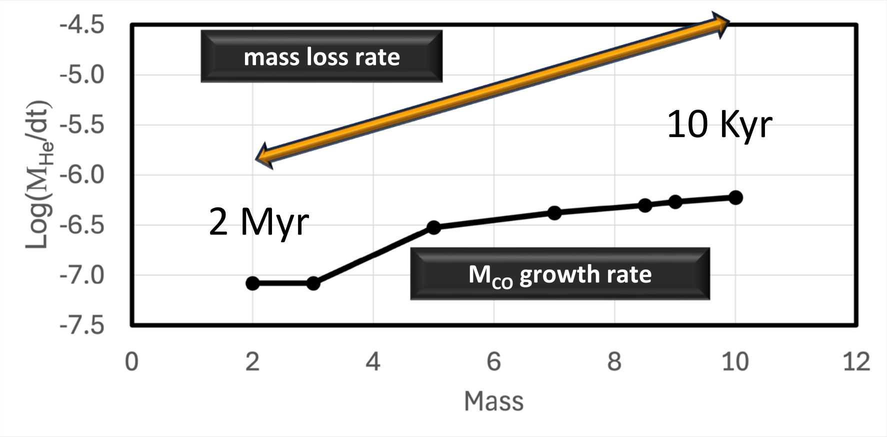

mass loss rate
10 Kyr
2 Myr
M$_{CO}$ growth rate
Log(M$_{He}$/dt)
-4.5
-5.0
-5.5
-6.0
-6.5
-7.0
-7.5
0
2
4
6
8
10
12
Mass

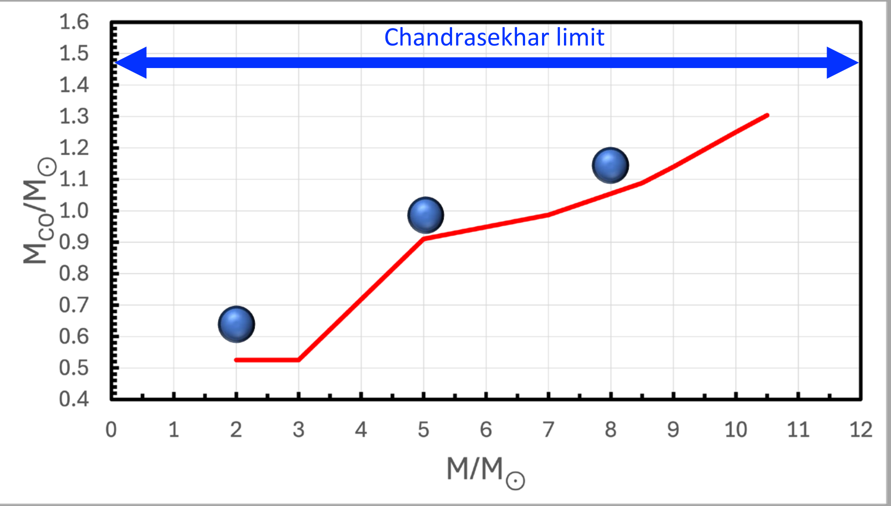

Chandrasekhar limit
$M_{CO}/M_\odot$
1.6
1.5
1.4
1.3
1.2
1.1
1.0
0.9
0.8
0.7
0.6
0.5
0.4
0
1
2
3
4
5
6
7
8
9
10
11
12
$M/M_\odot$

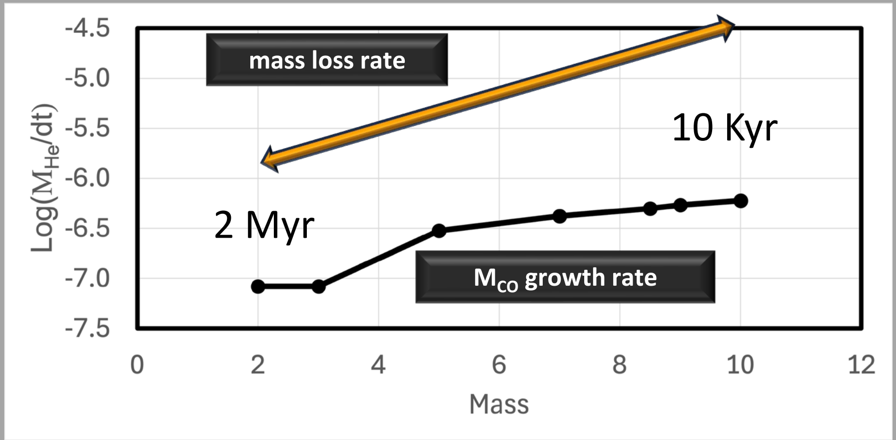

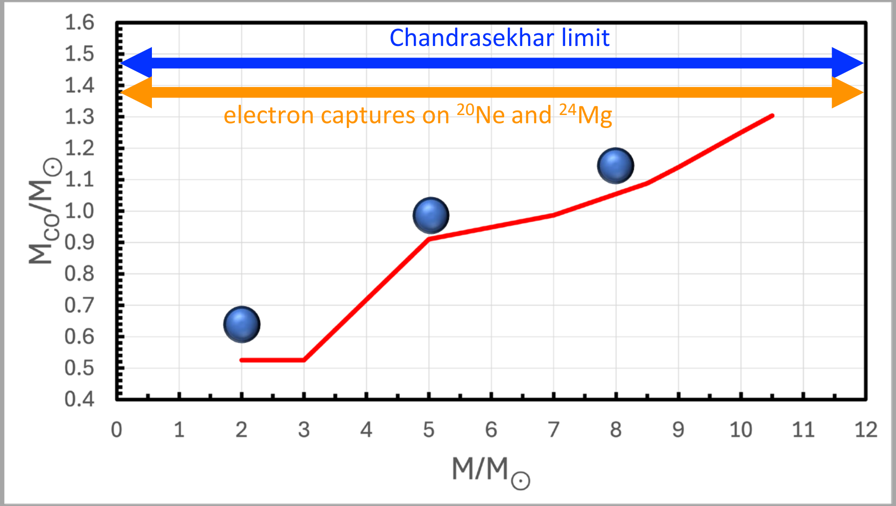

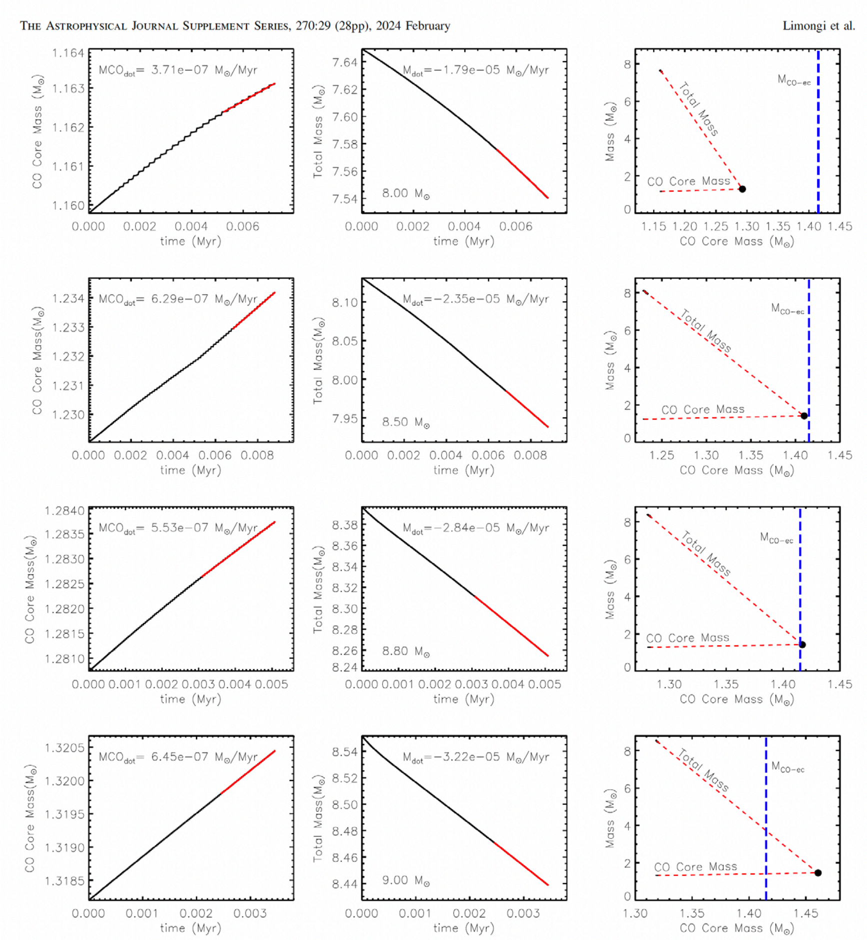

Limongi+ 2024 ApJS 270,29

Mass – central density relation for white dwarfs

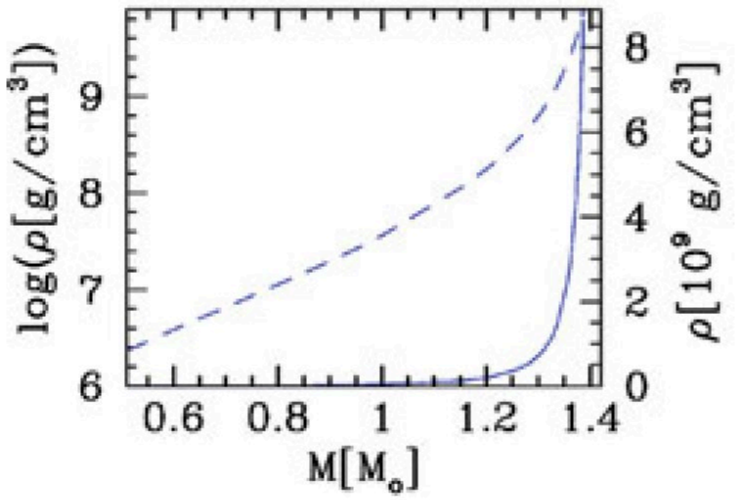

Hoeflich, Handbook of Supernovae (2016)
Springer International Publishing

fully electron degenerate Fermi gas of $M \approx 1.4\ M_\odot$ has a Fermi energy $E_F \approx 8$ MeV

electron capture on ^{24}Mg -> 6MeV

electron capture on ^{20}Ne -> 8MeV

TP-stars

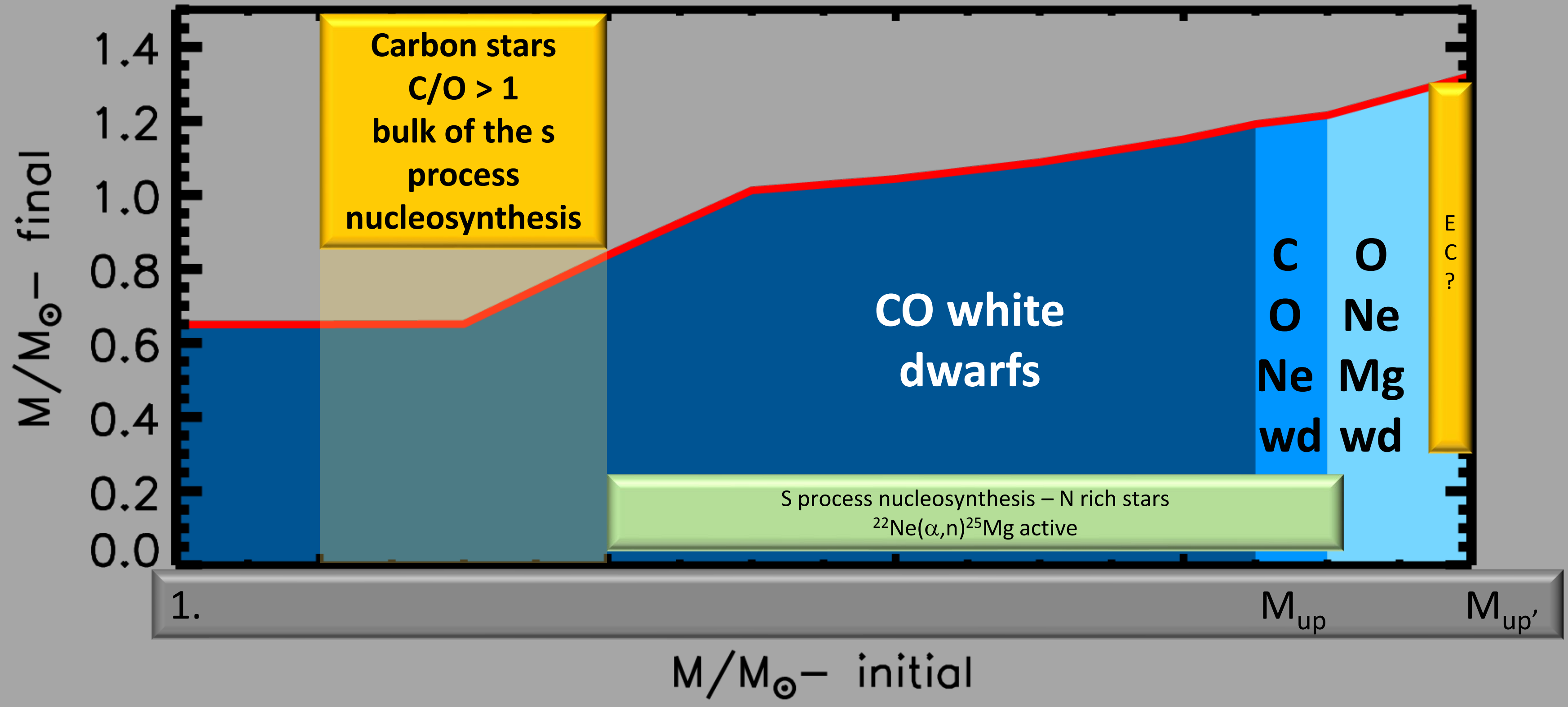

Carbon stars
C/O > 1
bulk of the s
process
nucleosynthesis
CO white
dwarfs
C
O
Ne
wd
O
Ne
Mg
wd
E
C
?
S process nucleosynthesis – N rich stars
$^{22}Ne(\alpha,n)^{25}Mg$ active
1.4
1.2
1.0
0.8
0.6
0.4
0.2
0.0
$M/M_\odot$ – final
1.
M_{up}
$M_{up'}$
$M/M_\odot$ – initial


THANK YOU
stjerner
sterren
istilel
izarrekin puntuatua
zvijezde
ulduz
gwiazdy
sвезди
Sterne
bintang
sao
steloj
zvaigznes
estrelas
שטערן
明星
stele
etoiles
stjörnur
žvaigždės
Hviezdičky
sterre
stars
yjet
sidera
зірки
bituin
Звездице
yıldız
estrelas
tähte
כוכבים
csillagok
Tähdet
звезди
sêr
estrellas

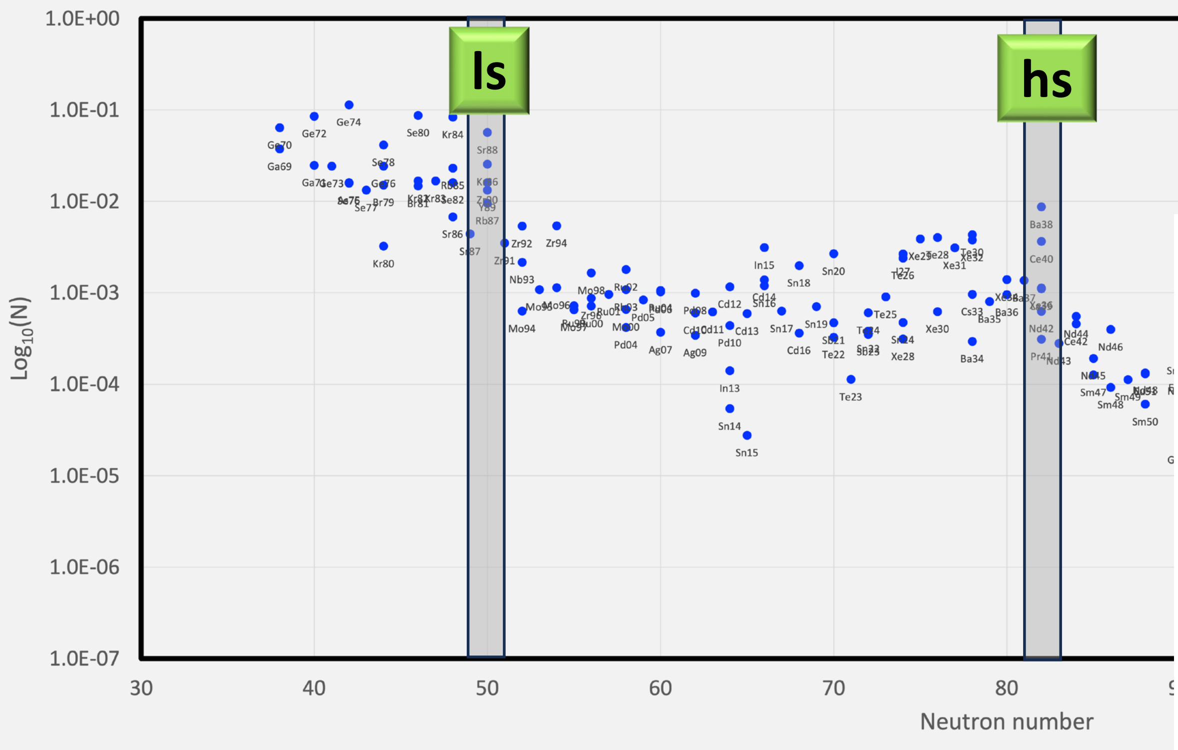

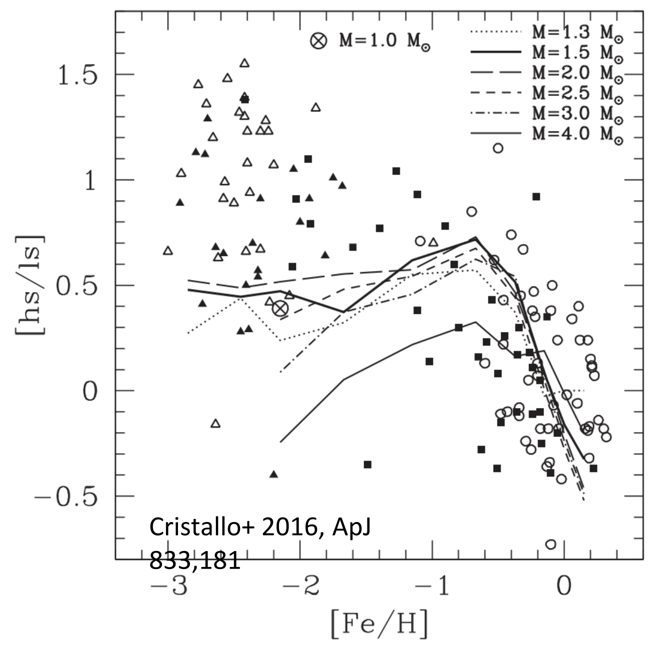

Cristallo+ 2016, ApJ 833,181

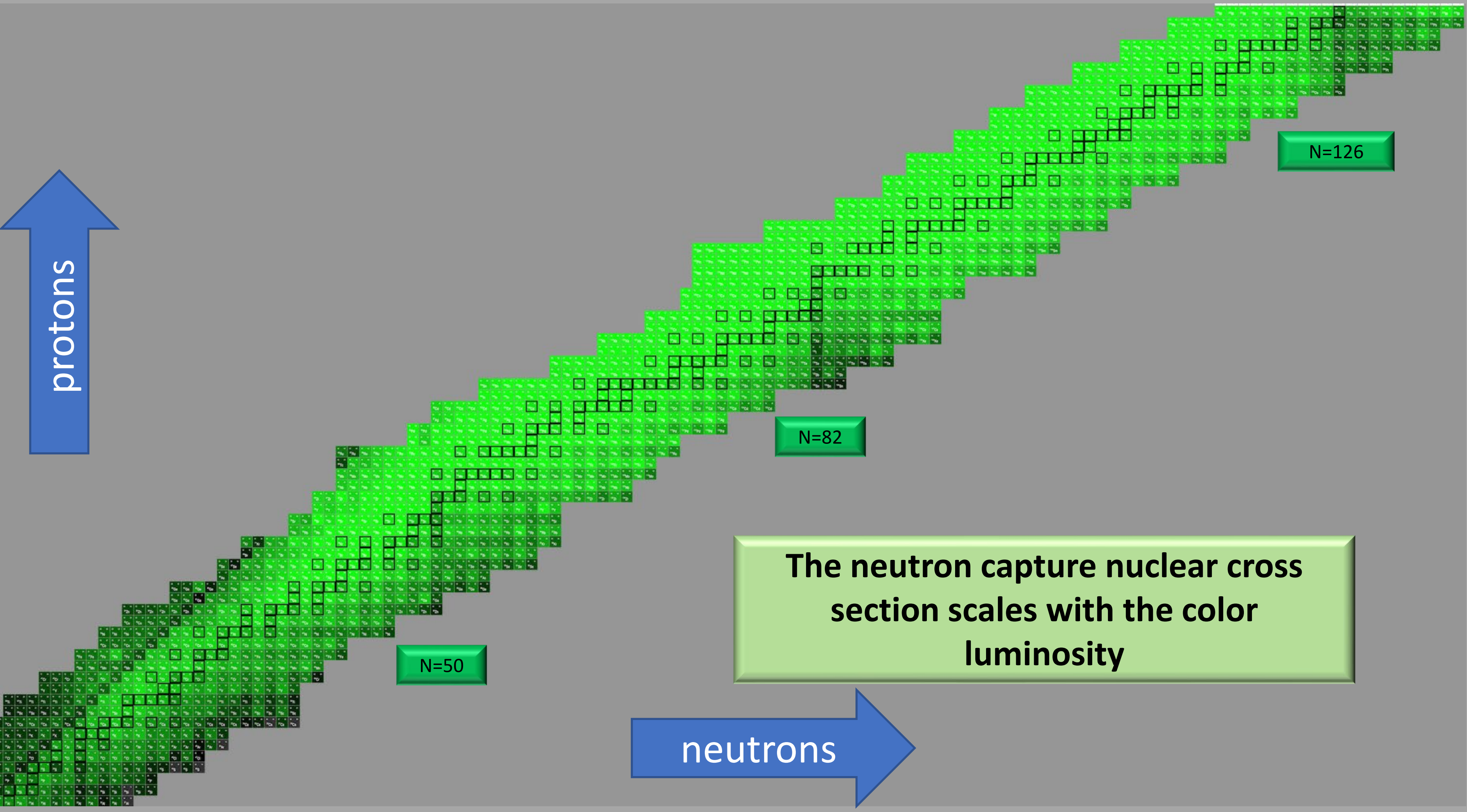
protons
N=126
N=82
N=50
The neutron capture nuclear cross section scales with the color luminosity
neutrons

$$N_n \cdot \langle N_A \sigma v \rangle_{in} = \frac{N_A}{\tau_i}$$

$$N_n = \frac{N_A}{\langle N_A \sigma v \rangle_{in} \cdot \tau_i} \quad [\# \ cm^{-3}]$$

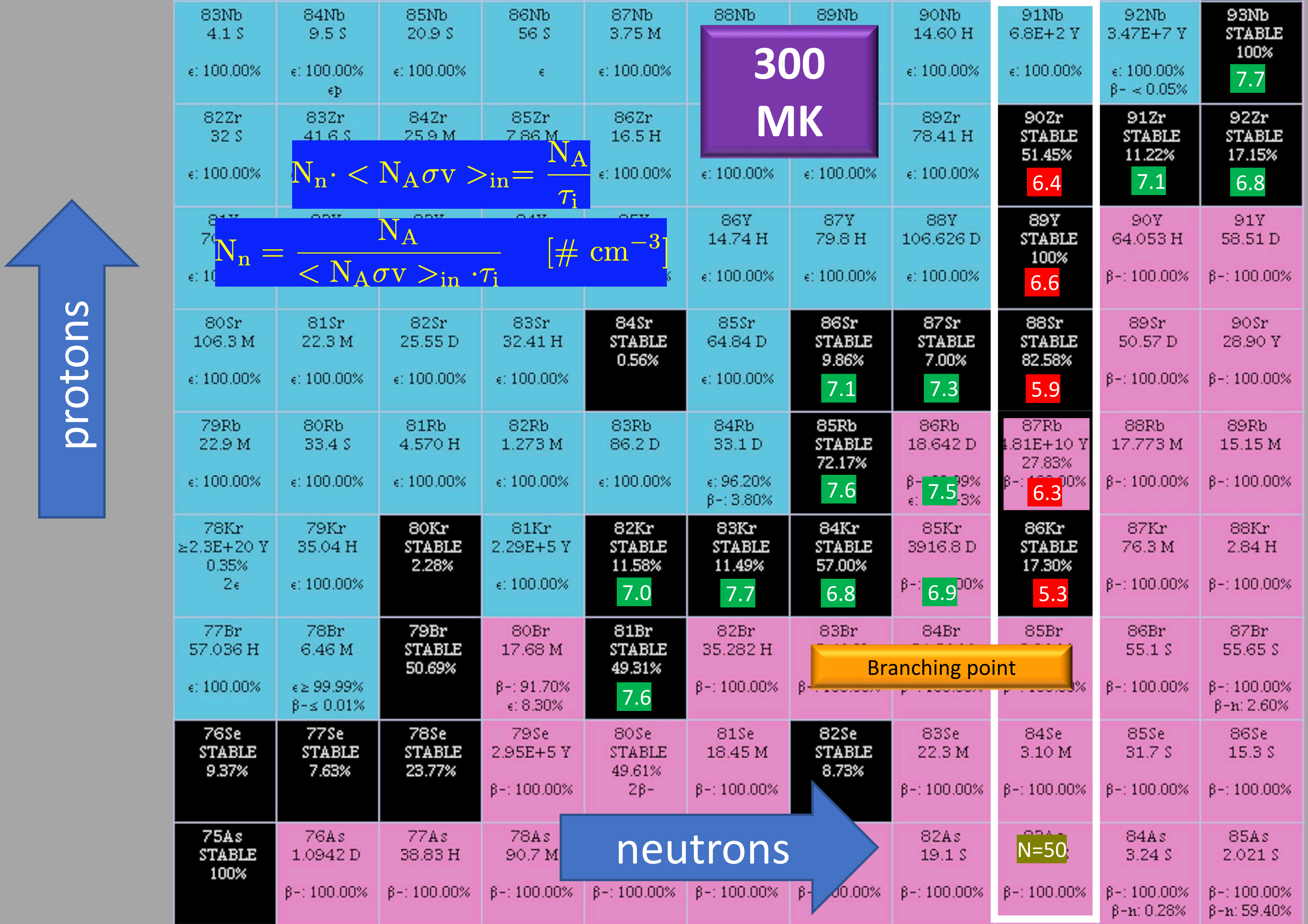

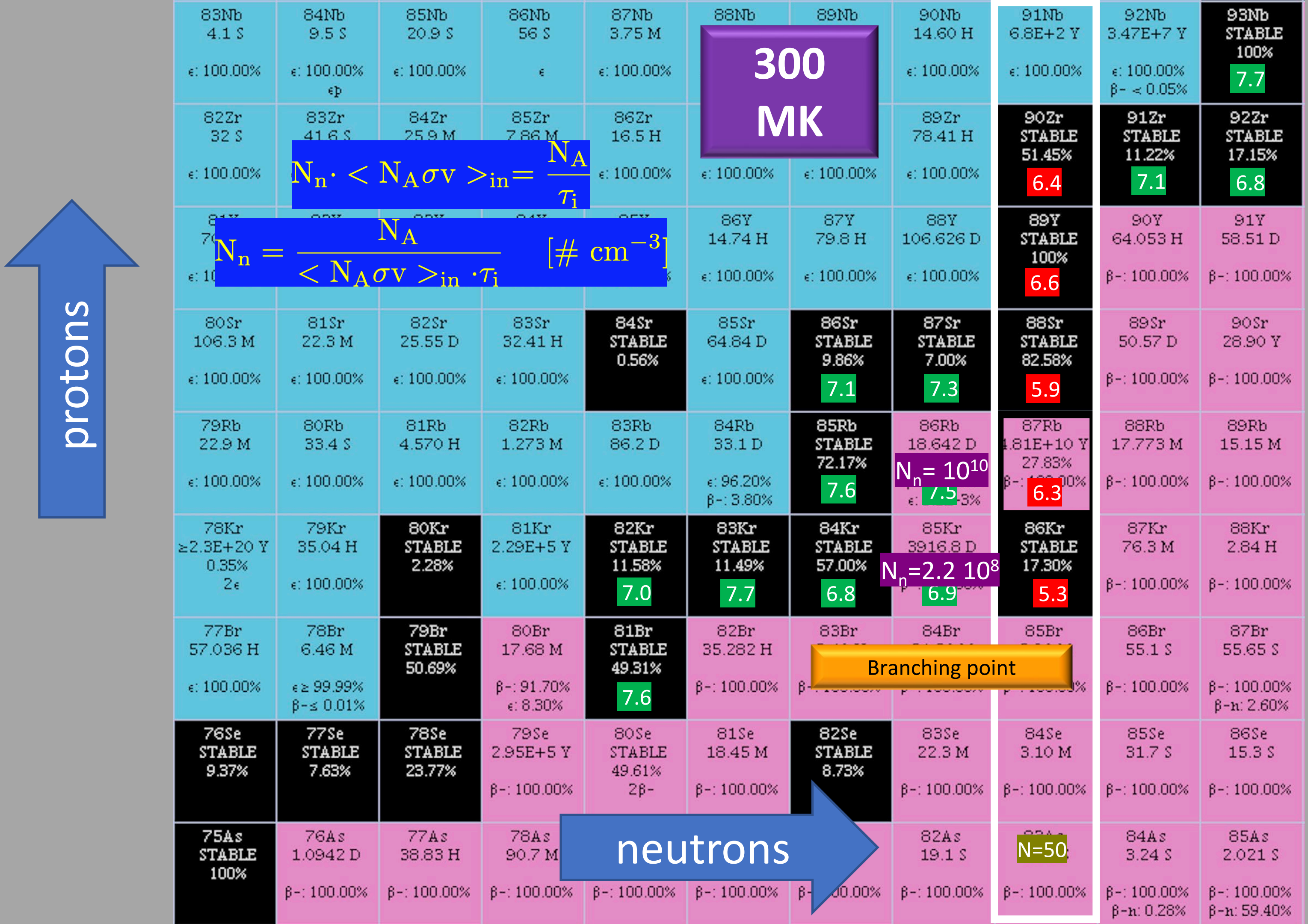
300 MK
$N_n \cdot <N_A\sigma v>_{in} = \frac{N_A}{\tau_i}$
$N_n = \frac{N_A}{<N_A\sigma v>_{in} \cdot \tau_i}$ [# cm^{-3}]
protons
neutrons
Branching point
$N_n = 10^{10}$
$N_n = 2.2\ 10^8$
N=50
83Nb 4.1 S ε: 100.00%
84Nb 9.5 S ε: 100.00% εp
85Nb 20.9 S ε: 100.00%
86Nb 56 S ε
87Nb 3.75 M ε: 100.00%
88Nb
89Nb
90Nb 14.60 H ε: 100.00%
91Nb 6.8E+2 Y ε: 100.00%
92Nb 3.47E+7 Y ε: 100.00% β- < 0.05%
93Nb STABLE 100% 7.7
82Zr 32 S ε: 100.00%
86Zr 16.5 H ε: 100.00%
89Zr 78.41 H ε: 100.00%
90Zr STABLE 51.45% 6.4
91Zr STABLE 11.22% 7.1
92Zr STABLE 17.15% 6.8
86Y 14.74 H ε: 100.00%
87Y 79.8 H ε: 100.00%
88Y 106.626 D ε: 100.00%
89Y STABLE 100% 6.6
90Y 64.053 H β-: 100.00%
91Y 58.51 D β-: 100.00%
80Sr 106.3 M ε: 100.00%
81Sr 22.3 M ε: 100.00%
82Sr 25.55 D ε: 100.00%
83Sr 32.41 H ε: 100.00%
84Sr STABLE 0.56%
85Sr 64.84 D ε: 100.00%
86Sr STABLE 9.86% 7.1
87Sr STABLE 7.00% 7.3
88Sr STABLE 82.58% 5.9
89Sr 50.57 D β-: 100.00%
90Sr 28.90 Y β-: 100.00%
79Rb 22.9 M ε: 100.00%
80Rb 33.4 S ε: 100.00%
81Rb 4.570 H ε: 100.00%
82Rb 1.273 M ε: 100.00%
83Rb 86.2 D ε: 100.00%
84Rb 33.1 D ε: 96.20% β-: 3.80%
85Rb STABLE 72.17% 7.6
86Rb 18.642 D 7.5
87Rb 4.81E+10 Y 27.83% 6.3
88Rb 17.773 M β-: 100.00%
89Rb 15.15 M β-: 100.00%
78Kr ≥2.3E+20 Y 0.35% 2ε
79Kr 35.04 H ε: 100.00%
80Kr STABLE 2.28%
81Kr 2.29E+5 Y ε: 100.00%
82Kr STABLE 11.58% 7.0
83Kr STABLE 11.49% 7.7
84Kr STABLE 57.00% 6.8
85Kr 3916.8 D 6.9
86Kr STABLE 17.30% 5.3
87Kr 76.3 M β-: 100.00%
88Kr 2.84 H β-: 100.00%
77Br 57.036 H ε: 100.00%
78Br 6.46 M ε ≥ 99.99% β- ≤ 0.01%
79Br STABLE 50.69%
80Br 17.68 M β-: 91.70% ε: 8.30%
81Br STABLE 49.31% 7.6
82Br 35.282 H β-: 100.00%
83Br
84Br
85Br
86Br 55.1 S β-: 100.00%
87Br 55.65 S β-: 100.00% β-n: 2.60%
76Se STABLE 9.37%
77Se STABLE 7.63%
78Se STABLE 23.77%
79Se 2.95E+5 Y β-: 100.00%
80Se STABLE 49.61% 2β-
81Se 18.45 M β-: 100.00%
82Se STABLE 8.73%
83Se 22.3 M β-: 100.00%
84Se 3.10 M β-: 100.00%
85Se 31.7 S β-: 100.00%
86Se 15.3 S β-: 100.00%
75As STABLE 100%
76As 1.0942 D β-: 100.00%
77As 38.83 H β-: 100.00%
78As 90.7 M β-: 100.00%
82As 19.1 S β-: 100.00%
84As 3.24 S β-: 100.00% β-n: 0.28%
85As 2.021 S β-: 100.00% β-n: 59.40%

Figure 40. Schematic view of some of the evolutionary properties and expected

Limongi+ 2024 ApJS 270,29

Convective envelope

H rich matter

He core

CO core

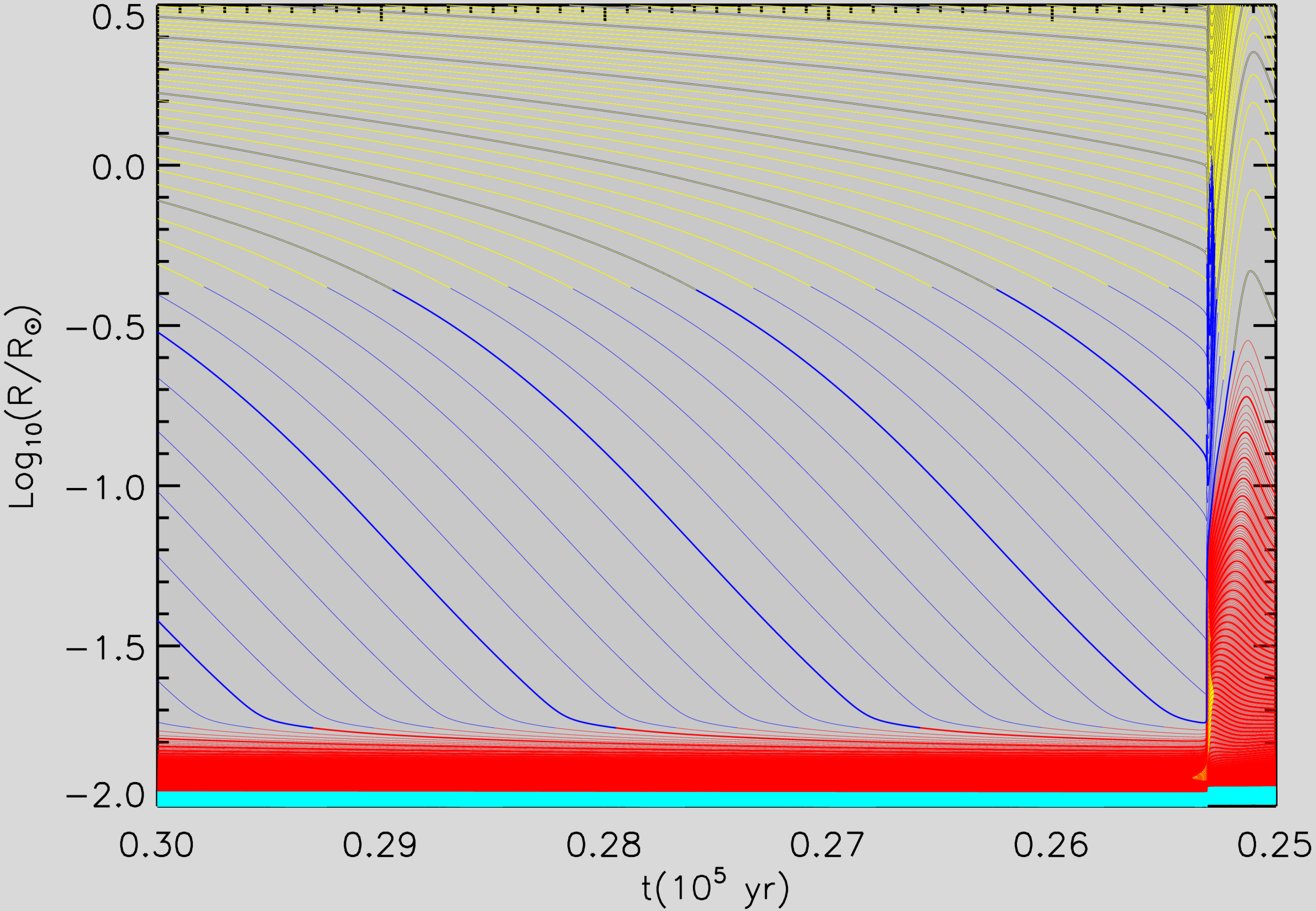

Convective envelope

H rich matter

He core

CO core

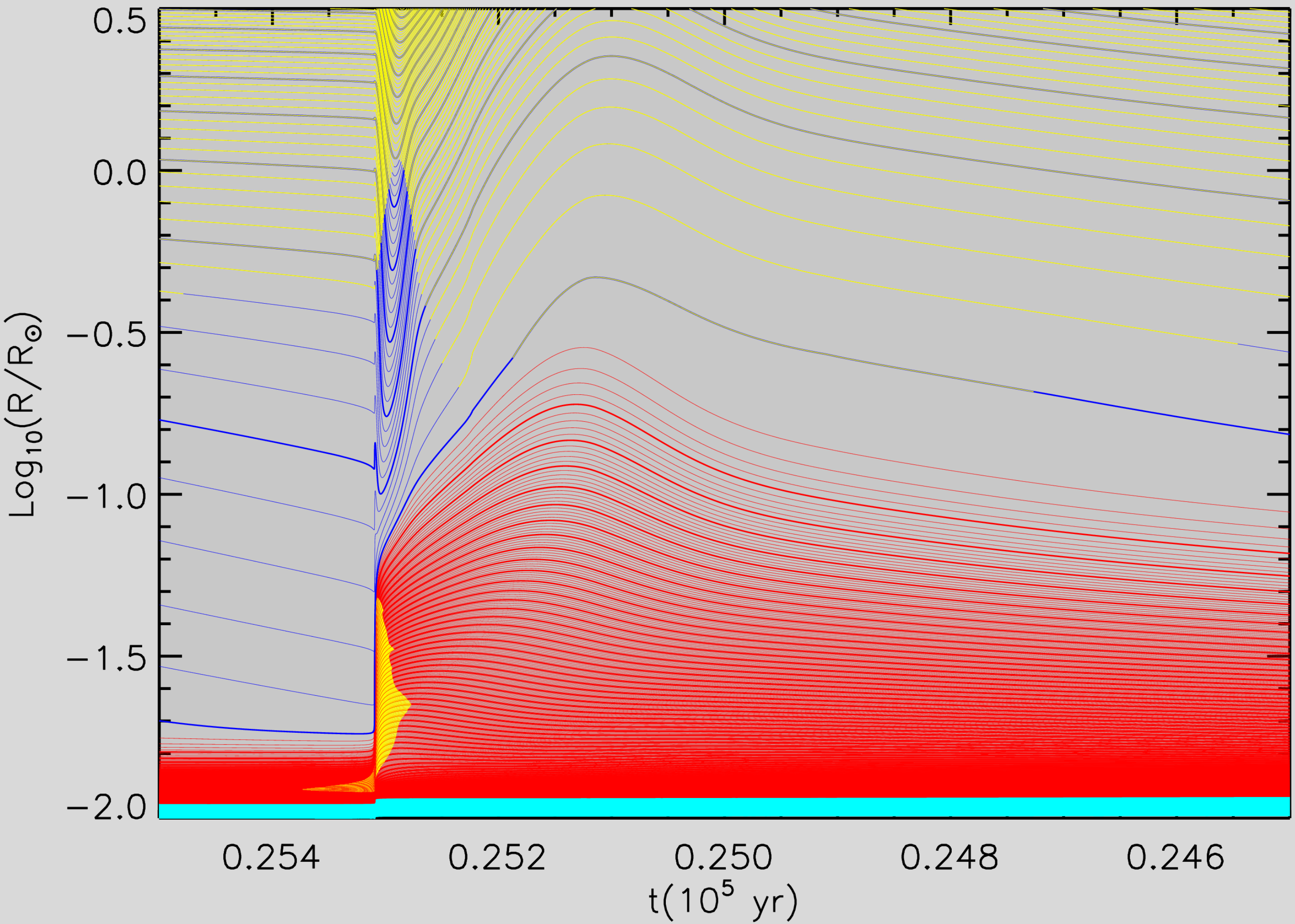

Convective envelope

H rich matter

He core

CO core

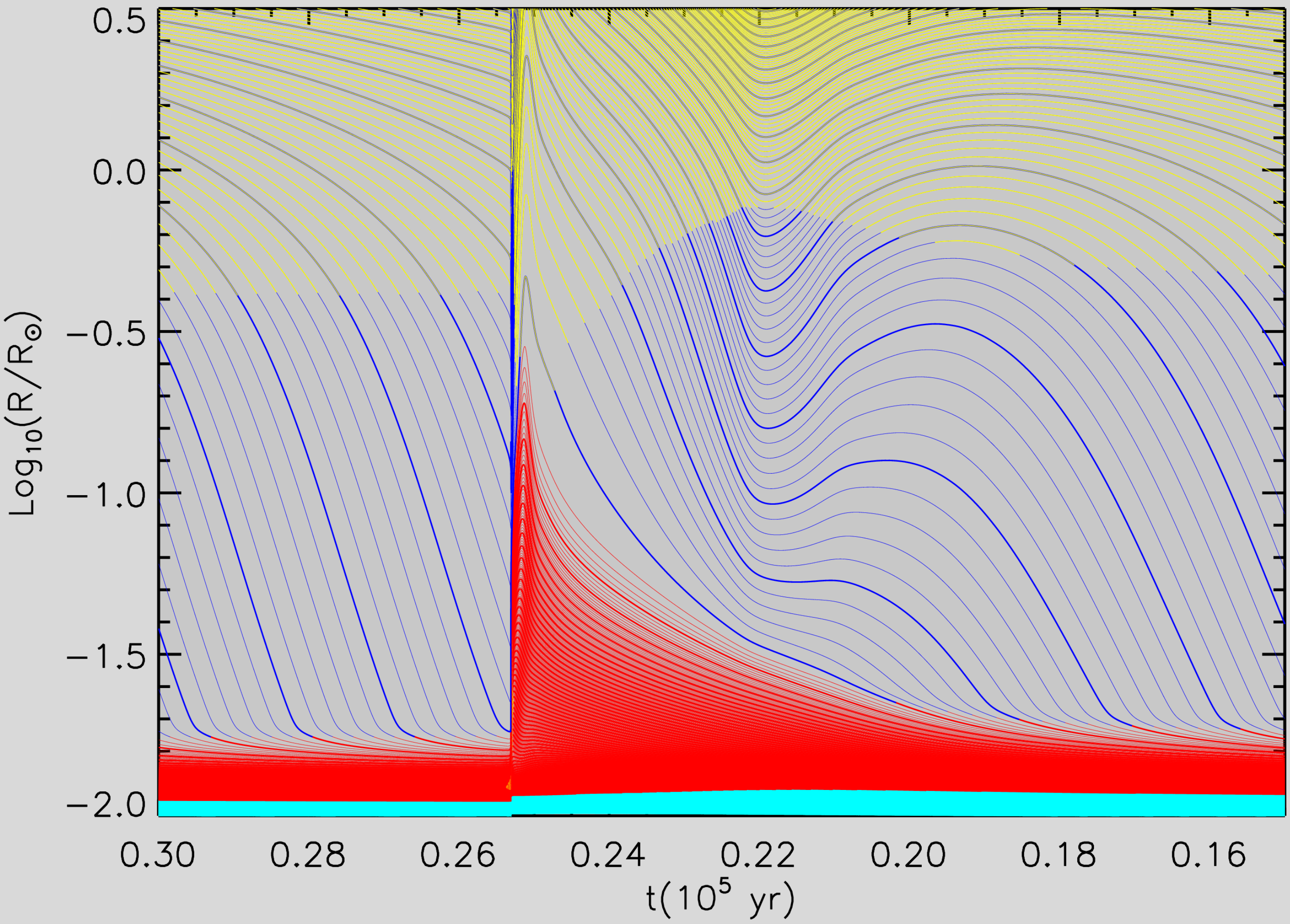

Convective envelope

H rich matter

He core

CO core

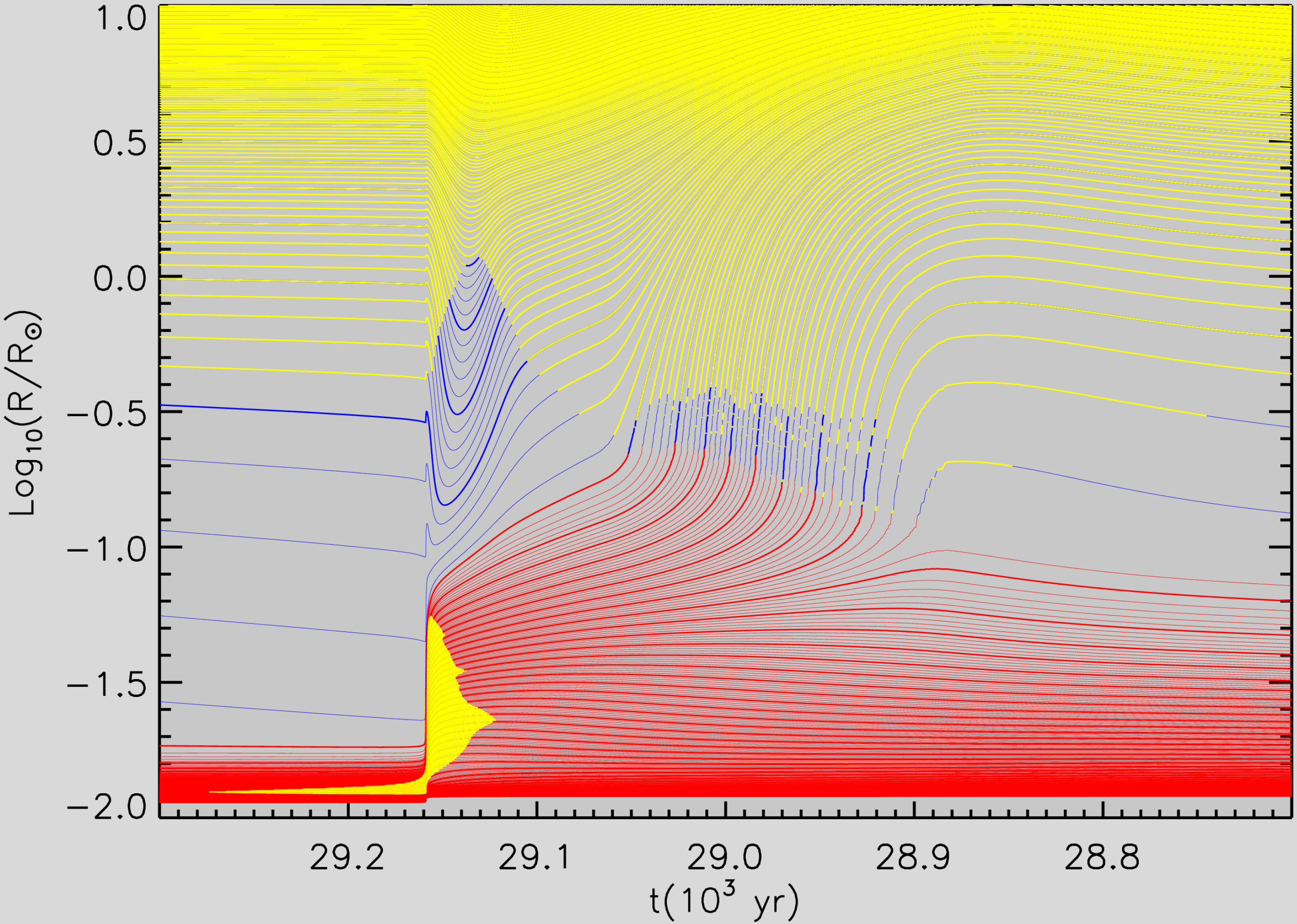

Convective envelope

H rich matter

He core

CO core

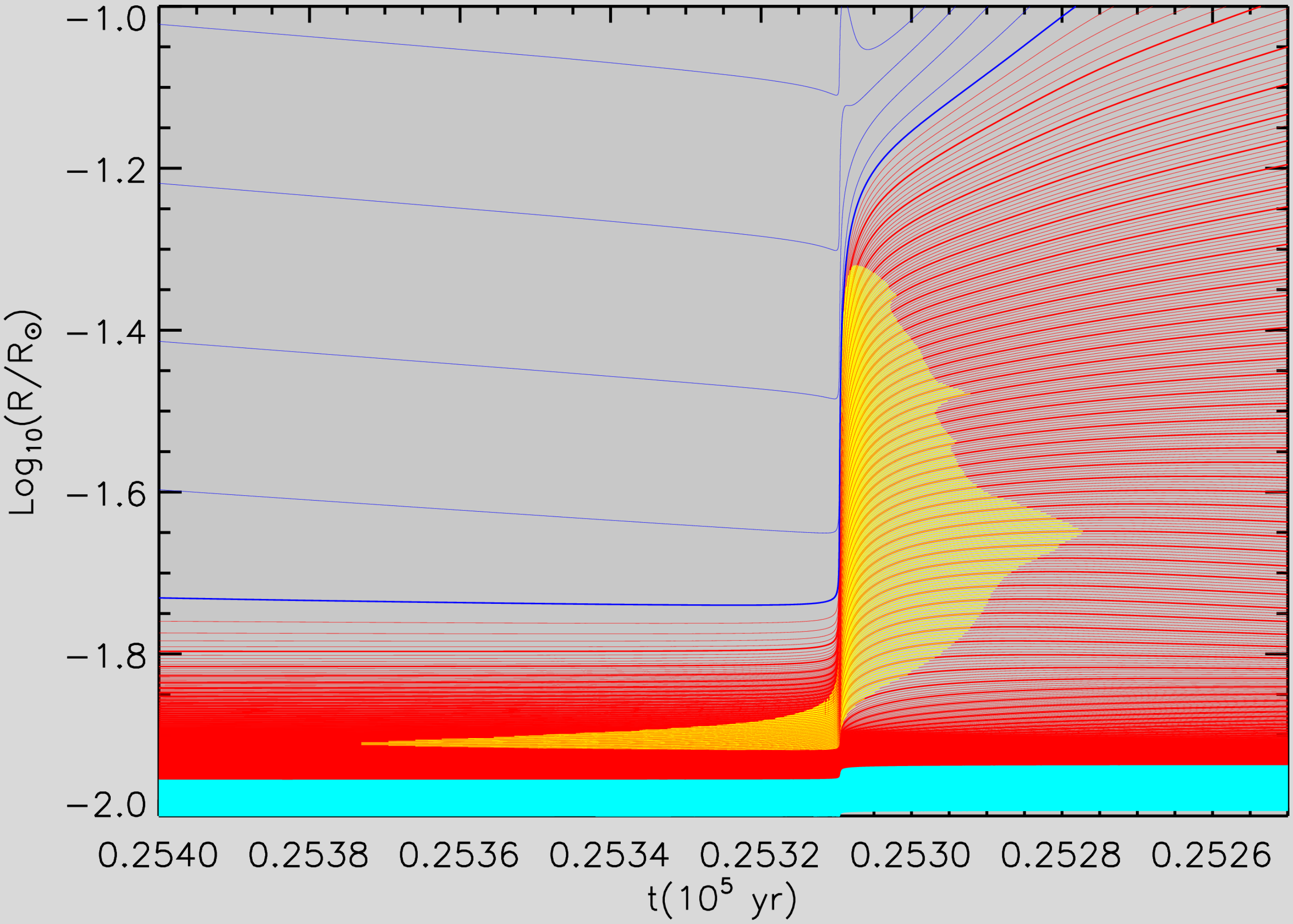

Convective envelope

H rich matter

He core

CO core